Effect of Culture Conditions on the Glycosylation Patterns of mAb

by

Hengameh Aghamohseni

A thesis

presented to the University of Waterloo

in fulfillment of the

thesis requirement for the degree of

Doctorate of Philosophy

in

Chemical Engineering

Waterloo, Ontario, Canada, 2015

©Hengameh Aghamohseni 2015

AUTHOR'S DECLARATION

I hereby declare that I am the sole author of this thesis. This is a true copy of the thesis, including any required final revisions, as accepted by my examiners.

I understand that my thesis may be made electronically available to the public.

Hengameh Aghamohseni

Statement of Contribution

Chapter 4 and partly of Chapter 6 are based on published work by Aghamohseni et al. entitled “Effects of nutrient levels and average culture pH on the glycosylation pattern of camelid-humanized monoclonal antibody” in *Journal of Biotechnology*, (2014) 186, 98–109, 2014.05.024, and are reported with permission from *Journal of Biotechnology*. The thesis author's contributions to this publication were to conduct all the cell culture experiments, experimental design, metabolites and mAb assays, sample preparation for the glycan analysis done at the University of Manitoba and providing all the data used for the dynamic extracellular metabolites’ and glycosylation models. Glycan analysis has been done by Dr. Maureen Spearman with the assistance of Natali Krahn at the laboratory of Professor Mike Butler at the University of Manitoba. In addition, the thesis author carried out the metabolic flux analysis, macro reaction implementation, dynamic-model-structure establishment and index-model- constitution according to the experimental results, and Kaveh Ohadi collaborated in the coding of mathematical equations and optimization of the dynamic model under the MATLAB environment. All plots and analysis of results were implemented by the first author. The thesis author also wrote the final manuscript and responded to the comments of reviewers. This work and journal paper preparation was conducted with direction from the project main supervisors Hector Budman and Jeno Scharer and co-supervisor Murray Moo-Young who are co-authors on the publication.

Abbreviations

CHO	Chinese hamster ovary
BHK	Baby Hamster Kidney
NS0	Mouse Myeloma-derived
GI	Galactosylation index
GI^{inst}	Instantaneous Galactosylation index
SI	Sialylation index
mAb	Monoclonal antibody
EPO	Erythropoietin
tPA	Plasminogen activator protein
INF	Interferon
HILIC	Hydrophilic interaction liquid chromatography
GU	Glucose unit
RA	Relative abundance
ER	Endoplasmic reticulum
ADCC	Antibody cell mediated cell cytotoxicity
CDC	Complement dependent cytotoxicity
ELISA	Enzyme-linked Immunosorbent assay
MFA	Metabolic flux analysis
Q_{mAb}	specific mAb productivity (pg/cell.h)
C_{Met}	metabolite concentrations (mM)
Q_v	volumetric mAb productivity (mg/l.h)
VCH	Volumetric cell-hours (10^6 cells.hr/ml)
[Ala]	Alanine concentration (mM)
[Amm], NH3	Ammonia concentration (mM)
[Asn]	Asparagine concentration (mM)
[Lac]	Lactic acid concentration (mM)
[Asp]	Aspartic acid concentration (mM)
fgr	growing fraction of viable cells
[Glc]	glucose concentration (mM)
[Gln]	glutamine concentration (mM)
[mAb]	Monoclonal antibody concentration (mg/l)
Kij	model parameters
µ	specific growth rate (day^{-1})
TCA	Citric acid cycle
GlcNAc	N-acetyl glucosamine
Man	Mannose

GDP	Guanosine diphosphate
CMP	Cytidine monophosphate
UDP-GNAc	Uridine diphosphate N-acetylhexosamine
UDP –GalNAc	Uridine diphosphate N-acetylgalactosamine
UDP –GlcNAc	Uridine diphosphate N-acetylglucosamine
G0	non-galactosylated glycan
G1	mono galactosylated glycan
G2	fully galactosylated glycan
S0	asialylated
S1	monosialylated
S2	disialylated
$[Sug]$	Nucleotide sugar concentration(mM)
Xd	specific death rate (day^{-1})
Xv	total viable cell density (10^6 cells/ml)
Gluc	glucosidase
Man I	Mannosyl-oligosaccharide 1,2-a-mannosidase
Man II	Mannosyl-oligosaccharide 1,3-1,6-a-mannosidase
GnT I	a-1,3-mannosyl-glycoprotein, 2-b-Nacetylglucosaminyltransferase
GnT II	a-1,6-mannosyl-glycoprotein 2-b- N-acetylglucosaminyltransferase
FucT	Glycoprotein 6-a-Lfucosyltransferase
GalT	b-N-acetylglucosaminylglycopeptide b-1,4-galactosyltransferase
SiaT	b-Galactoside a-2,3/6-sialyltransferase
R	vector of consumption and production rates of metabolites
ψ	vector of metabolite concentrations of all intercellular metabolites
SSE	sum of squared error
ODE	Ordinary differential equation
E	Activation energy
T	Temperature (K)
S_p	Specific mAb productivity (pg/ cell.hr)
F	Lactic acid feeding (mM)

Abstract

The importance of cell culture environment on the glycan distribution of a newly developed monoclonal antibody (mAb) has been comprehensively studied through a combination of experiment and mathematical modeling. The ultimate goal of this research was to formulate a mathematical framework that can be used to determine a set of operation conditions including essential nutrient levels, byproduct concentration as well as pH and temperature optimum conditions to control the glycan profiles. In this regard, CHO DUXB cells were cultivated at different levels of initial glutamine concentrations (0, 2, 4, and 8 mM), pH levels (Reduced from the beginning of the culture or shifted down after the exponential phase to 6.8±0.05) and temperature incubation (Reducing and Shifting temperature strategies to 33˚ C). The relative abundance of glycan structures was determined by hydrophilic interaction liquid chromatography and the galactosylation index (GI) and the sialylation index (SI) were formulated to monitor the time profile of GI and SI levels during cultures of typical 10 days duration. Increasing the initial level of glutamine from 0 to 8 mM glutamine at constant level of 25 mM glucose resulted in a higher consumption rate of glucose and consequently lowers galactosylation levels due to probable decrease of the nucleotide sugars pool at glucose limited condition. Increasing the initial glutamine up to 8 mM was not effective for cell growth, and some growth inhibition due to high concentration of ammonia was observed. The initial levels of glutamine concentration did not affect the specific mAb productivity and consequently, did not impact the residence time of mAb in the Golgi and evolution of glycosylation. For experiments initiated with different levels of

glutamine, the GI values were mostly affected by the availability of glucose and ammonia accumulation. The batches initiated without glutamine supplementation reached a higher value of GI than batches cultivated with glutamine supplementation. It was hypothesized that due to the observed co-metabolism of glucose and glutamine, glucose depletes faster in the presence of glutamine thus becoming unavailable for glycosylation earlier in the culture. It was also observed that the produced ammonia resulting from glutamine conversion had a main effect on the activity of glycosyltransferase enzymes and consequently, led to low levels of SI. pH reduction had negative effects on cell growth, mAb productivity but positive effects on galactosylation and sialylation. At lower pH operation, GI rose because of a low consumption of glucose for cell growth and SI improved because of higher sialyltransferases activity at Reduced-pH conditions. The mechanisms for the effect of pH on glycosylation were inferred from a combination of experimental observations and by using the GLYCOVIS software that describes all possible glycosylation reactions occurring in the Golgi.

Regardless of the initial levels of glutamine, mild hypothermia had a significant effect on the cell growth, mAb productivity and glycosylation profile. Cell growth was reduced at lower temperature and cell viability remained high for a longer time of cell cultivation. Temperature affected the specific glucose consumption rate and glucose was mainly consumed for mAb production as specific mAb productivity and volumetric mAb productivity were enhanced significantly. In the spite of a higher residual glucose concentration at lower temperature compared to the control batches, the GI and SI level were

not improved. This fact is likely to be correlated to the higher specific productivity of mAbs that results in a reduced residence time in the Golgi complex.

Finally, a novel dynamic model that relates culture conditions to glycosylation was proposed. The model consists of two sub-models: one describing the dynamic balances of extracellular metabolites whereas the other sub-model is based on a semi-empirical balance on a lump sum of nucleotides sugars and the correlation between these sugars' levels to the galactosylation index (GI). Both sub-models' predictions were found to be in a good agreement with the experimental data. These models can be combined together to relate the extracellular conditions to glycosylation indices thus opening the possibility to optimize the glycoprofiles by model based optimization. Such optimization may be able to address in future work the tradeoff that has been observed in this thesis between mAb productivity and glycosylation, i.e. higher productivity is generally accompanied by lower glycosylation and vice versa.

Acknowledgements

I would like to express my heart full thanks and appreciation to my outstanding supervisors, Professors Hector Budman and Jeno Scharer for their continual supports of my PhD study and research. Their patience, motivation, and immense knowledge added considerably to my graduate experience. I could not have imagined having a better advisor and mentor for my PhD study as Professor Budman. I appreciate his vast knowledge and valuable contributions after hearth-breaking decease of Professor Jeno Scharer. I would like to especially thank and appreciate my distinguished co-supervisor Professor Murray Moo-Young for his great advices and directions at all levels of the research project.

I would like to thank the other members of my committee, Professors William Anderson Frank Gu, Brendan McConkey for agreeing to be part of my PhD advising committee. I would like to gratefully thank Professor Margaritis for serving as my external committee member. My special thanks to Dr. Maureen Spearman for her tremendous efforts in helping me to carry out my data analysis.

University of Waterloo and Monoclonal Antibody Network (MabNet-NSERC) are also appreciated for the funding of this research.

I also want to thank all of my colleagues, Saeedeh Naderi, Kaveh Ohadi, Johannes Gädke Yuncheng Du, Otacilio Pereira, Noor Aljalam, Ali Nikdel, Keywan Norouzi, Abdul Murayyan, Jann Ang, Susan Gow and Mary McPherson and my lovely friends Hadis, Lena, Zohreh, Fariba, Tatyana and Zhenovy for all their help, support, and valuable hints.

In the end, I would like to extend my heart full appreciation to my wonderful husband Shahabedin and my kind parents Hamid and Nahid, and my thoughtful sisters Marjaneh and Azadeh, for their endurance, support, and encouragements especially during difficult times. Moreover, I like to appreciate the help and support of my in-laws during years of PhD studies.

Dedication

To my love and best friend

Shahabedin

for being a wonderful companion and support in all the stages of my study

This thesis and the pursuit of my goals would not have been possible without you

Table of Contents

List of Figures

List of Tables

.

Chapter 1

Introduction

1.1 Research Motivation

Over the past two decades, the exploration and development of biopharmaceutical proteins has been recognized as one of the major applications of biotechnology. In particular, recombinant human proteins have been produced in a wide range of hosts such as various mammalian (mainly murine) cell lines, bacteria, yeast and insect cells (Sethuraman and Stadheim 2006). Due to the similarity with their original form in humans, these recombinant proteins can be used for replacement or enhancement of naturally existing proteins for the treatment of numerous pathological conditions (Sethuraman and Stadheim 2006).

Monoclonal Antibodies (mAbs) are a class of therapeutic agents with high pharmaceutical market interest due to their application in the fields of immunology and oncology. Their capabilities have been proven successful, and thus, as of 2010, mAbs have claimed approximately 5% of the estimated $850 billion pharmaceutical market. Due to this success, rapid development in this field has been taking place, with around 40 new mAbs being studied each year since 2007. Seventy five percent of the current applications of mAbs are to fight various forms of cancer and arthritis, but applications to other chronic illnesses are also currently

being investigated. Some features of mAbs that makes them especially suitable for use in humans are their high specificity with substrates, and their minimal side effects (Li et al. 2010; Fekete et al. 2013).

The market for therapeutic glycoproteins produced by mammalian cells is expected to reach US $500 billion by 2020 (Kuystermans and Al-rubeai 2015). Among the various mammalian cell cultures, Chinese Hamster Ovary (CHO) cells have been found to be a very effective host for industrial production of recombinant protein therapeutics. CHO cells have protein processing machinery similar to that in humans and this can be exploited to create necessary modifications (Butler 2006a; Hossler 2012).

Glycosylation is one of the most important post translational processes occurring in mammalian that strongly affects the therapeutic properties of mAbs (Spearman and Butler 2015). Therefore, it is crucial to synthesize human mAbs in animal cell cultures which primary structure and conformation are as similar as possible to the naturally occurring proteins in the human body. Thus, conditions should be imposed to achieve the correct glycosylation patterns (Hossler et al. 2009).

The glycosylation process in eukaryotic cells is associated with numerous complex enzymatic reactions whereby sugar groups (oligosaccharides) are attached to the protein's backbone with covalent bonds. The conserved core sugars, which form five out of the fourteen common sugar-lipid-complexes, can be modified by trimming and branching reactions, while the proteins that are transported through the endoplasmic reticulum (ER) and Golgi apparatus undergo

modifications that result in various forms of glycoproteins (Restelli and Butler 2002). Based on the glycan binding site on the polypeptide backbone, glycans are categorized into two major groups: N-linked glycans, where the oligosaccharides attach to the side chain of asparagine, and O-linked glycans, where the oligosaccharides bind to serine or threonine. The former type predominates in animal cell culture. Since many of the reactions during the glycosylation process often do not proceed to completion due to the operating conditions occurring during synthesis, a pool of heterogeneous glycoforms is produced (Restelli and Butler 2002; Spearman and Butler 2015).

The diversity of glycoforms may manifest itself in site–occupancy (macro-heterogeneity) or in the structure of added glycans (micro-heterogeneity). The glycan conformations are important because they can influence the biological characteristics of the mAb products including secretion, solubility, receptor recognition, antigenicity, bioactivity and pharmacokinetics (Spearman and Butler 2015).

Human serum IgG and therapeutic mAbs are highly fucosylated. It has been demonstrated that antibody cell mediated cell cytotoxicity (ADCC) is affected by the fucosylation level of mAbs. ADCC is activated through attachment of lymphocyte receptors (FcγRs) to the Fc region of the antibody. The reduction of core fucose from the glycans has been found to improve the ADCC activity up to 50 fold (Shields et al. 2002; Konno et al. 2012). It has been observed that N-glycans of IgG1, that possessed a higher level of galactosylation, cooperated greatly in the activity of immune system. The normal level of agalactosylated Fc glycans of serum IgG is

between 25 and 35 %. In Rheumatoid arthritis, infection and inflammatory bowel diseases the level of agalctosylated glycans of serum IgG increases significantly (Karsten et al. 2012).

Galactosylation also plays an important role in the complement dependent cytotoxicity (CDC) of Mabs (Wong, et al., 2005a). The sialic acid content of N-glycans is also important in the regulation of anti-inflammatory immune response of IgG (Anthony et al. 2008). In addition, increasing the sialylation level of therapeutics could improve the serum half-life of therapeutic proteins by preventing the activity of asialoglycoprotein receptors available in the liver (Butler 2006a).

1.2 Research Objectives

Following the above-mentioned influences of glycoforms on the therapeutic efficacy of mAbs, it is necessary to identify the culture conditions that control the bioprocess for synthesizing mAbs with the desired spectrum of glycans. An appropriate model with the capability of correlating the mAb glycan profile to the cell culture conditions would be useful for bioprocess design and control, culture media formulation, and possible genetic engineering strategies (Del Val et al. 2010).

In view of the above, the major objective of the present study was to develop a systematic approach to determine a set of operational conditions, including essential nutrient levels as well as byproduct concentration, to produce a desired glycan profile. To accomplish this goal,

mathematical modeling was used in combination with extensive experiments to describe the correlations between culture conditions to the antibody productivity and glycoprofiles.

It was hypothesized that using the developed model, it will be possible in the future to accurately control the mAb productivity and the glycoprofiles by imposing the required set of culture conditions. Although several studies have evaluated the effects of particular nutrients (such as glucose, glutamine, galactose, etc.), culture supplements or inhibitors (ammonia, DMSO, etc.) on the glycan profile (Hossler et al. 2009), it was found that the literature is lacking with respect to the investigation of the combination of these factors on the glycan profile, cell growth and antibody productivity.

To our knowledge, before the current research, no other mathematical models were available that connected the extracellular culture conditions with the resulting glycoprofiles. Earlier models reported in the literature studied particular aspects of the problem. For example, Del Val et al. (2010) have developed a model to represent the N-glycosylation process within the Golgi apparatus while considering the transport of nucleotide sugar donors from the cytosol to the Golgi lumen. However, this model had not been coupled to the culture conditions at the time of starting this project (Del Val et al. 2010). Recently, these authors expanded their model to include the effect of extracellular glucose (Jedrzejewski et al. 2014). In contrast, the model framework developed in our study considers a number of environment factors such as glucose, glutamine, temperature and pH conditions.

Towards the goal of developing a comprehensive model connecting culture conditions with glycosylation and antibody productivity, this thesis research accomplished the following tasks:

1. Evaluated the effect of glucose and glutamine availability on mAbs' glycan profiles.
2. Assessed the effect of byproduct accumulation of ammonia on glycosylation by cultivation of cells at different initial levels of glutamine.
3. Investigated the effect of the environmental pH on glycosylation and productivity.
4. Studied the effect of temperature reduction on glycosylation due to the resulting changes of residence time of the antibody in the Golgi apparatus.
5. Developed a mathematical model that correlates the glycan profile with the factors studied in the above items.

With regard to objectives (1-2), the relative contribution of each essential nutrient, particularly glucose and glutamine, and byproduct accumulation, specifically ammonia, were investigated by carrying out an appropriate set of experiments at 25 mM of glucose concentration and four different levels of glutamine (0,2,4 and 8 mM). The specific production and consumption rates of extracellular metabolites have been assessed by a multi-parameter bioanalytical system, BioProfile 400 (Nova Biomedical, Waltham, MA). The mAb productivity was monitored by using an enzyme-linked Immunosorbent assay (ELISA) developed by MabNet for Eg2-hFc mAb. A hydrophilic interaction liquid chromatography (HILIC) followed by exoglycosidase enzyme array digestion were applied for glycan analysis.

It was found that the culture with medium levels of glucose and glutamine reached the highest level of cell density, but the mAb productivity was almost the same for all conditions. The population of dead cells was found to be correlated with higher levels of ammonia that mostly resulted from the metabolism of glutamine. Glycosylation levels changed significantly with the initial glutamine level, and in the culture with a lower level of glutamine, a higher level of sialyation was observed. Galactosylation was affected by both glucose and glutamine levels.

Regarding objective (3) it was found that reducing the culture pH to as low as 6.8±0.05 has notable effects on sialyation and galactosylation levels. A model of the glycan reactions occurring in the Golgi (GLYCOVIS) was used to understand the particular pathways that determine the glycan profiles for the experiments conducted for the above objectives (1-3).

In objective (4) above, it was found that temperature changes can be used to manipulate the residence time of mAbs through the Golgi complex thus changing the exposure time of proteins to glycosyltransferase enzymes present in the Golgi apparatus. Later, by decreasing mAb productivity at Reduced-pH conditions but improving mAb glycosylation, attempts were made to apply mild hypothermia to improve protein productivity as well. In spite of the negligible effect of temperature on the glycan pattern of glycoproteins reported by researchers (Chen et al., 2011; Hossler, 2012; Rodriguez et al., 2010; Yoon, Song, & Lee, 2003), we did observe changes in the glycan profile for Eg2-hFc and, at the same time, the mAb productivity improved significantly. The lower galactosylation levels observed at the end of the exponential phase of growth at

Reduced-Temperature may be due to shorter residence time of mAbs in the Golgi complex rather than glucose limitations.

Objective (5) focused mostly on the construction of a mathematical approach for correlating variables presented in items (1-4) to the mAbs glycosylation profile. To this end, we first formulated a model to describe the extracellular culture conditions including cell growth, antibody productivity and extracellular concentrations of main metabolites.

This dynamic model was based on a preliminary metabolic flux analysis (MFA) that was applied to eliminate insignificant metabolic pathways and adding appropriate ones based on the experimental results. The dynamic model was implemented according to the systematic approach proposed by our group previously (Naderi et al. 2011). The parameters of the dynamic model were calibrated based on the experimental data (Ohadi et al. 2013; Aghamohseni et al. 2014). After, the effects of Reduced-pH and Reduced-Temperature were applied on the dynamic model to create a descriptive dynamic model for a wider range of set of experiments and the model parameters were recalibrated.

Then, to connect this model of extracellular properties to glycosylation two different approaches were pursued: 1- a semi-empirical model was develop to correlate directly the extracellular conditions to the glycosylation indices through the solution of a lumped quantity representing nucleotides' sugars levels (defined in Chapter 6) and 2- a mechanistic model was formulated to correlate the extracellular culture conditions to the individual glycans' levels through the solution of three connected sub-models: i) a dynamic model of extracellular

metabolites, ii) a nucleotide sugars production model in the cytosol and iii) a model of glycosylation occurring in the Golgi apparatus (Ohadi et al. 2013).

Although the second modeling approach is very rigorous, because it considers nucleotide and nucleotide sugar donor networks and the kinetics of the individual reactions, we have found the parameter optimization for this model to be very challenging. In addition, to achieve an acceptable optimized model, many data points are required. In particular, the culture samples needed for analysis of intracellular metabolites are relatively large as compared to the total working volume in the flask. In this regards, the first approach regarding a semi empirical model was expended in this thesis. This model speculates a lumped profile of nucleotide sugars and an instantaneous galactosylation index (GI^{inst}). The nucleotide sugar concentration $[Sug]$ per one day interval is associated with the nucleotide sugar production, glucose and glutamine concentration, and specific growth rate of that day. The GI^{inst} model correlates to $[Sug]$ profile, glucose concentration and mAb specific productivity. The combination of this model was accomplished to predict the galactosylation indices for a wild range of culture condition over seven days of cell cultivation.

The semi-empirical model proposed above is easier to calibrate and it can serve to easily elucidate correlations between extracellular properties and glycosylation while avoiding the very challenging parameter estimation task required for the second more rigorous model.

This thesis comprises seven chapters organized as follows:

Chapter 1 introduces the topic, objectives and approaches of the current research.

Chapter 2 reviews the relevant literature, including monoclonal antibody productions, the Chinese hamster ovary cell host, animal cell culture modes, glycosylation and control of oligosaccharide processing under different culture conditions and mathematical modeling of glycosylation process.

Chapter 3 summarizes the methodology and techniques used in the experiments.

Chapter 4 emphasizes on the effects of glucose and glutamine depletion, ammonia accumulation and, Reduced-pH on the mAb's glycan profiles. This Chapter has been published in *the Journal of Biotechnology* (Aghamohseni et al. 2014).

Chapter 5 demonstrates the effect of Reduced-Temperature on the mAbs' glycan profiles.

Chapter 6 introduces the modeling strategies used to connect the extracellular environmental to the intracellular glycosylation.

Chapter 7 summarizes significant conclusions and recommendations for future work.

The thesis author publications are as follows:

I. A Silico Study of Glycosylation in a Camelid-Humanized Monoclonal Antibody at Different Cell culture Conditions, ready to submit to the *Journal of Biotechnology*, (H. Aghamohseni, K. Ohadi, M. Spearman, M. Moo-Young, M. Butler, H. Budman, 2015).

II. Novel Dynamic Model to Predict the Glycosylation Pattern of Monoclonal Antibodies from Extracellular Cell Culture Conditions, *12th IFAC Symposium on Computer*

Applications in Biotechnology (K. Ohadi, H. Aghamohseni, Y. Gädke , M. Moo-Young , Y. Scharer, R. Legge, H. Budman, 2013).

III. Effects of Nutrient Levels and Average Culture pH on the Glycosylation Pattern of Camelid-humanized Monoclonal Antibody, *Journal of Biotechnology*, (H. Aghamohseni, K. Ohadi, M. Spearman, N. Krahn, M. Moo-Young, Y. Scharer, M. Butler, H. Budman, 2014).

IV. Fluorescence-based Soft Sensor for at Situ Monitoring of Chinese Hamster Ovary Cell Cultures, *Biotechnology and Bioengineering*, (K. Ohadi, H. Aghamohseni, R. Legge, H. Budman ,2014).

Chapter 2

Literature Review

2.1 Monoclonal Antibody Production

Since 1994, when the first mAb product was approved by the US FDA, the share of therapeutic mAbs in the pharmaceutical market has rapidly increased. Currently, over 30 therapeutic mAb are available. Previously they have been used to treat a wide range of cancers and disorder of the autoimmune system, and more recently as carriers of various cytotoxic drugs (Munro et al. 2011).

As of 2003, the worldwide biopharmaceutical investment was estimated at more than $30 US billion. In 2010, the marketing of biological products surpassed $100 US billion and reached $142 US billion as of 2011, with five out of ten of the current world's dominant pharmaceuticals being antibodies (Munro et al. 2011; Jedrzejewski et al. 2014).

Initially, therapeutic proteins were extracted from human sources such as blood clotting factors, human serum albumin from plasma, and insulin from pancreas. Concerns over product purity, conformity and the risk of viral infections as well as significant progression in genetic engineering tools, motivated the adoption of recombinant expression systems. Based on the similarity of the recombinant protein with its original form in humans, a wide range of hosts such

as mammalian cell lines, bacteria, yeast and insect cells, have been utilized as platforms (Sethuraman and Stadheim 2006).

The commercial production of therapeutic mAbs was initiated using various continuous hybridoma cell lines with the capacity of creating the desired antibodies (Elvin et al. 2013). The earliest mAbs were involved purely murine sequences. To reduce human anti-murine antibody responses (HAMA) and to increase their efficiency, the mAbs format was shifted to "chimeric" type involving both murine variable and human constant domains and, more recently, to fully human mAbs (Munro et al. 2011; Elvin et al. 2013).

Chinese hamster ovary (CHO) cells are currently the most desired expression systems used for the manufacturing of biopharmaceuticals due to their high productivity, adaptability to industrial scale production and the ability to produce human-like glycoforms (Hammond et al., 2012).

2.2 Chinese Hamster Ovary Cells

The primary goal of cell culture development is the selection of an animal cell line that enables the production of desirable cell concentration, viability and productivity (Taschwer et al. 2012). An additional consideration for selecting a cell line is obtaining the required post-translational modification, mainly glycosylation, of the synthesized protein skeleton.

Since their isolation in 1958, CHO cell lines have been successfully used in a wide range of research areas such as genetics, pharmacology, toxicology and cancer (Hammond et al. 2012). In

addition to providing appropriate glycoforms, CHO cells are known to produce genetically stable clonal cells. They can be cultured to high density in simple bioreactors as suspended cells and can be easily adapted to proliferate in protein-free media (Butler, 2005a; Hammond et al., 2012; Taschwer et al., 2012). However, despite their advantage, they exhibit certain characteristics such as shear sensitivity, low yield, and medium complexity which has motivated intensive research on bio-process and media optimizations (Butler 2006a).

At present 60 to 70% of all the recombinant pharmaceuticals are produced in CHO cells with a value of $100 US billion on the global market (Ahn and Antoniewicz 2012). In addition to CHO cells, Mouse Myeloma-Derived (NS0), Baby Hamster Kidney (BHK), Human Embryo Kidney (HEK), Human-Retina-Derived (PER-C6) cells have been used as alternative platforms for the production of recombinant proteins. Although all these cell lines have been found to adapt well for growth in suspension cell cultures, CHO and NS0 cell lines are considered superior candidates in this group (Taschwer et al. 2012).

2.3 Glycosylation

Most proteins secreted by mammalian cells are glycoproteins (Hauser and Wagner 1997). The diversity of carbohydrate components of glycoproteins is a key factor for their therapeutic efficacy, since it can influence many of their characteristics, including pharmacokinetics, secretion, solubility, bioactivity, recognition and antigenicity.

Glycosylation is one of the most important modifications that can be carried out to glycoproteins in mammalian cells. This post-translational modification involves a series of reactions causing the formation or cleavage of covalent bonds to the nascent synthesized polypeptide chain (Hauser and Wagner 1997).

During glycosylation, oligosaccharides are added to the protein in a step-wise manner while being transported through the endoplasmic reticulum (ER) and Golgi apparatus (Hossler et al. 2009). Depending on the glycan binding site on the polypeptide backbone, glycans are categorized into two major groups: N-linked glycans referring to the case when the oligosaccharides attach to the side chain of asparagine and O-linked glycans when the oligosaccharides bind to serine or threonine. The N-linked glycans are more prevalent type in mammals (Restelli and Butler 2002).

2.3.1 N-Glycans

N-linked oligosaccharides are composed of three main groups: high-mannose, hybrid and complex-type. They all have a same pentasaccharide core structure but with different outer branches as follows:

1) High-mannose (Man) type: typically has two to six additional Man residues linked to the core, 2) Complex type: contains two or more outer branches containing N-acetyl glucosamine (GlcNAc), galactose, and sialic acid and 3) Hybrid type: has features of both high-Man and

complex type oligosaccharides (Hauser and Wagner 1997; Restelli and Butler 2002; Butler 2005).

Human native IgG is mostly composed of N-linked Fc- complex biantennary type oligosaccharides with heterogeneity in core fucosylation, terminal sialylation and galactosylation (Wacker et al., 2011).

The precursor for N-glycosylation contains a lipid (dolichol) linked to an oligosaccharide (Glc3Man9GlcNAc2). The first seven sugars of the precursor (two GlcNAc and five Man) are obtained from nucleotide sugars, (UDP-GlcNAc and GDP-Man), respectively. The N-glycosylation starts in the ER, where the precursor is attached to the Asn side chain of the amino acid sequence of mAb by the oligosaccharyltransferase enzyme (Butler 2006a).

This process is followed by a series of trimming reactions for glycan removal. The first terminal glucose is removed by α-1,2 glucosidase I (Gluc I), and the other two glucose molecules are eliminated by a single α-1,3 glucosidase II (Gluc II). Before leaving the ER and entering the Golgi, the newly synthesized glycoprotein may lose at least one mannose by mannosidase I (Man I). All the mentioned consecutive reactions occur successfully in the ER if the protein has an appropriate folding pattern. Thus, there is always a need to control the mechanism so that it yields a required protein tertiary structure (Restelli and Butler 2002).

Following the aforementioned reactions, N-glycosylation results in the formation of complex-type glycans by step-wise addition of monosaccharides including, GlcNAc, galactose, fucose and sialic acid, through a series of transferases that are present in the Golgi

compartments. However, many of the enzymatic reactions cannot be completed, leading to enhanced heterogeneity of the final glycan structure (micro-heterogeneity). Heterogeneity can take different forms such as antennarity, with the number of branches from the central mannose of the core structure, terminal sialylation, core fucosylation and addition of a 'bisecting' GlcNAc to the central core Man residue (Butler 2005).

2.4 Control of Oligosaccharide Processing in Mammalian Cell Culture

Translation of gene expression occurs according to the mRNA (messenger RNA) template thus resulting in high constancy of the protein structure. In contrast, oligosaccharides processing occurs in the presence of several successive enzymatic reactions in different intracellular compartments. Therefore, the outcomes of these series of reactions differ depending on the environmental conditions affecting this reaction (Hauser and Wagner 1997).

Because of the paramount impact of glycan profiles on properties that determine the therapeutic efficacy of glycoproteins, such as solubility, resistance to thermal inactivation and protease digestion, secretion, biological activity and immunogenicity, there is always a strong incentive for optimally manipulating external factors that influence intercellular glycosylation (Andersen and Goochee 1994; Hauser and Wagner 1997). The awareness of such effects has

increased the importance of developing and optimizing the culture environment to manipulate the glycan-profiles (Restelli and Butler 2002).

The following section covers the main factors determining the heterogeneity of the final glycan patterns.

2.4.1 Host Cell Line

The glycan patterns of a protein depend on the expression level and the availability of various glycosyltransferase enzymes that are present in the Golgi apparatus of the cell. Analysis of the glycoforms occurring in the same proteins but from different species and/or from different tissues discloses that a key factor in determining the synthesis of particular N-linked oligosaccharides depends on the relative activity of these enzymes (Butler 2006a).

Raju et al. (2000) reported that the glycan structures of IgG produced from 13 different species were very different. They have found a significant variation in the proportion of terminal galactose, core fucose and bisecting GlcNAc among these different species (Raju et al. 2000).

Structural changes of glycans can also be effected through metabolic engineering of the host cell line, for instances by gene knockout of the already expressed corresponding glycosyltransferases or by insertion of novel functionalities (Butler 2005). Structural changes such as adding the bisecting N-acetyl glucosamine (Umaña et al. 1999) or removing fucose

(Konno et al. 2012) from the glycan of an IgG can improve the attachment of the antibody to Fc receptors leading to increased antibody-dependent cell mediated cytotoxicity (ADCC).

2.4.2 Culture Environment

Cell culture conditions affect the glycosylation process as a result of changes in either the general cell-culture method or in specific culture variables (Hauser and Wagner 1997; Restelli and Butler 2002).

The potential mechanisms and approaches to explain such effects are summarized as:

- Depletion of the cellular energy state
- Variability in glycosidase and glycosyltransferase activities
- Variation of nucleotide and nucleotide sugars and lipid precursors
- Disruption of the local ER and Golgi environment
- Degradation of extracellular glycan by glycosidase
- Prolongation of protein residence time in the Golgi (Nabi and Dennis 1998; Valley et al. 1999; Restelli and Butler 2002; Wong et al. 2010).

These mechanisms were explicitly taken into account in this thesis when devising strategies for altering the glycoprofiles as further discussed in the modeling section of Chapter 7.

➢ *Mode of Culture*

A number of techniques are generally used for growth of mammalian cells, including suspension growth in batch, fed batch and perfusion cultures.

Batch culture has been the most common mode of operation in the pharmaceutical industry. However, although batch operation is a cost-effective, simple and reliable production system, it is limited in terms of growth and productivity (Ozturk and Hu 2006). The limitations are often due to the accumulation of metabolic by-products, such as ammonia and lactate, or the depletion of nutrients, such as glucose or glutamine. To address these limitations, cultures are cultivated using alternative modes such as fed-batch or perfusion.

In a fed-batch culture, avoiding complete depletion of nutrients is operationally simple using continuous or intermediate feeding of nutrients. Its advantages are ease of use, reliability and adaptability (Cruz et al. 2000; Raju et al. 2000). Optimal operation strategies for fed-batch cultures involve optimal feeding of nutrients according to the cell's requirements for appropriate growth and maximal productivity. For instance, maintaining the major carbon sources at low concentrations leads to a more-efficient primary metabolism because the concentrations of toxic metabolic by-products such as ammonia and lactate are kept at low levels. Consequently, the cells remain in a productive state for a longer time (Raju et al. 2000; Butler 2006a).

Unlike batch cultures which require temporary adjustments, with continuous cultures different culture parameters can be monitored under steady state conditions (Ozturk and Hu 2006). In addition, continuous operations have been reported as the most-effective processes for

maintaining more consistent and stable products while minimizing the amount of inhibitory substances. Thus, the specific growth rate and physiological state of cells as well as environmental conditions can be better controlled (Chu and Robinson 2001; Vergara et al. 2014).

In perfusion cultures, the constant supply of nutrients and continuous or intermittent removal of media result in higher cell densities (from 10^6 cells/ml in batch culture to at least 10^7 cells/mL in perfusion mode) (Xie et al. 1997; Taschwer et al. 2012). Vergara et al., (2014) capitalized on the ability of controlling the physiological state of cells in chemostat to investigate the effect of mild hypothermia on specific productivity independently from the cell growth reduction occurring at lower temperature. At a lower dilution rate of 0.012 h^{-1} and lower temperature of 33ºC, a higher level of protein productivity was observed (Vergara et al. 2014).

However, the selection of the culture operation mode and operational strategies are strongly dependent on a number of issues such as product secretion (growth or non-growth associated), quality and stability of the final product in the culture and on limitations imposed by industrial-scale production (Meuwly et al. 2006).

The choice of culture methodology also affects the properties of glycoproteins and the time evolution of the oligosaccharide structures. For example, glucose depletion, occurring in batch cultures in contrast with fed-batch operation where such depletion is avoided, has a significant effect on glycosylation (Andersen and Goochee 1994). Specifically, the level of galactosylation

and sialylation levels of a Camelid mAb produced by CHO cells were depleted due to unavailability of glucose at different levels of glutamine in batch condition (Liu et al. 2014).

Significant differences in the degree of sialylation were found in an immobilized culture in comparison to free suspension conditions. The recombinant human thyrotropin (TSH) glycan profile was examined in both hollow fiber and micro-carriers bioreactors. The TSH produced in the hollow fiber bioreactor contained less sialic acid and galactose compared to the TSH produced in micro-carriers beads in a larger bioreactor (Hauser and Wagner 1997). The perfusion mode of culture has been reported as an effective and economical way to enhance the quality of glycoproteins while combined with controlled-glucose feeding (Yang et al. 2014). Recombinant β-IFN produced at a lower temperature in a perfusion culture provided 43% less aggregation than in the batch process while the sialylation levels of -IFN were found to improve significantly (Rodriguez et al. 2010).

The influences of fetal bovine serum (2%) on glycosylation patterns were investigated in serum free medium in both suspension and micro-carrier cultures. It was found for both modes of operation that the N-linked glycosylation, specifically fucosylation and galactosylation, was higher in the serum-free medium than in a serum-containing medium (Gawlitzek et al. 1995).

➢ *Nutrient Availability*

Different studies have been conducted to investigate the effects of nutrients on mammalian cells that produce recombinant proteins. The glycosylation of mAbs was shown to significantly change when glucose as the main carbon source is limited or is completely substituted with other monosaccharides (del Val et al. 2010; Liu et al. 2014). Glucose starvation was explained to generate two main deficiencies in glycoprotein synthesis: abnormal precursor attachment and reduction of glycosylation at the expected sites of the protein. Both-mentioned irregularities result from insufficiency of glucose-derived oligosaccharide precursors of glycans (Restelli and Butler 2002; Liu et al. 2014).

It has been demonstrated that a reduced level of intracellular uridine triphosphate N-Acetyl glucosamine (UDP-GlcNAc) is the main reason for the lower level of glycosylation in both glucose and glutamine depleted media (Nyberg et al. 1999). It is also reported that the antennarity of the glycan structure produced in BHK increases at higher levels of UDP-GlcNAc (Valley et al. 1999). Hayter et al. (1991) showed that in a CHO chemostat culture producing gamma interferon, the degree of glycosylation decreases at lower levels of glucose (Human et al. 1992). Fed-batch culture techniques have been used frequently to resolve this problem by maintaining the level of glucose and glutamine above the critical concentration (Restelli and Butler 2002). For example, the glycan profile of produced gamma interferon was monitored at levels below 0.1 mM glutamine and 0.7 mM glucose in a CHO fed-batch culture. A significant

decrease in sialyation proportion and an increase in the hybrid and high mannose glycan ratio were observed (Chee Furng Wong et al. 2005).

Burleigh S. et al. (2011) carried out a batch culture of CHO cells under different glutamine levels in order to investigate glutamine's effect on the efficacy of the glycosylation. Using a glutamine-free medium resulted in lower cell growth rate, slower glucose metabolism, lower sialylation, reduced intracellular UDP-GlcNAc sugar pools, smaller glycolytic flux and lesser complexity of N-linked glycans (Burleigh et al. 2011). In contrast, Taschwer et al. (2011) observed improvement in production of complex N-linked glycans of EPO produced in glutamine-free condition (Taschwer et al. 2012).

Glucosamine is another potential substrate that was used for glycosylation modification. Yang and Butler (2002) investigated the effect of glucosamine and ammonia on the intracellular UDP-GNAc pool and glycosylation patterns of EPO by CHO cells cultivated in a serum-free medium. Results showed that the presence of glucosamine or ammonia enhances the heterogeneity of EPO due to an increase in the production of UDP-GNAc, and decreases the production of tetra-sialylated and tetra-antennary glycan structures (Yang and Butler 2002). In the other hand, human IgG-IL2 produced in a continuous culture of BHK-21 with low supplementation of glucose and glucosamine exhibited the same glycosylation profile as a control culture without glucosamine and glucose limitations (Hossler et al. 2009).

Terminal galactosylation of glycans was found to be highly correlated to the level of galactose in the medium. Feeding the culture with higher levels of galactose increases the

proportion of galactosylated glycans in a variety of mAbs. However, the use of galactose instead of glucose by galactose as a major carbon source affects the cell growth, byproduct accumulation and protein quality (Altamirano et al. 2006).

The combinations of different nutrients affecting glycosylation have been recently recognized as an effective strategy to modulate the Mabs' glycosylation. For example, a combination of manganese, galactose and uridine have been found to induce 1,4-galactosylation of IgG4 produced by different CHO cell lines while appropriate levels of all three substances were maintained in the culture (Grainger and James 2013). More recently, Liu et al. reported the significant increase of the galactosylation index of two different antibodies, IgG1(DP12) from 0.30 to 0.43 and EG2 mAb from 0.73 to as high as 0.83 when cells supplemented by uridine, manganese and galactose cocktails (Liu et al. 2014).

Amino acids present in growth media have been reported to profoundly affect glycosylation. The addition of amino acids (cysteine, isoleucine, leucine, tryptophan, valine, asparagine, aspartic acid and glutamine) was studied to determine their effects on the glycosylation pattern of recombinant human erythropoietin (EPO) secreted by a CHO cell line (Crowell et al. 2007). Although amino acid supplementation at the cell growth stages improved the protein productivity, the sialic acid content of EPO was reduced. On the other hand, the addition of manganese as a cofactor of 1,4-galactosyltransferase improved sialylation and productivity. In 2014, Eli Lilly's researchers reported significant changes in the glycan structures of recombinant proteins produced by CHO cells cultivated in a new chemically defined medium. Further studies

revealed that the higher level of asparagine in the new medium caused elevated levels of higher mono and di-galactosylated glycans compared to non-galactosylated structures. They hypothesized that the higher level of ammonia resulting from the metabolized asparagine caused higher heterogeneity in the final product quality (McCracken et al. 2014).

➢ *Ammonia and pH*

Ammonia (NH3) or the ammonium ion ($NH4^+$) is produced as the main by-product of the cellular enzymatic glutamine utilization or the thermal decomposition of glutamine in a medium. Glutamine plays a key role in the generation of energy for cells and as a precursor for nucleotide synthesis (Restelli and Butler 2002; Butler 2006a). However, it is an unstable component which easily decomposes to ammonia when pH, temperature and phosphate concentration change significantly (Ahn and Antoniewicz 2012). In addition, metabolism of amino acids other that glutamine induce ammonia production (Crowell et al. 2007; McCracken et al. 2014).

The effect of ammonia accumulation has been considered as of great importance for process optimization due to inhibitory effect on cell growth (Butler 2005; Chen and Harcum 2006), on glycosylation alteration (Chen and Harcum 2006) and on galactosylation gene expression levels (Brodsky et al. 2014).

Ammonia has been reported to cause heterogeneity of the final product (Crowell et al. 2007; McCracken et al. 2014). The main effect of ammonia on mAb's glycan profile is related to changes in the terminal sialic acid (Andersen and Goochee 1994; Yang and Butler 2000; Hossler

et al. 2009). Yang et al., (2000) reported that the addition of NH4Cl to CHO cell cultures not only significantly increased the glycan heterogeneity, but it also reduced the terminal sialic acid concentration. They also reported that the ammonium produced as a result of glutamine metabolism had greater effect on glycoproteins than ammonium present from NH4Cl supplemented media (Yang and Butler 2000). Ammonia also has been reported to negatively impact the efficacy of sialylation glycans secreted by NS0 cells (Brodsky et al. 2014).

There are two possible mechanisms to explain the effect of ammonia on glycosylation: i) the increase of the Golgi's pH level and ii) significant impact on the nucleotide sugar concentrations. The accumulation of ammonia inside the cells raises the pH level where the latter impacts the activity of transferases in the Golgi. Thus, changes in the environmental conditions of enzymes consequently affect the final glycosylation profile. Also, the enhanced incorporation of ammonia into glucosamine increases the level of the intermediate GlcNAc. This nucleotide sugar competes with the sialic acid-nucleotide sugar precursor, which is the critical substrate for the sialyation process (Valley et al. 1999; Restelli and Butler 2002; Butler 2006a). The expression levels of 12 associated glycosylation genes of CHO cells were investigated at different ammonia concentrations by Chen et al., (2005). They reported that the deficiency in galactosylation and sialylation is mainly due to suppression of genes of galactosyltransferase, sialyltransferase and the CMP-sialic acid transporter at elevated levels of ammonia. These observed correlations mostly happens in the Golgi apparatus rather than in the cytosol and/or endoplasmic reticulum (ER) (Chen and Harcum 2006).

Extracellular pH conditions affects different intracellular properties including cell metabolism, glucose transport, ATP/ADP ratios and the intracellular pH environment. Under unfavorable extracellular pH conditions, the internal pH of the Golgi changes, and the activity of key enzymes involved in glycosylation decreases (Borys et al. 1993; Butler 2006a). In addition, it has been reported that higher levels of pH cause dislocation of the glycosyltransferase enzyme along the Golgi compartment thus negatively impacting galactosylation and sialyation in N-linked oligosaccharides (del Val et al. 2010). The most favorable pH levels for sialylation were found to be in the range of 6.8-7.2, although this range was found to be dependent on the cell line type and glycoprotein product (Trummer et al., 2006; Yoon et al., 2005).

Borys et al., (1993) found that the glycosylation patterns of a recombinant protein, mouse placental lactogen produced by CHO cells, changed over the culture pH range of 6.4 to 8.7 (Borys et al. 1993). A notable decrease in the extent of glycosylation was observed at pH lower than 6.9 and higher than 8.2. Muthing et al., (2003) reported that the bioreactor pH for a hybridoma cell line had a significant effect on the galactosylation of mAbs (Müthing et al. 2003). In that work, the maximum levels of non-galactosylated (G0), mono galactosylated (G1) and fully galactosylated (G2) glycans were detected at pH levels of 7.2, 6.9 and 7.4, respectively, whereas the lowest level of sialyation occurred at a pH of 6.9. These results can be explained by mislocalization of galactosyltransferase (GalT) and sialyltransferase (SiaT) (del Val et al. 2010).

➢ *Temperature*

In general the productivity of recombinant proteins is correlated to cell viability. Due to its strong effect on viability, temperature has been often manipulated for optimizing productivity. Several studies have reported the significant effects of temperature on different cell culture variables, including growth rate, cell metabolism and protein production (Ahn et al. 2008; Hossler et al. 2009; Spearman and Butler 2015). Although the desired culture temperature is correlated to other environmental parameters, researchers generally agree that for a specific cell line there is an optimal temperature for which productivity is maximized (Chen et al., 2011; Ivarsson, 2014; Rodriguez et al., 2010).

Reducing temperature mostly leads to reduced cell growth, but longer cell life and cell productivity (Chen and Harcum 2006; Rodriguez et al. 2010; Vergara et al. 2014). To explain this contradictory observation, Mason et al., (2014) compared the productivity of two antibody mutant cells from stable CHO cell lines. The productivity of highly expressing mutant cells did not improve at 32º C compared to 37ºC while the productivity of poorly expressing mutant cells was enhanced. These authors proposed that protein types, protein folding and protein assembly determine the effects of reduced temperature on protein production (Mason, et al., 2014).

Although, the benefit of reduced temperature has been studied by several researchers, the mechanism by which reduced temperature enhance specific productivity has not been resolved conclusively. The possible mechanism includes increased mRNA stability of recombinant proteins, improved transcription and arrest of the cell cycle in the G1 phase since cell arrest

results in energy savings and reduced metabolism of carbon sources (Butler 2005; Vergara et al. 2014).

More recently, the possibility of controlling glycosylation by reducing the culture temperature has been reported (Spearman and Butler 2015). However, the outcomes of temperature reduction on glycosylation evolution are highly dependent on cell line and protein type thus explaining contradictory observations reported in the literature. Moreover, since the regulation of enzymes during the progress of glycosylation in the ER and Golgi is not well understood the effect of temperature on enzyme activity and the resulting glycosylation cannot be clearly elucidate (Butler 2005; Hossler et al. 2009; Stanley 2011).

Wang et al., (1991) investigated the effect of temperature on the residence time of proteins in the Golgi. Incubation of the cells under lower temperature conditions (21°C) resulted in decreasing flow rates of glycoproteins through the Golgi and longer exposure of the protein to glycosyltransferase enzymes. The glycoprotein incubated under the above conditions, had a higher percentage of N-acetyllactosamine in its structure (Wang et al., 1991). The effect of lower temperature conditions on the production rate and quality of EPO secreted by recombinant CHO cells was studied at 30, 33, and 37° C (Yoon et al. 2003). Reducing the culture temperature below 37° C increased the volumetric product titers and cell viability but hindered cell growth. The sialic acid content of EPO produced at lower temperature than 37º C remained at higher concentration until the late death phase of growth while it dropped significantly in the dead phase operated at 37° C.

In contrast to the aforementioned studies, reduction of terminal sialyation was reported at low temperature in some studies. As an example, the sialyation level of EPO-FC decreased by 20% and 40% at 33° C and 30° C, respectively. In this particular case, a correlation between increased specific productivity and reduced sialyation was suggested as the probable reason (Hossler et al. 2009). For CHO cells, the synergistic effects of low temperature operation (30º C) and cultivation under 0-5 mM sodium butyrate (NaBu) supplementation were investigated (Chen et al., 2011). In spite of longer cell viability in the presence of NaBu and lower temperature, the total sialic acid content of mAbs produced by CHO cells did not change. However, the researchers observed that the level of N-glycolylneuraminic acid (Neu5Gc), an uncommon form of sialic acid in human, was reduced by up to 10% under both NaBu or (and) low temperature conditions. They hypothesized that lower production of NADH due to lower consumption of glucose did not provide an optimum condition for activity of responsible enzymes for production of this type of sialic acid.

Temperature reduction was also found to reduce the aggregation of glycoproteins at higher protein productivity, while cell density was improved by perfusion culture (Rodriguez et al. 2010). In the perfusion operation, the aggregation of β-INF was reduced by 43% compared to batch operation, and the sialylation content of β-INF was improved as well. It has been reported that non-glycosylated β-INF had a higher level of aggregation comparing to glycosylated ones.

To ensure consistency in mAb quality, a thorough understanding of the relationship between cell metabolism, mAb synthesis and Fc-glycosylation is necessary.

➢ *Dissolve Oxygen Concentration*

The effect of oxygen on the growth and viability of cells has been observed in several studies (Restelli and Butler 2002; Butler 2006a). Also, the dissolved oxygen level (DO) has been shown to have a significant effect on the glycan profile of proteins. Chotigeat et al. (1994) reported that at higher levels of oxygen in CHO cell culture, the level of sialyation of recombinant proteins improved as a result of higher activity of sialyltransferases (Chotigeat et al. 1994).

The effect of DO on the galactosylation of the IgG produced by hybridoma cells has been investigated by Kunley et al., (1998). By reducing the level of oxygen in the culture, the glycan profile changed from digalctosylated (G2) at 30 % oxygen level to monogalctosylated (G1) and agalctosylated (G0) at 10% oxygen level (Kunkel et al. 1998).

➢ *Extracellular Degradation of Glycoprotein Oligosaccharides*

The presence of extracellular enzymes such as fucosidase, galactosidase and sialidase that may cause glycan degradation has been previously reported (Restelli and Butler 2002). The level of glycan degradation in the culture depends on several factors, including culture pH and temperature, time of glycans exposure to extracellular enzymes and their activities. In this regard, culture processes such as fed-batch and perfusion, that prolong the cell viability longer, may cause an increase in glycan degradations and glycan heterogeneity (Restelli and Butler 2002).

- ***Stirring Speed***

Adequate stirring of the culture is a key parameter for transferring sufficient nutrients to cells. However, excessive stirring may cause negative effects on cell viability, mAb productivity and mAb glycosylation (del Val et al. 2010). Senger et al. (2003) studied the effect of shear stress in suspension culture on glycosylation of the recombinant tissue-type plasminogen activator protein (r-tPA) produced by recombinant CHO cells. They reported that by increasing the stirring speed from 40 to 200 rpm, the level of partially galactosylated tPA increased from 31 to 72%. They proposed that at higher stirring speed, protein synthesis increases resulting in a reduced retention time of glycoproteins in the ER. This reduction in retention time negatively affects the N-glycan site occupancy (Senger and Karim 2003).

2.4.3 Modeling of The Extracellular environment

Metabolic analysis is helpful for in-depth understanding of mammalian cell metabolism and their intracellular physiology. Metabolic flux analysis (MFA) is a mathematical method that can be applied for quantitative studies of cell metabolism (Sanfeliu and Stephanopoulos 1999; Ahn and Antoniewicz 2012). It provides fundamental understanding about the metabolic pathways involved in the overall cellular metabolism by quantifying intracellular fluxes from measured metabolites' production or consumption rates. In the classical MFA approaches the flux analysis is based on the steady-state mass balance of intracellular species (Gao,et al., 2007; Naderi et al.,

2011). However, the steady state assumption may not be maintained in batch and fed-batch operations used for industrial production of biologics.

Recent research has focused on dynamic MFA models with the ability to reflect the culture variation during phase transition at different culture conditions (Naderi et al., 2011; Wahrheit, et al., 2013). Naderi et al., (2011) adjusted the metabolic changes of a CHO cell line by developing a kinetic model for growing and non-growing cells. A dynamic model of cell growth and metabolism for a CHO cell cultures was developed for different glutamine concentrations and feeding strategies in an attempt to understand the effects of glutamine on intracellular and extracellular fluxes (Wahrheit et al. 2013). These researchers observed a strong link between extracellular and intracellular availability of glutamine and specific metabolic pathways.

Glycosylation significantly affects the therapeutic characteristic of mAbs that can be influenced by many operational parameters. A mathematical model with the capability of correlating the mAb glycan profile to the cell culture conditions would be useful for bioprocess design and control, culture media formulation, and possible genetic engineering strategies (Del Val, et al., 2011).

Although several studies have been conducted to evaluate the effects of culture conditions on glycan profiles, including the impacts of particular nutrient concentrations such as glucose, glutamine, and galactose (Burleigh et al. 2011; Taschwer et al. 2012; Grainger and James 2013; Liu et al. 2014), culture supplementation and inhibitors such as ammonia (Yang and Butler 2002; Chen and Harcum 2006; Crowell et al. 2007), nucleotide sugar feeding (Gu and Wang 1998;

Wong et al. 2010) and, environmental pH and temperature alternation (Yoon et al. 2005; Ahn et al. 2008; Rodriguez et al. 2010; Seo et al. 2013), studies exploring how the combination of these factors affects the glycan profile are not numerous. Also, the numbers of mathematical models that connect these factors with the resulting glycoprofiles are quite limited. Earlier models focused on the reactions occurring in the Golgi complex but did not correlate these reactions to the extracellular culture conditions (Hossler et al., 2006; Del Val et al., 2011). For example, Del Val et al., (2011), presented a model of the N-glycosylation process occurring within the Golgi apparatus while considering the transport of nucleotide sugar donors from the cytosol to the Golgi lumen. However, this model was not coupled to the culture conditions (Del Val et al., 2011). Such coupling is essential because the process can be manipulated solely through these conditions. More recently, Jedrzejewki et al., (2014), extended their previous study and presented a model frame work connecting the extracellular conditions to the intracellular nucleotide sugar donors and glycosylation process for a mAb produced by a hybridoma cell line (Jedrzejewski et al. 2014). They developed a mechanistic nucleotide sugar network involving sixty metabolic reactions to connect the extracellular environment to the glycosylation process in the Golgi apparatus.

Chapter 3

Experimental Studies and Analysis Techniques

Some sections of the experimental methodology presented in this chapter are based on work published by Aghamohseni et al. (2014) and cited accordingly by permission of the *Journal of Biotechnology*. The thesis author's contributions to this publication were to conduct all the cell culture cultivations, experimental designs, amino acids, metabolites and mAbs assays and protein A purification and sampling preparation for the glycan analysis, the latter carried out by others at the university of Manitoba. The research work and journal paper preparation were conducted with direction from the project supervisors, who are co-authors of the aforementioned publication.

3.1 Cell Line

This study, used a transfected CHO (DUXB) cell line expressing a chimeric human-llama heavy chain monoclonal antibody (cHCAb) received from Yves Durocher, NRC, Montreal (Zhang et al. 2009), a member of MabNet (National Science and Engineering Research Council monoclonal antibody network (MabNet)). The produced mAb, EG2-hFc, contains a single N-linked glycan at Asn-297, a variable region of the heavy chain camelid (llama) antibody with a humanized Fc region attached at the hinge section. Its smaller size (~ 80 KD), longer serum half-life and distinctive tumor accumulation are comparable to that of human IgGs (~ 150 kD) (Bell et al. 2010). The cell line is adapted to grow in a serum-free medium and in suspension culture (Aghamohseni et al. 2014).

3.1.1 Initiation of Cell Culture

The cell vials of CHO (DUXB) were preserved in a liquid nitrogen tank. The frozen vials contained 1ml of cell suspension in a cryoprotectant medium at density 5×10^6 to 10×10^6 cells/ml. At the time of use, a frozen vial was recovered by rapid thawing in a 37˚C water bath while shaking for two minutes. Usually the water bath was sanitized with an anti-microbial reagent (such as Acryl AquaClean, WAK–Chemie) to prevent any microbial contamination. Then, the vial's contents were quickly transferred to 40 ml of pre-warmed BioGro-CHO medium

in an Erlenmeyer polycarbonate shake-flask (125 ml) with a vented cap. The BioGro-CHO medium was a serum-free medium optimized and provided by MabNet for this cell line.

Before cell inoculation, the flask containing the medium was kept in a humidified CO_2 incubator (Sanyo IR Sensor, 37 °C, 5 % CO2) for 15 minutes for pH and temperature adjustment. Then, the seed culture was placed on an orbital shaker at 120 rpm (MaxQ 2000 orbital shaker) in the humidified incubator for 24-48 hours. The cell concentrations and viability were determined by Trypan Blue staining and by counting the cells in a hemocytometer right after inoculation.

3.1.2 Cell Passaging and Maintenance

The average doubling time of CHO (DUXB) cells is approximately 16 hours, and depending on their rate of growth, cells are passaged 2 to 3 times a week. The maximum cell density during the maintenance period should not exceed $2.5x10^6$ cells/ml to maintain cells in the exponential growth phase and to prevent cell aggregation. Cell viability is not allowed to drop below 97 % during this maintenance period.

Based upon the cell density determination, a new subculture was prepared by diluting the cell suspension to $0.25x10^6$ cells/ml in the BioGro-CHO medium. After 48 hours, the cell density reached approximately $2x10^6$ cells/ml. Then, the culture was ready for the next passage.

All maintenance procedures were performed under aseptic conditions and in a laminar flow cabinet. To ensure conditions for optimal cell growth, the maintenance shake-flasks were changed every 10-14 days.

3.1.3 Cryogenic Preservation

For long-term storage of CHO (DUXB) cells and for the purpose of maintaining a cell bank reserve, cryogenic preservation of cells is necessary. For this reason, BioGro-CHO medium containing 8 % (v/v) DMSO (dimethyl sulphoxide) was prepared and stored at 4°C for use with the cells during freezing. The concentration of cells was determined after harvesting during their exponential growth phase when their viability was greater than 90%. Then, the cells were centrifuged at 300 g for 5 minutes, and the supernatant is decanted. The cell pellets were diluted by adding the freezing medium to obtain the final desired cell concentration (5×10^6 - 10×10^6 cells/ml). The prepared suspension was quickly subdivided into pre-labeled 1 ml cryo-vials which were placed overnight in a -80°C freezer. Then, the cryo-vials were transferred into a liquid nitrogen container on the following day.

3.2 Batch Culture

In the early stages of this research, we attempted to perform cell culture passage and maintenance in T-flasks, and then transferred them to spinners. In spite of substantial cell growth in the T-flasks, there was only very small growth in the suspension culture in spinners. Untreated T-flaks and Erlenmeyer shaker flasks were also used to eliminate the probable effect of Trypsin on growth. Trypsin is the enzyme that is routinely used for detaching attached cells from the T-flask surface. After numerous trials, the polycarbonate shaker flask was found to be the best option for maintaining sufficient growth in serum-free suspension.

The initial experiments were designed to assess the effect of essential nutrient concentrations on the glycan patterns of mAb. To that purpose, experiments were conducted for different initial levels of glucose and glutamine. These experiments were performed in a batch culture adapted to suspension growth in the shake-flask by the method described in section 3.1.2, in 500 ml flasks with 200 ml working volume and an initial cell density of $0.2x10^6$ cells/ml. The regular serum free BioGro-CHO medium was supplemented at the beginning of the cultures with different glucose (25 to 45 mM) and glutamine (0, 2, 4 and 8 mM) concentrations.

The flasks were placed on a 120 rpm shaker and incubated at 37°C and 5% CO2. The growth profile, extracellular glucose and amino acid-consumption as well as ammonia and lactate production were monitored over 10 days. Four ml of culture were removed every day, one ml for the immediate analysis of the viable cell concentration and viability index and the other three ml

for later analysis of glucose, amino acids, mAb, ammonia and lactate. Ten ml of samples were also removed every other day for glycan profile analysis. The samples were centrifuged at 1000 rpm for 10 minutes, and the supernatants were stored at -20˚C for further analysis. The analytical procedures are explained in section 3.3.

3.2.1 Reduced-pH Adjustment

pH changes were implemented only in the culture with 25 mM glucose and 4 mM glutamine concentrations (i.e., normal condition) that were found to be optimal for cell growth. Attempts for altering the pH at lower initial glutamine concentration and lower pH than 6.8±0.05 were not successful since the growth and mAb productivity were negligible for these conditions.

Two strategies were applied for manipulating the pH: i) maintaining the average pH of culture at 6.8±0.05 at the start of the batch operation - referred to hereafter as the Reduced-pH strategy - and ii) shifting the average pH to 6.8±0.05 at the time period of peak cell density - referred to hereafter as Shifted-pH strategy. Maintaining the average pH at 6.8±0.05 for reduced-pH and Shifted-pH cultures was achieved by daily additions of pre-determined amounts of 1 M lactic acid or HCl solutions calculated based on an a priori obtained calibration curve. These additions achieved a required pH level of 6.8±0.05 (Aghamohseni et al. 2014).

To provide complete CO2 equilibrium, the medium was incubated in 5 % CO2 and 37 ºC while shaking at 120 rpm for one hour before the experiments were carried out.

3.2.2 Reduced-Temperature Adjustment

Two strategies were applied for investigating the effect of temperature changes on cell metabolism and mAbs' glycosylation; i) maintaining the culture temperature at 33ºC from the start of the batch operation - referred to hereafter as the Reduced-Temperature strategy - and ii) shifting the temperature from 37ºC to 33ºC on day 3 of the exponential phase of growth - referred to hereafter as Shifted-Temperature strategy.

3.2.3 Specific Metabolites Production and Consumption Rates

The specific mAb productivity (Q_{mAb}) and production or consumption rates of metabolites (Q_{Met}) such as glucose, glutamine, lactate, ammonia and etc. were calculated from the slope of the linear regression of the cumulative mAb (C_{mAb}) or metabolite concentrations (C_{Met}) against the volumetric cell-hours (VCH) as proposed before (Dutton et al. 1999) according to the following equations.

$$VCH = \sum \frac{X_v(i+1) - X_v(i)}{\ln(X_v(i+1)/X_v(i)} \ (\triangle t) \qquad (3\text{-}1)$$

$$Q_{Mab/Met} = {}^{C_{Mab/Met}}/_{VCH} \qquad (3\text{-}2)$$

The volumetric productivity of mAbs, was calculated based on the equation presented by (Yoon et al. 2006) by dividing the mAbs' concentrations by the corresponding culture time.

$$Q_v = {}^{C_{Mab}}/_{time} \quad (3\text{-}3)$$

3.3 Analytical Procedures

3.3.1 Viable Cell Concentration and Viability Index

The Trypan Blue exclusion test was used to determine the number of viable and dead cells present in the suspension culture. This method is based on the principle that only live cells possess intact cell membranes that enable the exclusion of certain dyes such as Trypan Blue. One hundred µl of a cell suspension were taken and mixed well with the same volume of 5% Trypan Blue.

At higher levels of cell concentrations (greater than $5x10^5$ cells/ml) a higher level of cell dilution had to be used. After applying a drop of Trypan Blue cell mixture (approximately 10 µl) to a hemocytometer, the number of viable (unstained) and nonviable (stained) cells were counted under a microscope. Cells were counted within 3 to 5 min of mixing with Trypan Blue because

longer times were expected to result in viability reduction and cell death. The percentage of viable cells is calculated by the ratio of viable cells to the total cell number. Fifteen percent errors of analysis for viable cell counting by hemocytometer were calculated for triplicated samples.

A Moxi™ Z Mini automated cell counter, ORFLO Technologies was also applied as a second method of cell counting for comparison with the Trypan Blue method. The errors of analysis by the Moxi™ Z were less that hemocytometer equal to 5 % for triplicated samples.

3.3.2 Glucose, Glutamine, Lactate and Ammonia Assay

A multi-parameter bioanalytical system, BioProfile 400 (Nova Biomedical, Waltham, MA), was used to measure the glucose, glutamine, glutamate, lactate and ammonia concentrations in the culture (Aghamohseni et al. 2014). Five hundred µl of stored supernatants were purified by 0.2 µm filters prior to their injection into the device. In addition, an enzymatic glucose assay kit (K-GLUC, Megazyme, Ireland) was used for glucose analyses according to the company instruction as a backup method.

The Nova Biomedical Lactate Plus meter and the ammonia ion-selective electrode connected to a pH/ISE meter (model 710A of VWR) were utilized to analyze lactate and ammonia, respectively, as the backup methods for the measurements obtained with the BioProfile 400.

3.3.3 Amino acids Assay

In addition to glutamine other amino acids were analyzed according to the AccQ-Tag method, with a reverse phase C18 column using a Waters HPLC device (WATERS E 2695, Milford, MA) equipped with a UV detector (Waters 2489, Milford, MA) with amino acid standard (Sigma Aldrich AAS18 FLUKA) (Cohen et al. 1993; Aghamohseni et al. 2014). The errors in amino acid analysis were up to 10% as determined from triplicated samples.

3.3.4 Monoclonal Antibody Purification and Analysis

Protein A HP spin trap ^{TM} columns (GE Healthcare 28-9031-32) were used for purification of mAb prior to the glycan analysis, according to the manufacturer's instructions.

An enzyme-Linked Immunosorbent Assay (ELISA) method, developed by MabNet for Eg2-hFc, was used for monoclonal antibody analysis. According to the protocol, the 96-well flat-bottom high binding plate, Costar® HB was used for reading the optical density of each sample against the blank at 450 nm with a micro-plate reader (Aghamohseni et al. 2014).

Following this protocol, the anti-human IgG1 (Fc- specific) (Sigma Aldrich I2136) and the anti-human IgG (Fc- specific)-peroxidase antibody (Sigma Aldrich A0170), both produced in goats, were used as the primary and secondary antibodies, respectively, with 3,3',5,5'-

tetramethylbenzidine dihydrochloride (sigma T3405) as the substrate for the peroxidase. Samples were incubated at room temperature for 30 minutes immediately after adding the substrate solution to develop the complete color (Aghamohseni et al. 2014).

A dilution series of standard concentrated Eg2-hFc (provided by MabNet) was applied to find an appropriate standard curve. The mAb concentration was calculated by comparing the optical density of each sample with respect to the standard curve. The errors of ELISA for the replicated samples in the same plate were less than 5%. However errors reached a maximum value of 20% for independent tests performed at different days.

3.3.5 Glycan Analysis

Following release from the gel using sonication and desalting, the glycans were labelled with 2-aminobenzamide (2-AB) (Bigge et al. 1995). The glycans were analyzed by hydrophilic interaction liquid chromatography (HILIC) with fluorescent detection using a Waters X-Bridge 3.5 um amide column (4.6 x 250 mm) with the column heated to 30ºC and a flow rate of 0.86 ml/min. Then, they were eluted using 50 mM ammonium formate, pH 4.4: acetonitrile, starting with an initial ratio of 20:80, followed by a gradient to 50:50 over 48 minutes. Peaks were calibrated with a 2-AB labeled glucose ladder and glycan standards (Prozyme) (Guile et al., 1996) and compared to a glycan database (www.glycobase.nibrt.ie) for preliminary identification (Figure **1**). Further structural assignments were performed by exoglycosidase array analysis

(Royle et al. 2006) using sialidase A (recombinant from A. ureafaciens), bovine kidney α-fucosidase, bovine testis β-galactosidase, Jack Bean β-N-acetylhexoaminidase (Prozyme). Digested glycans were re-analyzed using HILIC analysis, and shifts of glycan GU values were compared (Aghamohseni et al. 2014) (Figure 2).

For this project, the database Glycobase (Campbell et a., 2008) was applied as a reference to predict the glycan structures based on their glucose unit (GU) values. The entire assay procedure was performed by the Department of Microbiology of University of Manitoba as part of the MAbNet project. Five percentage errors were calculated for overall glycan analysis based on the average differences in individual glycans RA% for the two duplicates.

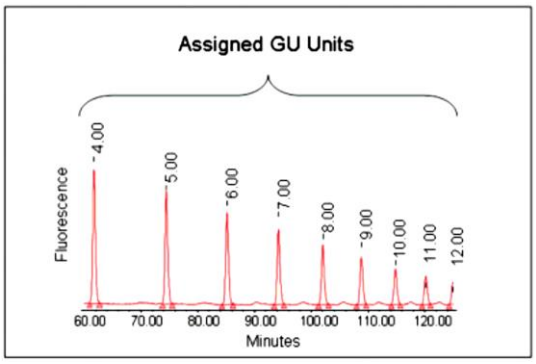

Figure 1, Normal phase HPLC elution times of dextran ladder with GU units assigned (Domann et al. 2007)

3.3.6 Glycosylation Indices

The predominant glycan structures found in EG2-hFc were complex biantennary fucosylated types with different amounts of terminal galactose and sialic acid. Regarding the occupancy of one, two or none of the available positions in the biantennary structures, G_i^1 (monogalactosylated), S_i^1 (monosialylated), G_i^2 (digalactosylated), S_i^2 (disialylated), G_i^0 (agalactosylated) and S_i^0 (asialylated) were found (Table 1). The glycan structures with lower relative abundance, RAs (less than 1%) were not considered, and their abundances were normalized to give a total area of 100%. In order to simplify the analysis of the results glycosylation indices were used to quantify the overall levels of galactosylation and sialylation. Accordingly, the RAs of each specific glycan were added together to calculate the galactosylation index (GI) and sialylation index (SI) as per the following equations:

$$GI = \frac{\sum G_i^2 + 0.5 \times \sum G_i^1}{\sum G_i^2 + \sum G_i^1 + \sum G_i^0} \quad (3\text{-}4)$$

$$SI = \frac{\sum S_i^2 + 0.5 \times \sum S_i^1}{\sum S_i^2 + \sum S_i^1 + \sum S_i^0} \quad (3\text{-}5)$$

The values of the indices were determined by considering all the glycan structures determined for EG2-hFc (Aghamohseni et al. 2014).

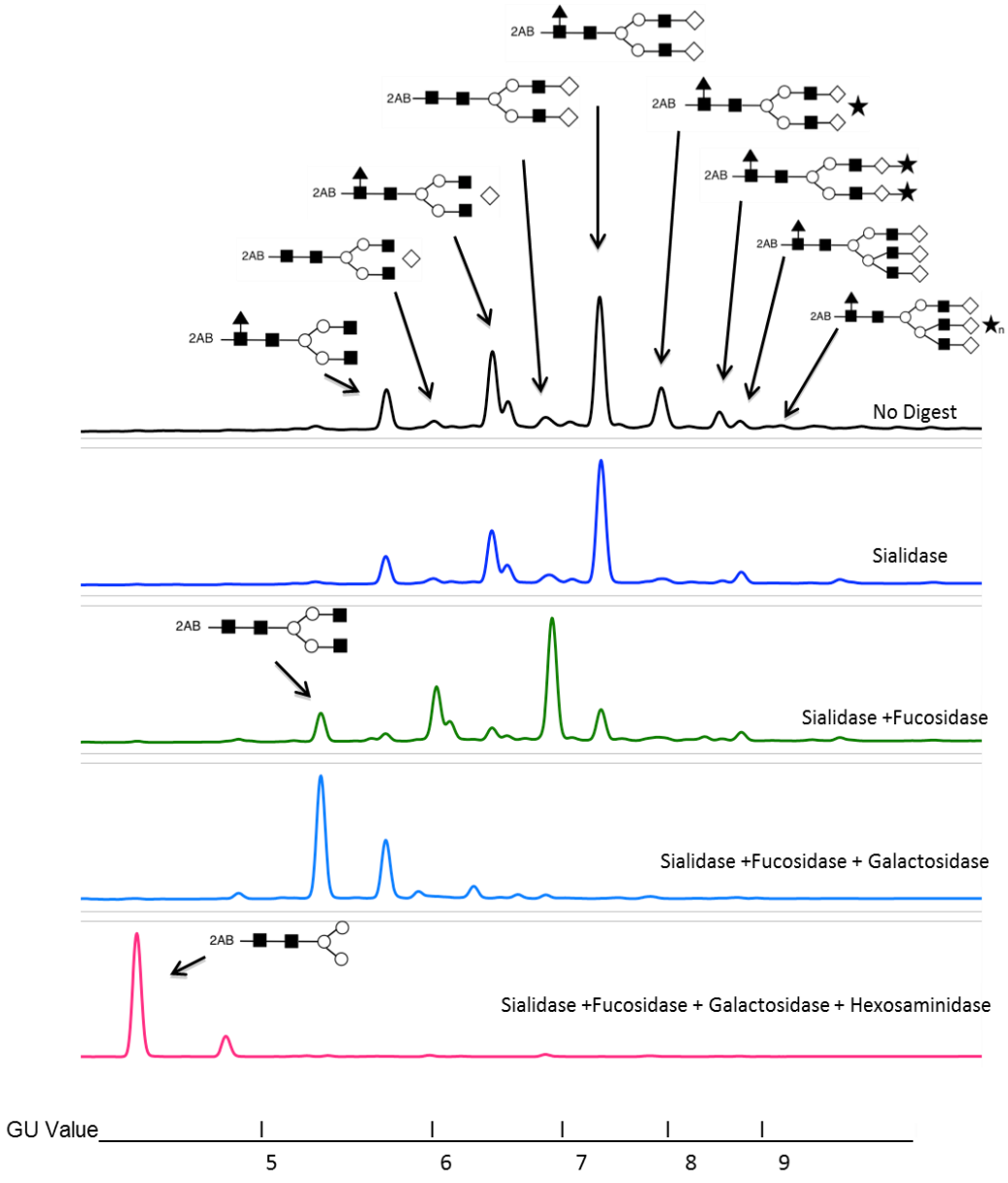

Figure 2, Structural assignments of the CHO-EG2 glycan were confirmed using shifts of GU values of major peaks using exoglycosidase digests : Sialidase (Sial), Sialidase A (recombinant from A. ureafaciens); fucosidase (Fuc), bovine kidney α-fucosidase; galactosidase (Gal), bovine testis β-galactosidase; hexosaminidase (Hex), Jack Bean β-N-acetylhexoaminidase (Aghamohseni et al. 2014)**.**

Table 1, Glycan structures of Eg2-hFc based on the Glycobase

Glycan name (Glycobase)	Glycan Structure
A2	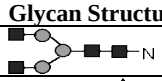
F(6)A2G0	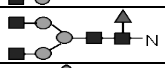
A1G1	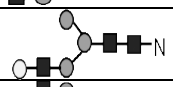
A2G1	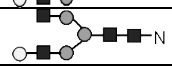
F(6)A2B	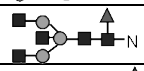
F(6)A1G1	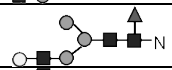
A2BG1	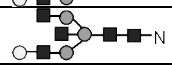
(6)A2 G1 Isomers	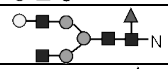
F(6)A2G1	
A2G2	
A2BG2	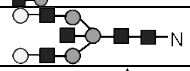
F(6)A2G2	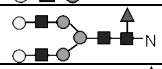
F(6)A2G2S1	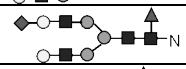
F(6)A2G2S2	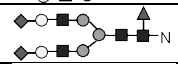
A4G3	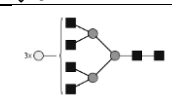
A4G4	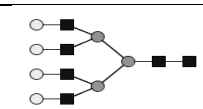
$A4G4S_n$	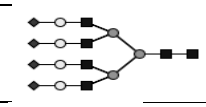
F(6)M2	
F(6)M3	
M3	

Chapter 4

Effects of Nutrient Levels and Average Culture pH

Materials presented in Chapter 4 are based on the published work by Aghamohseni et al. (2014) by permission of the *Journal of Biotechnology*. The thesis author's contributions to this publication were to conduct all the cell culture experiments, experimental design, metabolites and mAb assay, and sample preparation for glycan analysis at university of Manitoba. In Addition all plots and analysis of results were implemented by the first author. The other contributions are writing the final manuscript and respond to the comments of reviewers. This work and journal paper preparation was conducted with direction from the project supervisors who are co-authors on the publication (Aghamohseni et al. 2014).

4.1 Introduction

The key therapeutic properties of mAbs are strongly related to the post-translational process of glycosylation (Butler 2006a; Hossler et al. 2009). The complex process of glycosylation that occurs in eukaryotic cells involves several enzymatic reactions whereby oligosaccharide chains are added to the polypeptide through a complex series of reactions in the endoplasmic reticulum (ER) and the Golgi apparatus. In N-linked (asparagine-linked) glycosylation, the predominant type in animal cells, a high mannose oligosaccharide is transferred en block to asparagine residues from a lipid carrier molecule in the ER and they further processed and modified to add heterogeneity and complexity to the glycoforms.

The degree of glycosylation depends on general cell-culture conditions including the mode of culture operation, i.e. batch, fed-batch or continuous, temperature, pH, dissolved oxygen, pCO_2 and shear stress or changes in the specific culture variables including glucose, glutamine, ammonia, lactate and amino acids levels (Butler, 2006; Hossler, 2012).

Among the culture conditions that could affect the final glycan patterns, the nutrient levels and the concentrations of byproducts such as ammonia have been identified as very significant (Restelli and Butler, 2002 ; Yang and Butler, 2000). To achieve higher cell growth and productivity, mammalian cells need to be cultivated at the higher level of essential nutrients, mainly glucose and glutamine. However, the increased level of initial nutrients results in accumulation of cell metabolism byproducts, in particular lactate and ammonia, which in return

can result in lower cell densities and product titres (Nyberg et al., 1999; Taschwer et al., 2012;Yang and Butler, 2000).

Nutrient levels influence the final glycan profiles by changing the intracellular nucleotide sugar pools that are the precursors for oligosaccharide synthesis(Nyberg et al. 1999). For example, high levels of UDP–GlcNAc result in significant increase of antennarity and reduction of sialylation in baby hamster kidney (BHK) cells expressing IL-Mu6 glycoprotein (Valley et al. 1999) and for a CHO Epo-Fc fusion producer cell line (Taschwer et al. 2012).

High levels of ammonia also can result in lower glycosylation by perturbing the balance of the nucleotide sugar pool (Chen and Harcum, 2006 ; Gawlitzek et al., 1999). However, the reports regarding the effects of ammonia and pH on glycosylation are sometimes contradictory and may be highly dependent on the cell line, cultivation process and glycoprotein type (Raju et al., 2000; Butler, 2006 ; Chen and Harcum, 2006).

Our ultimate goal was defined to produce a descriptive model to assess the effects of nutrients, by-products and culture pH on the cell growth, mAb productivity and glycosylation progress that could be used for process optimization (Ohadi et al. 2013). Towards this objective the current study reports a combination of experiments and modeling results that were used to demonstrate and quantify impact of these parameters on the quality of the produced mAb under study.

To further understand the particular tradeoff between mAb productivity and glycosylation indices, the first objective of this study, was defined to reveal the relative correlation between

essential nutrients depletion and inhibitory effects of byproduct accumulation which have been demonstrated in this chapter. The sets of experimental designs are based glucose and glutamine concentration levels reported as the main energy sources biomass production and posttranslational process of glycosylation. The importance of this examination relates to fact that, the optimum nutrient conditions for cell growth are not always the same optimum conditions of cell productivity and protein quality.

4.2 Materials and Methods

4.2.1 Batch Condition and Experimental Design

Preliminary research comprised a set of batch cultures with different combinations of initial concentrations of glucose (25 and 45 mM) and glutamine (0, 2, 4 and 8 mM) Table 2. These experiments were performed in 500 ml polycarbonate vented-cap shaker flasks with a 200 ml working volume.

Depending on the desired initial nutrient concentration, appropriate amounts of concentrated glucose (Sigma G8644) and glutamine (Sigma 59202C) were added to the regular BioGro-CHO medium. To investigate glutamine-free and low glucose conditions, a special glutamine and glucose free BioGro medium was employed and glucose and/or glutamine were added as needed. The glucose and glutamine concentration in the regular BioGro-CHO medium are 25mM and 4-mM, respectively. All the set of experiments were performed in triplicate. The same seed culture

cultivated in regular BioGro-CHO was used for all batches as explained in section with 0.2 x 10^6 cells/ml inoculum concentration.

500 polycarbonate shaker flasks were used for each set of experiment and incubated in 37 ºC and 5 % incubator and 120 rpm shaker for ten days. Each set of samples run in duplicate except control (4 mM Gln, 25 mM Glc) which was triplicate.

Samples were taken according to the procedure mentioned in section 3-2 of Chapter 3 . Table 2 shows the preliminary experimental designs investigated for initial effect of glucose and glutamine.

Table 2, Experimental design for four initial glutamine concentrations at 25 mM glucose. Letter n, shows number of flakes in each set of experiment

	Glutamine (mM)				
Glucose (mM)		**0**	**2**	**4**	**8**
	25	**n=3**	**n=2**	**n=3**	**n=2**

4.2.2 Analysis

Viable cell density, viability index, metabolite profiles including lactate, ammonia, glucose, glutamine, mAb concentration and glycan analysis examined according to the techniques described in Chapter 3 section 3.3.

4.3 Results and discussion

4.3.1 Cell Density and Metabolite Profiles

- ***Glucose and Glutamine Depletion Effect***

The changes in viable cell density, glucose, glutamine, ammonia and lactate are presented in Figure 3, over the course of the cultures. The high initial level of glucose of 45 mM was found to inhibit cell growth as compared to lower initial glucose levels regardless of the glutamine level (data not shown). Therefore, all remaining experiments for different levels of glutamine were conducted with a glucose level of 25 mM that is recommended by the BioGro CHO suppliers. It should be noted that the culture with 0 mM initial glutamine in the medium is expected to contain some residual glutamine that was introduced with the inoculum.

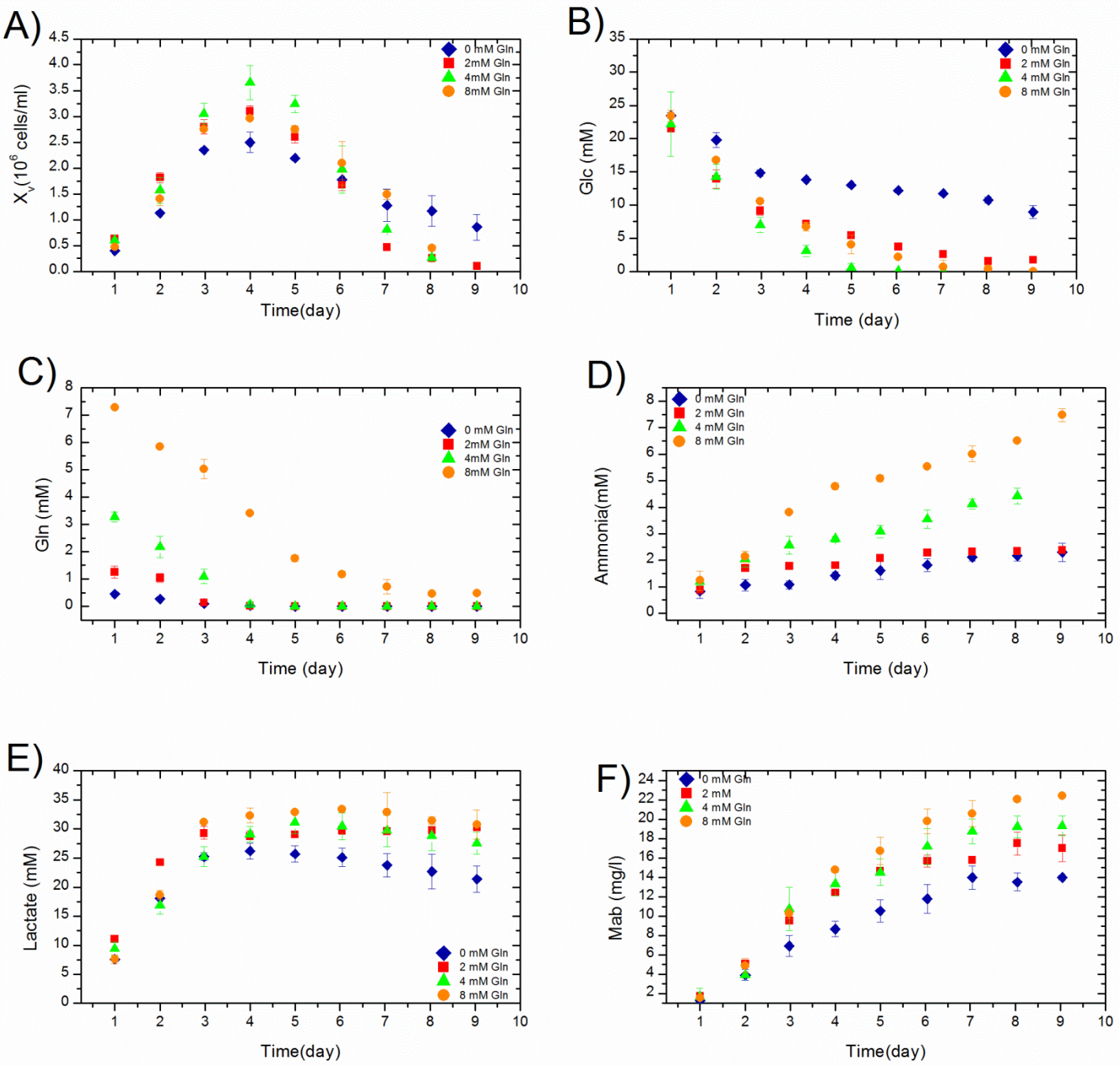

Figure 3, Viable cell density and metabolite profiles. Data points represent mean ± SD for two independent experiments except for experiments with initial 4 mM glutamine repeated three times. Closed symbols: ◆ 0 mM glutamine, ■ 2 mM glutamine, ▲ 4 mM glutamine, ● 8 mM glutamine. A) viable cell density; B) glucose consumption; C) glutamine consumption; D) ammonia accumulation; E) lactate accumulation; F) monoclonal antibody production.

The biomass time profile shows that this particular CHO cell line is relatively fast growing having a minimum generation time of approximately 16.5 hours and a lag phase time of less than 24 hours. The cell yield was dependent on the initial glutamine concentration and increasing the glutamine level from 0 to 4 mM resulted in a higher peak of cell density. Providing a higher level of glutamine at 8 mM partially inhibited the cell growth. Maximal viable cell density (approximately $3.6x10^6$ cells.ml^{-1}) was observed after four days of incubation at 4 mM of glutamine. In contrast, the maximum cell density was much lower when 2 mM or no glutamine was added to the medium with maximal cell density of 3.1 and $2.5x10^6$ cells.ml^{-1} respectively. It is also evident from their specific consumption rates that glucose and glutamine were co-metabolized (Table 3) as the consumption of glucose was faster in the presence of glutamine and slower in its absence. For example, for the culture with zero initial glutamine (Figure 3), glucose was depleted very slowly and some residual glucose remained towards the end of the culture while for the culture with initial glutamine level of 4 mM glucose was almost totally depleted after 5 days. On the other hand, a higher cell viability or prolonged life span was observed for the initial glutamine free culture (Figure 4-A). Glutamine was consumed rapidly in the exponential phase of cell growth and the peak of cell density coincided with the exhaustion of glutamine in the culture cultivated at initial glutamine level of 4 mM. Cultures containing 4 and 8 mM glutamine produce a higher level of lactate approximately 32 mM at the time that the maximum cell density was reached as compared with no initial glutamine experiment. Also, ammonia production was higher in the batches supplemented with higher initial glutamine reaching its

highest level of 7.5 mM at the end of the batch initiated with 8 mM glutamine. A lower peak of cell density was observed for the culture with initial 8 mM glutamine compared to the initial 4 mM glutamine experiment leading to the speculation that higher levels of ammonia result in cell death thus reducing the value of maximal cell density.

The specific mAb productivity (Q_{mAb}) was calculated from the slope of the linear regression of the cumulative mAb concentration against the volumetric cell-hours (VCH), equation 3-3 of chapter 3. Since the slopes were observed to decrease during the post-exponential phase as compared to the slopes in the exponential phase for different glutamine concentrations, it was concluded that the mAb productivity is partly growth associated. On the other hand, the slopes were not exactly zero during the post-exponential phase suggesting that some non-growth associated productivity also occurred. In the exponential phase of cell growth, the mAb productivity was found to be approximately 0.1 pg mAb $(cell.h)^{-1}$ and it dropped to 0.033 pg mAb $(cell.h)^{-1}$ in the post exponential phase for all the tested initial glutamine conditions. The mAb productivity in the culture with 8 mM glutamine initially reached a slightly higher amount at 0.045 pg mAb $(cell.h)^{-1}$ in the post exponential phase of cell growth.

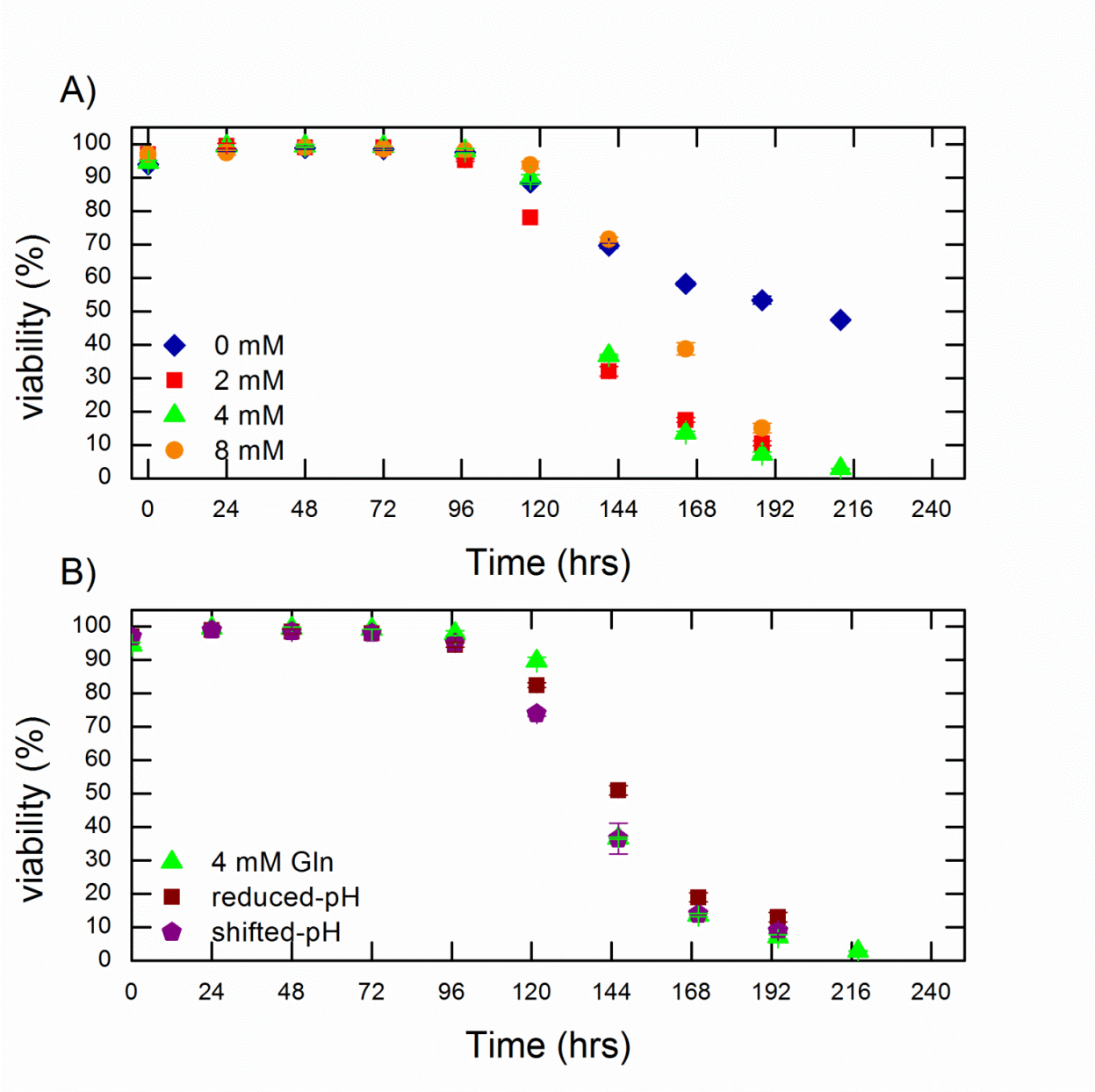

Figure 4, Cell viability profile. Data points represent mean ± SD for two independent experiments except for experiments with initial 4 mM glutamine repeated three times. Closed symbols: ◆ 0 mM glutamine, ■ 2 mM glutamine , ▲ 4 mM glutamine, , ● 8 mM glutamine, ■ reduced-pH (lactic acid), ⬟shifted-pH (lactic acid). A) Glutamine effect. B) pH effect.

Table 3, Specific glucose and glutamine consumption rates at different glutamine supplementation

Glutamine	Glucose Consumption rate (pmol/cell.hr)		Glutamine Consumption rate (pmol/cell.hr)	
	Exponential phase	Post- Exponential Phase	Exponential Phase	Post-Exponential Phase
0 mM	-0.15	-0.024	-0.004	0
2 mM	-0.15	-0.036	-0.011	0
4 mM	-0.2	-0.031	-0.027	0
8 mM	-0.2	-0.036	-0.029	-0.007

- ***pH Effect***

The objective of reducing the pH is that such reduction was expected to result in higher glycosylation. On the other hand the objective of shifting the pH only after reaching the cell density peak was to benefit from an increase in galactosylation and sialylation while preserving cell growth and mAb production mostly occurring during the exponential phase. For brevity the results of pH adjustment by HCl are shown in the Appendix A. The experimental results of viable cell density, glucose, glutamine and the byproduct accumulation of ammonia and lactate for the culture initiated with 4 mM glutamine and 25 mM glucose without pH reduction (control) were compared with the experiments of reduced-pH and shifted-pH conditions (Figure 5).

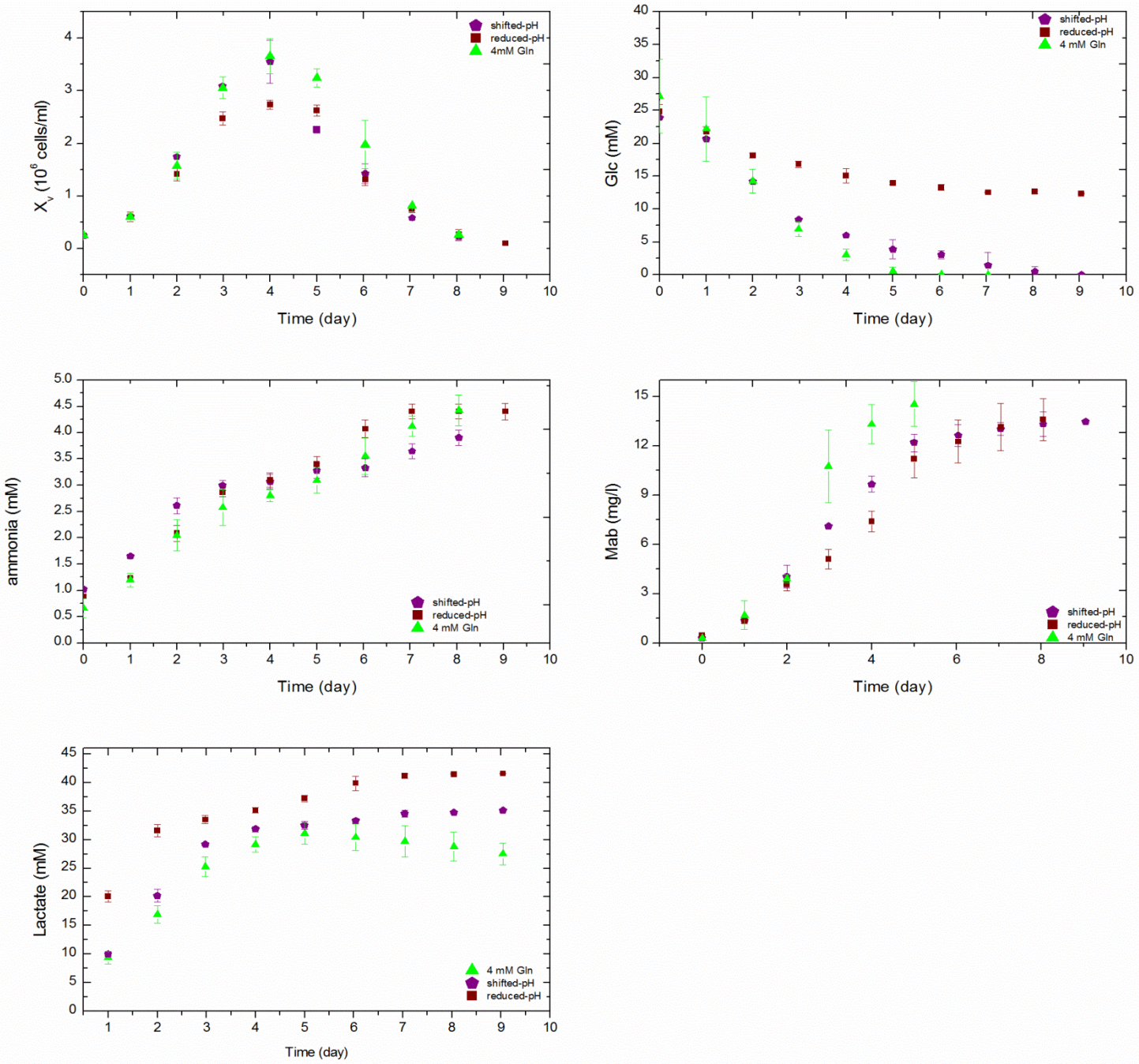

Figure 5, Viable cell density and metabolite profiles. Data points represent mean ± SD for two independent experiments except for experiments with initial 4 mM glutamine repeated three times. Closed symbols: ■ reduced-pH (lactic acid), ⬟ shifted-pH (lactic acid), ▲ 4 mM glutamine (Control). A) Viable cell density; B) glucose consumption; C) ammonia accumulation; D) monoclonal antibody production; E) Lactate accumulation.

Reducing the medium pH from 7.8± 0.05 to 6.8±0.05 along the entire culture duration resulted in lower cell growth and mAb productivity as compared to the culture without pH manipulation. Despite the fact that pH reduction was performed using lactic acid with the expectation of lactic acid being used as nutrient after glucose complete depletion, lactic acid accumulated in the culture and reduced cell growth due to non-optimal pH conditions. These findings differ from previous results that show that lactate can serve as nutrient in later stages of the culture and used as an effective method to reduce the ammonia production (Li, et al., 2012). The maximum peak of cell density with the reduced-pH operation was reached after 4 days of cultures with approximately $2.7x10^6$ cells.ml^{-1} which is significantly lower than the peak of $3.6x10^6$ cells.ml $^{-1}$ obtained for the control culture, also shown in Figure 5. The mAb productivity also decreased to 0.042 pg mAb (cell.hr)$^{-1}$ but it remained constant until the end of the culture. The shifted-pH cultures with the partial reduction of pH resulted in slight suppression of the cell growth and mAb productivity but cell growth was higher than for the culture operated with a lower pH from the start. Although reducing pH from the beginning of the culture had a negative impact on the cell growth and mAb productivity, it resulted in an almost three-fold lower rate of glucose consumption. This observation is relevant to glycosylation since glucose is correlated to the levels of nucleotide sugar pools (Liu et al. 2014). It is also noteworthy that ammonia levels were almost unchanged between the experiments with and without pH manipulation. This is important for the current study since the effect of pH changes on glycosylation has been previously assessed in the literature in cultures where these changes

were due to build-up or depletion of ammonia (Doyle and Butler 1990). Because in this case the external ammonia levels did not change, the results of pH experiments can be used to assess the effect of pH independent from the impact of ammonia levels.

4.3.2 Glycan Profiles

The predominant glycan structures determined in EG2-hFc mAb are predominantly fucosylated biantennary structures with different amounts of terminal galactose and sialic acid: agalactosylated (F(6)A2G0), monogalactosylated (F(6)A2G1) and digalactosylated (F(6)A2G2 , F(6)A2G2S1) oligosaccharides structures were identified based on the GU values from HILIC analysis compared to Glycobase 3.2 (NIBRT.ie) and verified with exoglycosidase digestions. Smaller amounts of other glycan structure were also identified: F(6)A1, A1G1, A2G1, F(6)A1G1, A2G2 and F(6)A2G2S2.

The time profiles for the observed dominant glycan structures for each batch at different glutamine levels and pH conditions are shown in Figure 6 and Figure 7, also the HILIC profile of glycans are provided in Appendix A. The glycosylation values at each day obtained from mAb supernatant samples represent a cumulative average of glycosylation from the start of the culture up to that day because the mAb is exposed to different glycosylation conditions at different times.

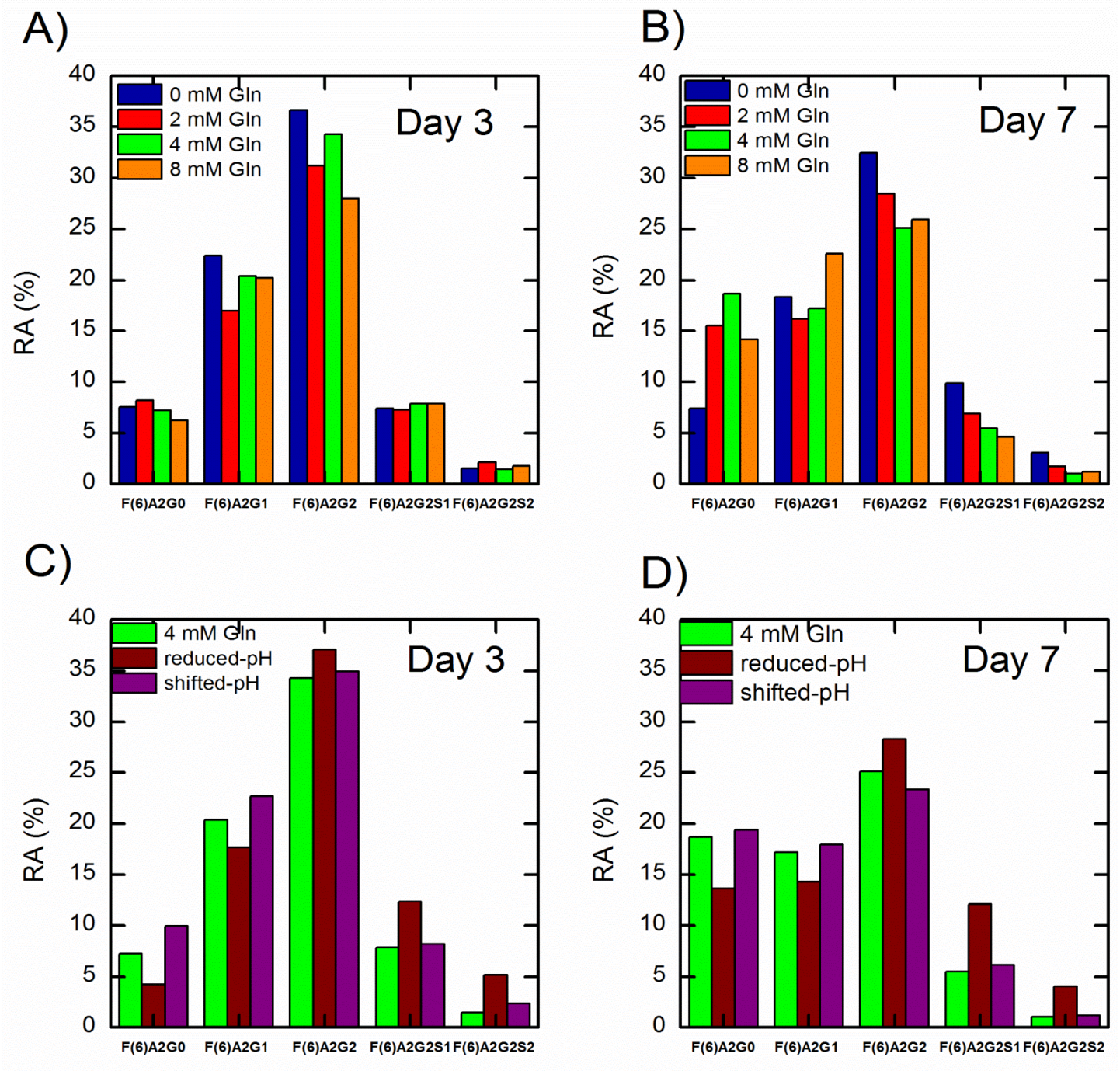

Figure 6, Individual glycans relative abundances (RA%) at different culture conditions. The error for F(6)A2G0, F(6)A2G1, F(6)A2G2 , F(6)A2G2S1, F(6)A2G2S2 are 1.42%, 0.79%, 0.56%, 1.17% and 0.11% respectively (100%=total area of glycans) which have been calculated based on a duplicated sample. A) Glutamine effect a day three, B) Glutamine effect at day seven, C) pH effect at day three, D) pH effect at day seven.

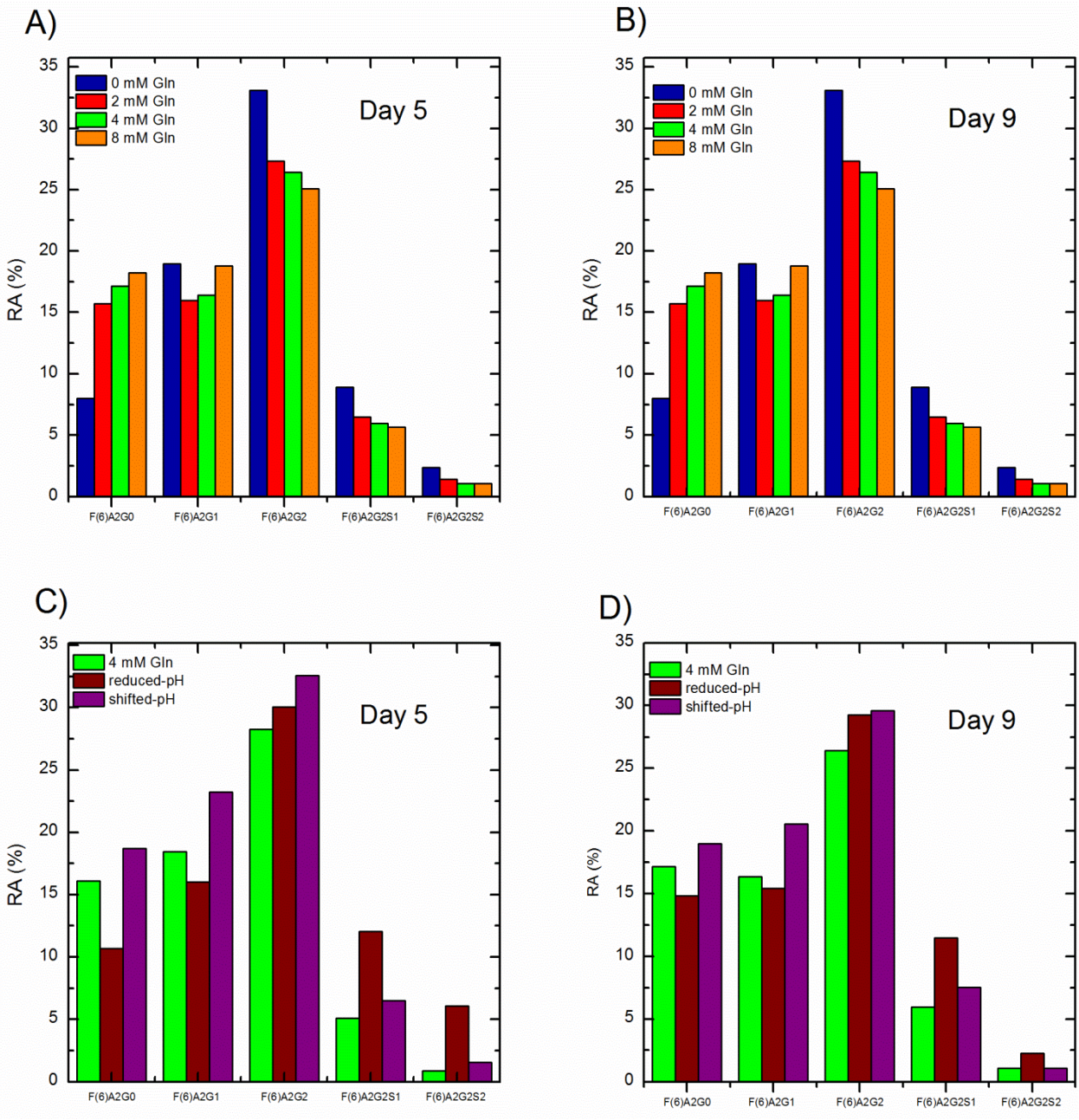

Figure 7, Individual glycans relative abundances (RA%) at different culture conditions. The error for F(6)A2G0, F(6)A2G1, F(6)A2G2, F(6)A2G2S1, F(6)A2G2S2 are 1.42%, 0.79%, 0.56%, 1.17% and 0.11% respectively (100%=total area of glycans) which have been calculated based on a duplicated sample. A) Glutamine effect a day three, B) Glutamine effect at day seven, C) pH effect at day three, D) pH effect at day seven.

According to Figure 6, the abundance of the agalactosylated glycan structure, F(6)A2G0, increased along the course of culture for all non-zero initial glutamine levels. In contrast, monogalactosylated glycan, F(6)A2G1 and digalactosylated structures, F(6)A2G2, F(6)A2G2S1 and F(6)A2G2S2 diminished temporally for all culture conditions except for the zero initial glutamine culture in which a slight increase in sialylation was observed. There was an exception for 8 mM culture in which the abundance of F(6)A2G1 increased form day 3 to day 7 but its value dropped again towards the end of day 9 (Figure 7). The decline of galactosylated glycans during the course of culture can be attributed to glucose reduction that influences nucleotide sugars availability for further galactosylation (Nyberg et al. 1999; Ohadi et al. 2013) and partly to the activity of glycosidase enzymes at lower cell viability in the post exponential phase of growth (Andersen and Goochee 1994).

Ammonia levels reached to 1.6 mM in culture without glutamine supplement at day 5 while with 2 and 4 mM initial glutamine the cultures reached higher ammonia concentrations of 3.1 and 5.1 mM respectively at the same day. These results might confirm a negative correlation between ammonia to sialylation and explaining the higher sialylation in the glutamine free culture. The pH in the culture with 4 mM of initial glutamine was slightly higher than the pH of the culture with 0 mM initial glutamine although the ammonia buildup was higher in the former culture as compared to the latter. This observation may be explained by the higher buildup of lactic acid (Figure 3) in the 4 mM glutamine culture as compared to the 0 mM glutamine culture following fast conversion of glucose to lactate. Thus, the experimental results suggest that

accumulation of ammonia should be avoided due to its negative impact on sialylation by, for example, operating the culture with lower or zero initial levels of glutamine.

Furthermore, the sensitivity of the cell line in terms of the impact of ammonia levels on glycosylation is higher than those reported in other studies (Yang and Butler 2000, 2002). For example, the culture started with 4 mM of glutamine reached a level of 3.1 mM of ammonia and exhibited 13% less RA of digalactosylated glycan as compared to the culture started with 0 mM of glutamine that reached a maximum of 1.6 mM of ammonia at day 5 of culture.

The effect of external pH on glycosylation is shown in Figure 7, C and D. The reduced-pH culture by lactic acid addition had a higher level of disialylated glycans than monosialylated and asialylated types. A similar impact of pH was observed in shifted-pH operation. It is important to notice that the ammonia concentrations for the cultures with or without pH manipulation resulted in almost identical levels of extracellular ammonia Figure 5.

Previous researchers have explained the effect of pH through the correlation of environmental pH levels with ammonia introduction into mitochondria (Doyle and Butler 1990; Schneider et al. 1996). However, in the current work pH and ammonia are not significantly correlated. Thus, the experiments with pH reduction can be used to elucidate the effect of pH independent from any effect associated with ammonia changes as shown later. pH reduction by HCl resulted in similar reduced growth and higher SI as with lactic acid but SI was lower that with lactic acid due to higher levels of ammonia (Appendix A).

4.3.3 Glycosylation Indices

The galactosylation and sialylation indices (GI and SI) were calculated according to the equations 3-4 and 3-5 defined in Chapter 3. Since improved therapeutic properties of mAbs are generally related to overall levels of sialylation and galactosylation (Butler 2006a) it is suggested that tracking the evolution of the process by monitoring the indices, can be a useful tool for further process improvement and optimization.

The time profiles of the indices for different initial glutamine concentrations are presented in Figure 8, A and B. The maximum GI was 0.74 and observed at the exponential phase of cell growth (day 3) of the culture supplemented with 0 mM and 4 mM glutamine.

To calculate the errors of GI and SI, a duplicates' analysis was done for day 7 of the culture with 4 mM glutamine and 25 mM glucose (control). The GI and SI values were calculated for each case and the error was then obtained based on the differences of final value of GI and SI between two cases. The errors for GI and SI were 0.5% and 0.9% respectively.

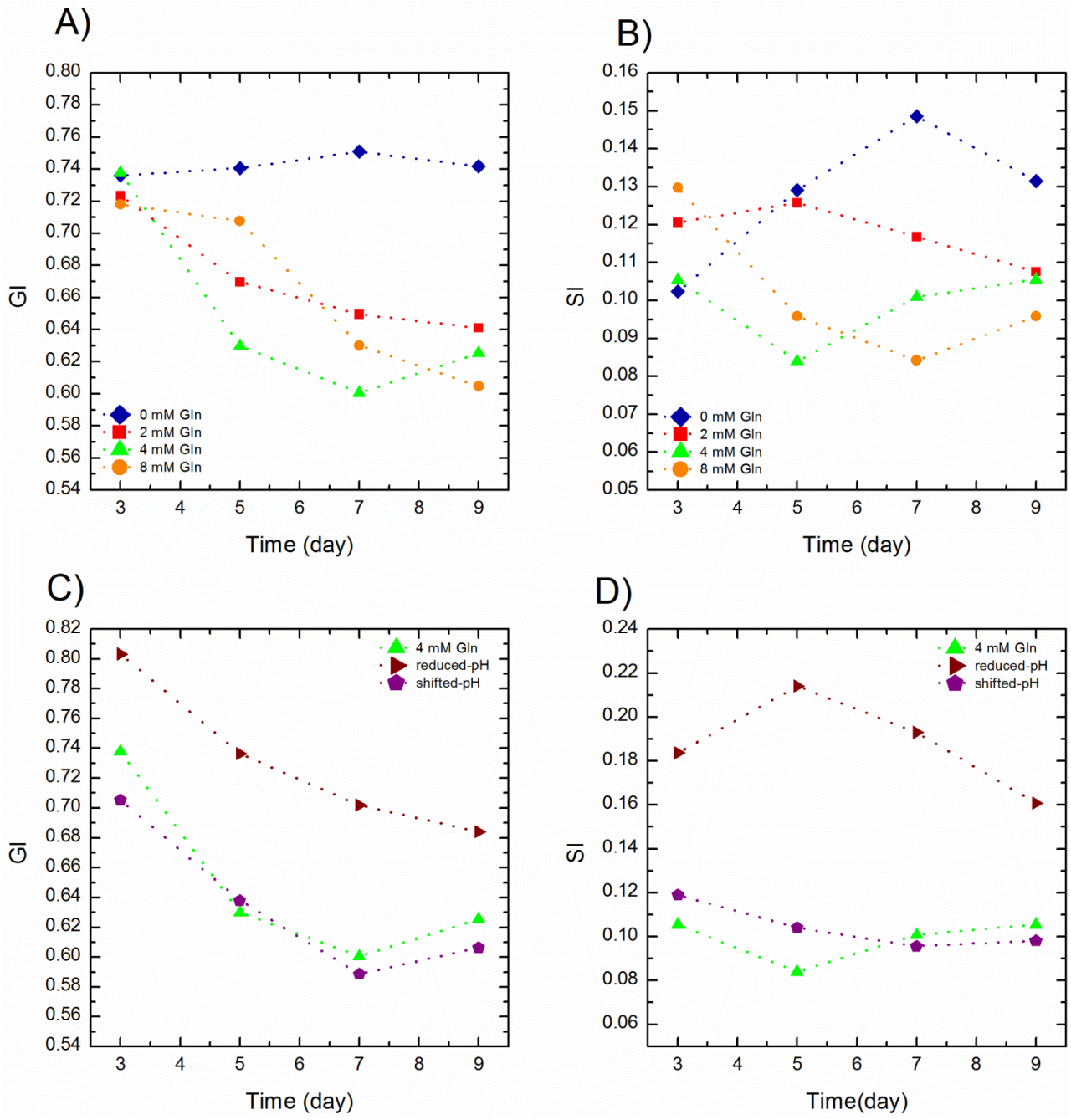

Figure 8, Galactosylation index, GI and sialylation index, SI at different culture conditions. The errors in the GI and SI index are 0.5% and 0.9% respectively which have been calculated based on a duplicated sample. ◆ 0 mM glutamine, ■2 mM glutamine , ▲4 mM glutamine, ● 8 mM glutamine, ▶reduced-pH (lactic acid),⬟ shifted-pH (lactic acid). A) GI and glutamine effect, B) SI and glutamine effect, C) GI and pH effect D) SI and pH effect.

GI variations were noticeable during the course of the culture for all experiments with nonzero initial glutamine levels. For the experiment with initial 4 mM of glutamine, the highest variation corresponded to a 15% decrease in GI between the exponential phase of cell growth (day 3) and the post exponential phase (day 5). For 0 mM glutamine culture, the GI level was 0.74 and stayed constant for the duration of the experiment. The consistent higher level of galactosylation in the 0 mM glutamine culture can be explained by lower consumption and higher availability of glucose when glutamine is not present due to the aforementioned co-metabolism mechanism between glutamine and glucose. For instance, for the culture with initial 4 mM glutamine the glucose was almost completely exhausted at the beginning of the post exponential phase (day 5) while 13 mM of glucose were still available for the culture with zero initial glutamine at the same day. These results suggest a correlation between the galactosylation level and glucose consumption rate (Ohadi et al. 2013; Liu et al. 2014).

In the culture with 0 mM glutamine slightly better sialylation was also observed (Figure 8, A). The SI level was 0.15 at day 7. In the cultures with higher initial glutamine levels, SI generally decreased over the culture. The 4 mM glutamine supplemented culture exhibited the lowest SI level at the post exponential phase (day 5) approximately 0.08 comparing to 0 and 2 mM glutamine supplemented cultures which had at least a SI of 0.12 by the same day. This reduction might be pertinent to higher ammonia in the culture initiated with 4 and 8 mM glutamine.

It is also worth mentioning that the SI range for EG2-hFc is low (0.08 to 0.2) compared to galactosylation (0.6 to 0.8). The sialic acid levels of commercial antibodies has been reported to be approximately 10% to be similar to the levels observed for in human antibodies (Raju et al. 2000). Therefore the EG2-hFc falls within the typical sialylation range for IgG. However, depending on the application achieving a higher level of sialylation might be of interest (Butler 2006a).

Figure 8, B and C, shows the effect of pH on GI and SI indices. Both GI and SI levels were higher in the reduced-pH culture. In the latter, the highest level of GI was 0.8 in the exponential phase (day 3) but its level dropped to 0.68 at the end of that culture indicating that the galactosylation was very low for the mAb produced during the post-exponential phase. However, the GI was still higher at the end of the culture as compared to the GI for the culture with the same initial concentration of glutamine but without pH reduction for which the GI was about 0.6. In the shifted-pH culture, similar GI and SI as compared to the culture where pH was not reduced (control) were observed. The maximum level of SI was observed in the reduced-pH culture at the beginning of the post exponential phase (day5) at approximately 0.21. The average SI was 0.19 as compared to the average SI observed for the culture without pH reduction which was 0.1.

4.4 Modeling of the glycosylation Process

The GLYCOVIS software (Hossler et al. 2006) was used to identify the most significant glycosylation pathways for the cell line under study. The program uses the amounts of the individual glycans as inputs. The code produces a graphical description of the glycosylation pathways where each pathway is described by a particular color corresponding to a specific range of glycan abundance in terms of percentages. For example, Figure 9 describes the pathways corresponding to the measured glycans at day 5 and 7 of the culture started with 0 and 4 mM glutamine and for the experiment where pH was reduced towards the end of the culture time (reduced-pH). The bold lines in Figure 9 correspond to the most significant pathways corresponding to the most abundant glycans levels measured along this pathway.

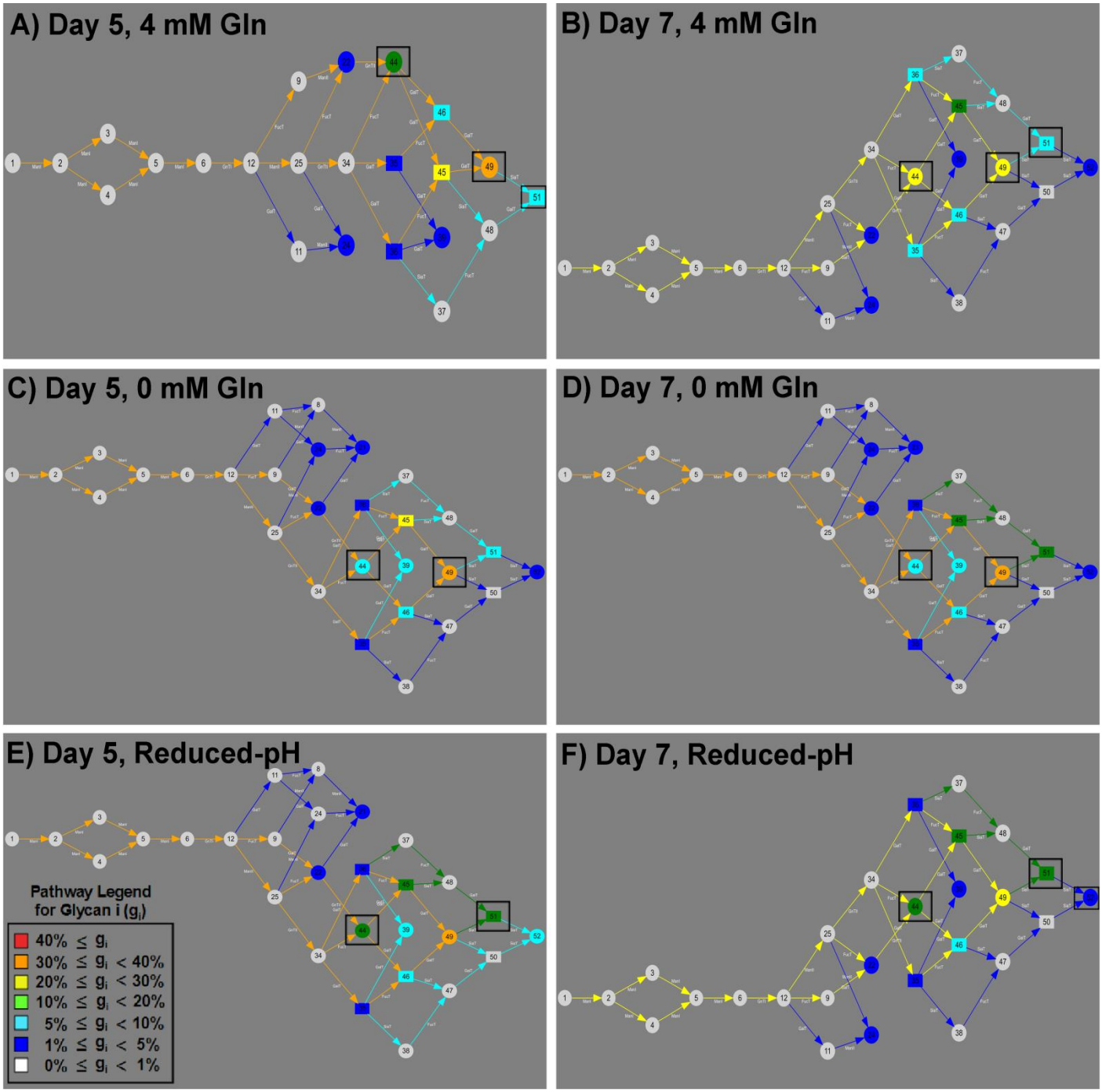

Figure 9, Glycan distribution network from GLYCOVIS at different days of batch cultures. Numbers indicates individual glycans and labels on arrows describe enzymes that trigger those specific reactions. G44 or F(6)A2G0, G45 and G46 or F(6)A2G1, G49 or F(6)A2G2, G51or F(6)A2G2S1, G52 or F(6)A2G2S2 . A) 4 mM Glc at day 5, B) 4 mM Gln at day 7, C) 0 mM Gln at day 5, D) 0 mM Gln at day 7, E) reduced-pH (lactic acid) at day 5, F) reduced-pH (lactic acid) at day 7.

The numbers in Figure 9, correspond to different glycans where the numbers in bold are glycans that were actually measured in the experiments whereas the others must occur as intermediates to enable the occurrence of the measured ones. The correspondence between the numbers and their chemical compositions was provided before (Hossler et al. 2006)

Similar GLYCOVIS plots were obtained for each day of a particular culture conducted in the current study. First, it was found that the pathways of significant reactions as well as glycans remained the same for all cultures. The only differences between the experiments were in terms of strengths (i.e. colors) of the pathways. For example, in day 5 of the culture with initial 4 mM glutamine the range of the most significant pathway (bold line) terminating in a digalctosylated glycan (glycan 49) is at 30-40% whereas in day 7 the same pathway is at 20-30%. For the initial zero glutamine culture for both days 5 and 7 the level of glycan 49 remained at 30-40% (Figure 9, A to D) thus explaining the overall higher galactosylation observed in the 0 mM glutamine as compared to the 4 mM glutamine culture. Beyond the identification of significant glycosylation pathways the results of GLYCOVIS in combination with the measured distribution of glycans abundances can be used to correlate the evolution of the glycosylation process with different culture conditions tested in the current work.

As it shown in Figure 9, A and C, agalactosylated glycan (Glycan 44) is higher in the 4 mM glutamine culture as compared to the 0 mM glutamine culture at day 5. A plausible reason is that UDP –GlcNAc, one of the precursors of glycan 44, increases with higher levels of ammonia as occurring in the culture with 4 mM glutamine as compared to the culture with initial 0 mM

glutamine. UDP –GlcNAc has been reported as a competitor for sialic acid transport (Valley et al. 1999; Butler 2006a) resulting in the lower observed sialylation for the 4 mM glutamine culture.

The lower level of galactosylation index observed for the 4 mM glutamine culture is that the reaction from glycan 44 to monogalctosylated isomer glycans (glycan 45 and 46) and then to digalctosylated glycan (glycan 49) cannot proceed forward due to unavailability of galactose pool resulting from early depletion of glucose by day 4. This is further corroborated by comparing the glycans distributions for day 7 (Figure 9, B and D).

When comparing the reduced-pH culture with 4 mM initial glutamine culture with normal pH levels (Figure 9, A, B, E and F) the distribution of glycans in day 5 indicates that the abundance of glycan 44 is similar for both cultures corroborating the correlation of this glycan with ammonia since in both cultures the ammonia levels are similar. On the other hand the abundances of glycans 51 (monosialylated glycan) and 52 (disialylated glycan), which corresponding reactions are regulated by sialyltransferase, are higher in the reduced pH culture. The higher observed activity in this pathway indicates an effect of pH on the activity of sialyltransferase (Borys et al. 1993).

Chapter 5

Effect of Mild Hypothermia

5.1 Introduction

Improvement of mammalian cell productivity have mostly focused on the use of fed-batch modes (Li et al. 2010; Naderi et al. 2011) and the optimization of cell culture media compositions (Butler 2005; Kim et al. 2013). Optimization of the cell culture's operating conditions plays a significant role in achieving higher productivity along with required quality in larger scale production. Among process parameters that can be optimized, temperature has been reported as a highly effective means for raising the mAbs' productivity (Trummer et al. 2006).

Applying mild hypothermia techniques has been reported as a feasible industrial solution (Chen et al. 2011; Vergara et al. 2014) that mostly leads to reduced cell growth, but longer cell life and cell productivity (Chen and Harcum 2006; Rodriguez et al. 2010; Vergara et al. 2014). Although, the benefits of reduced temperature have been utilized by several researchers, its mechanism on specific productivity enhancement has not been conclusively resolved. The mechanisms that were suggested to explain temperature effects on productivity include increased mRNA stability of recombinant proteins, improved transcription levels and cell cycle arrest in

the G1 phase that leads to energy savings and reduced consumption of carbon sources towards cell growth (Butler 2005; Vergara et al. 2014).

However, reducing the culture's temperature not only influences cell growth and protein expression but also influences the posttranslational process of glycosylation (Mason et al. 2014; Sou et al. 2014). The effects of mild hypothermia on glycosylation are highly dependent on cell line and protein type thus explaining the contradictory observations reported in the literature. Moreover, since the regulation of enzymes during the progress of glycosylation in the ER and Golgi are not well understood, the effect of temperature on enzyme activity and the resulting glycosylation have not been conclusively elucidated (Hossler et al. 2009; Stanley 2011). According to our previous observations (Chapters 5) (Aghamohseni et al. 2014), consistently higher glycosylation indices were obtained for two cases: i) glutamine-free cultures with resulting lower ammonia levels and higher availability of residual glucose and ii) in Reduced-pH conditions. However, it was also found for these two cases that productivity is negatively impacted thus leading to a tradeoff between productivity and glycosylation levels. This chapter explores the effects of mild hypothermia on both glycosylation and productivity to test whether there are similar tradeoffs between these two properties as obtained in the previous investigations with different levels of glutamine and culture pH. The results of this investigation were also used to further calibrate the mathematical model presented in Chapter 6.

5.2 Materials and Methods

5.2.1 Batch Conditions and Experimental Designs

According to the results presented in Chapter 4, at the medium level of glutamine (4 mM Gln) and 25 mM Glc, cell growth was higher. On the other hand, for glutamine-free conditions and 25 mM of glucose, higher levels of glycosylation indices were observed. Due to these competing outcomes, the effect of temperature manipulation was tested for only these two set of conditions to assess whether it is possible to obtain better tradeoffs between productivity and glycosylation.

Experiments were performed in 500 ml polycarbonate vented-cap shaker flasks with 200 ml working volumes. Each set of experiments was performed in triplicate.

The experimental design for this chapter is described in Table 4. The same seed culture cultivated in regular BioGro-CHO (4 mM Gln, 25 mM Glc) was used for all batches (Chapter 3 section 3.2), with 0.2 x 10^6 cells/ml inoculum concentration (Chapter 3, section 3.2).

Temperature adjustments were applied as per the steps explained in Chapter 3, section 3.2.1. Briefly, flasks with 0 and 4 mM Gln and 25 mM Glc were either kept in a 37ºC incubator through ten days of culture, to be referred to as "Reduced-Temperature" mode or transferred to a 33ºC incubator on day three after inoculation where cells were expected to still be in their exponential phase of growth, to be referred to as "Shifted-Temperature" mode. Two different incubators operated with two different temperature set points, 33ºC and 37ºC, were used to effect

the temperature changes. All flasks were maintained for a 10-12 days period during which the viability never dropped below 40%.

Table 4, Experimental design for temperature effects at two initial concentrations of glutamine and constant level of glucose (25 mM). The letter n, represents number of flasks in each set of experiments.

		Glutamine (mM)	
		0	**4**
Temperature	**Control (37ºC)**	**n=3**	**n=3**
	Reduced (33ºC)	**n=3**	**n=3**
	Shifted to 33ºC	**n=3**	**n=3**

5.2.2 Analysis

Samples were taken daily for analysis of viable cell density; viability index; metabolite profiles, including of lactate, ammonia, glucose, glutamine and mAbs concentrations. Since for the initial 3 days, mAb productivity was very low, samples for glycan analysis were taken every other day starting from day three when appropriate amounts of mAbs were produced. All the analyses were carried out according to the techniques explained in Chapter 3, section 3.3.

5.3 Results and Discussion

5.3.1 Cell Growth Characterization

- ***Temperature Effect and 4 mM Glutamine Condition***

The cell density profile and viability indices for cultures cultivated at 4 mM glutamine and mild hypothermia conditions are compared with a control (Figure 10). The control culture at 37ºC reached a higher peak of cell density $3.6x10^6$ cells/ml, at day four after inoculation. As for the Temperature-Shifted batch, for which the temperature was reduced from 37ºC to 33ºC on day 3, the cell density peak was lower as compared to the control and it occurred at day 3. Thus, cell growth dropped as soon as the temperature change was applied. However, for the shifted temperature culture, cells entered their predominantly death phase more slowly which, led to a higher viable cell density at day 7 of $1.4x10^6$ cells/ml as compared to the control, which reached $0.8x10^6$ cells/ml at that day.

The impact of lower temperature was even more evident when cells were cultured at 33ºC for the entire experiment (Reduced-Temperature mode). As shown in Figure 10 the cells exhibit a lag phase of more than 24 hours for this condition as compared to a much smaller lag phase for the control culture. The cell density peak was delayed to day 6 and the maximum cell density was 44% lower as compared to the control. The highest cell density observed for the Reduced-Temperature batch was $2x10^6$ cells/ml at day 6. Although at lower temperature the cells did not

reach the same viable cell density as shown in Figure 3, they stayed in the stationary phase for a longer time and consequently entered their dead phase later.

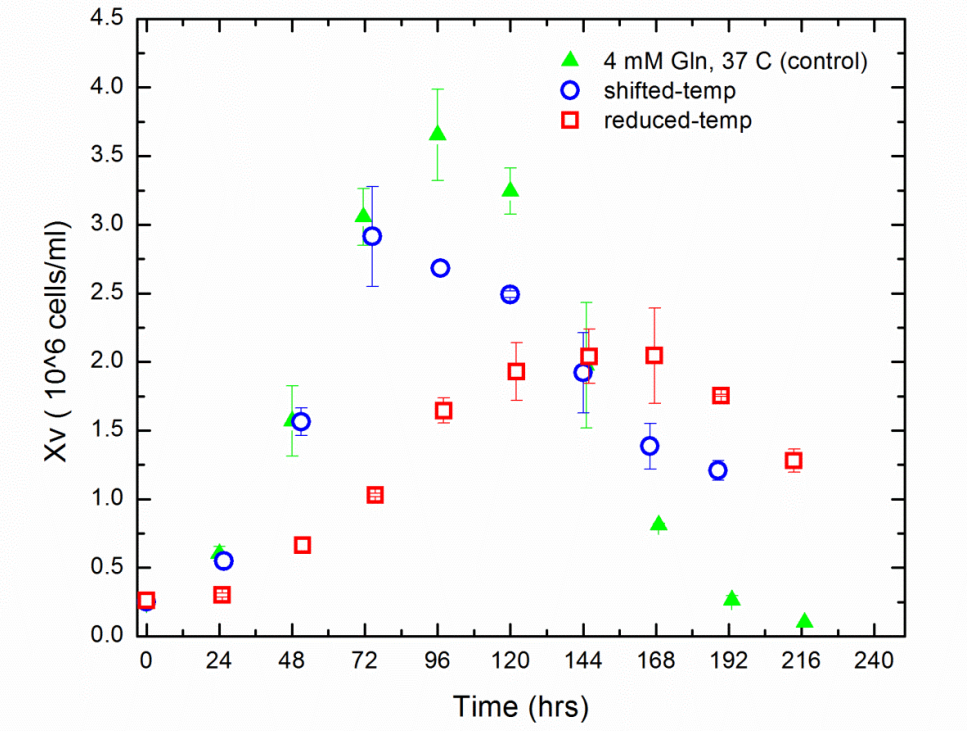

Figure 10, Time profile of total viable cell density of CHO cells cultivated at 4 mM glutamine and different temperature conditions. Data points represent mean ± SD for triplicate experiments. ▲ Control at 37ºC, ○ Shifted-Temperature and, □ Reduced-Temperature.

According to the Figure 11, the viability index of Reduced-Temperature stood above 90% until day 7 post inoculations, while for the control and Shifted-Temperature, this value was maintained for a shorter period of 5 days.

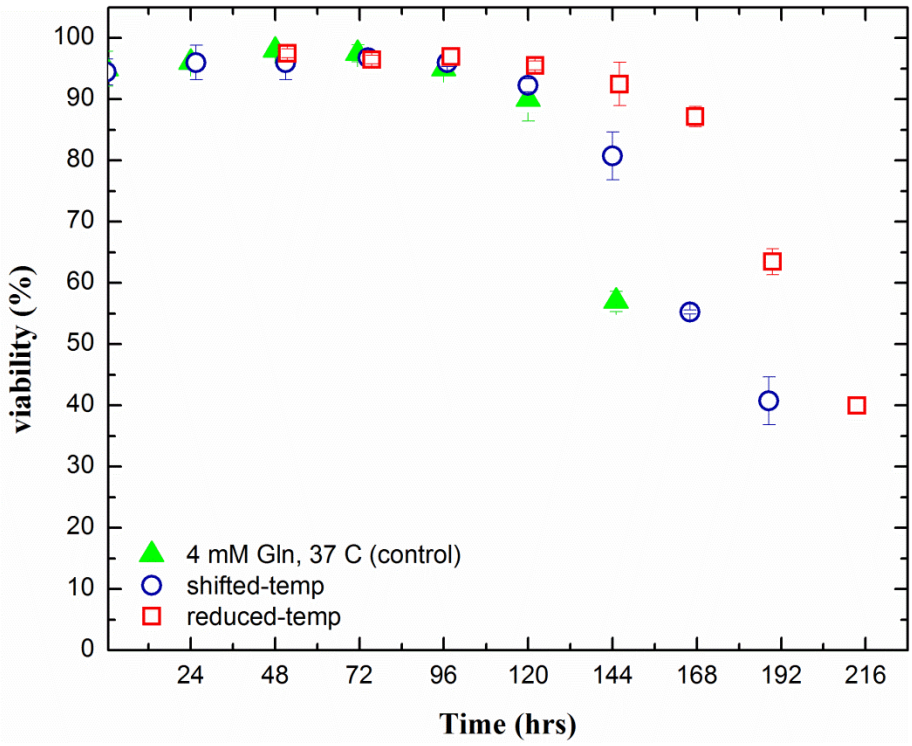

Figure 11, Time profile of viability index of CHO cells cultivated at 4 mM glutamine and different temperature conditions. Data points represent mean ± SD for triplicated experiments. ▲ Control at 37°C, ○ Shifted-Temperature and, □ Reduced-Temperature.

➢ *Temperature effect and Glutamine-Free Condition*

As shown in Chapter 4, glutamine is a key nutrient for cell growth of this cell line and, in a particular proportion with glucose (4 mM glutamine and 25 mM glucose), resulted in optimal cell growth. Thus, lack of glutamine was found to hinder the ability of cells to reach higher

viable cell densities. Figure 12, presents the time profiles of viable cells cultivated at different temperature settings without glutamine supplementation.

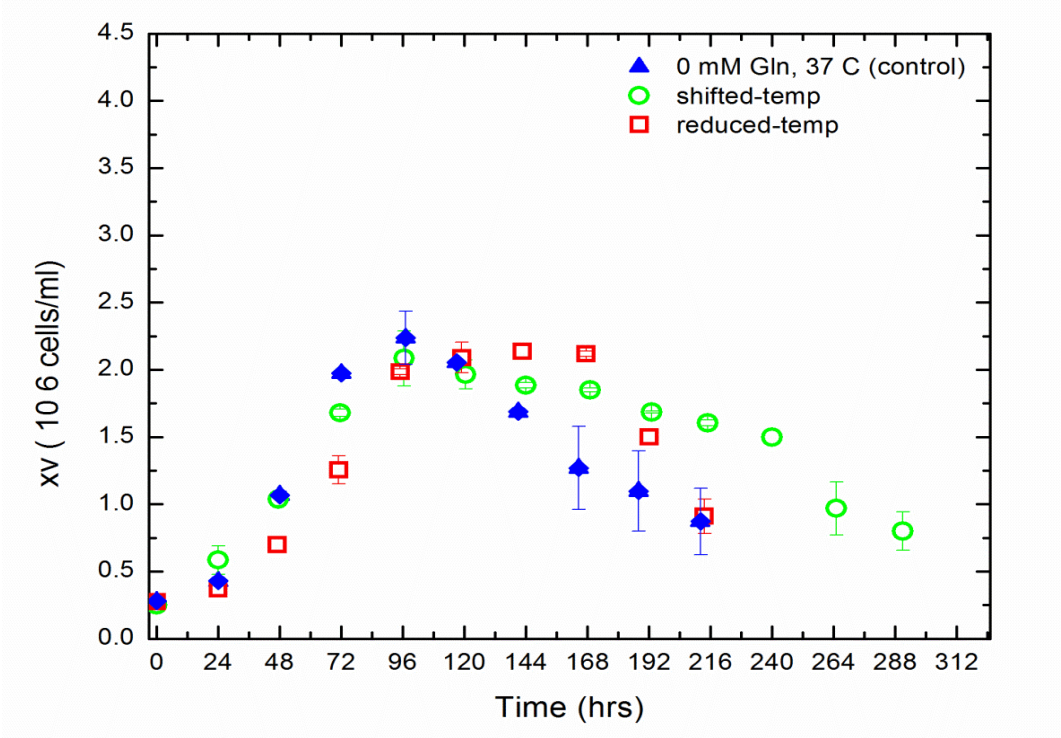

Figure 12, Time profile of total viable cell density of CHO cells cultivated at 0 mM glutamine and different temperature conditions. Data points represent mean ± SD for triplicated experiments. ◆ Control (37ºC), ○ Shifted-Temperature and, □ Reduced-Temperature.

The control (Glutamine-free and 37˚C) and Shifted-Temperature cultures both reached their peaks of cell density on day 4 of the culture with densities of 2.23±0.37 and 2.08±0.2 x 10^6 cells/ml, respectively while the peak of cell density for the Reduced-Temperature operation occurred on day 5 and it was equal to 2.09±0.11 x10^6 cells/ml. As for the 4 mM glutamine

culture, the rate of dead cells was slower at lower temperature conditions. The cell viability over 50% under the Shifted-Temperature condition increased to almost 12 days, which was a record value among all the experimental conditions investigated in the current research.

Overall, cells reacted to lower temperature more moderately under glutamine-free conditions as compared to cultures initially supplemented with glutamine. This observation can be explained by the fact that under glutamine starvation the specific growth rate was already low so the contribution of lower temperature to cell growth was less noticeable than for the cultures initiated with 4 mM glutamine.

The viability index profiles for glutamine-free batches at different temperature regimes are displayed in Figure 13. The viability index for both the Shifted-Temperature and Reduced-Temperature modes of operation remained above 90% until day 6 after inoculation, while for the control, this value started to drop on day 5.

Comparing of results of temperature effect with and without glutamine supplementation (Figure 10 and Figure 12) disclosed that the main effect of mild hypothermia on cell population was the reduction of specific growth rates and increasing the cell life. Table 5 summarizes the specific growth rates, μ (1/h), and death rates (negative values), during the exponential and post-exponential phases of growth. The reported values in the table were calculated based on the equation 3-1 and 3-2 presented in Chapter 3.

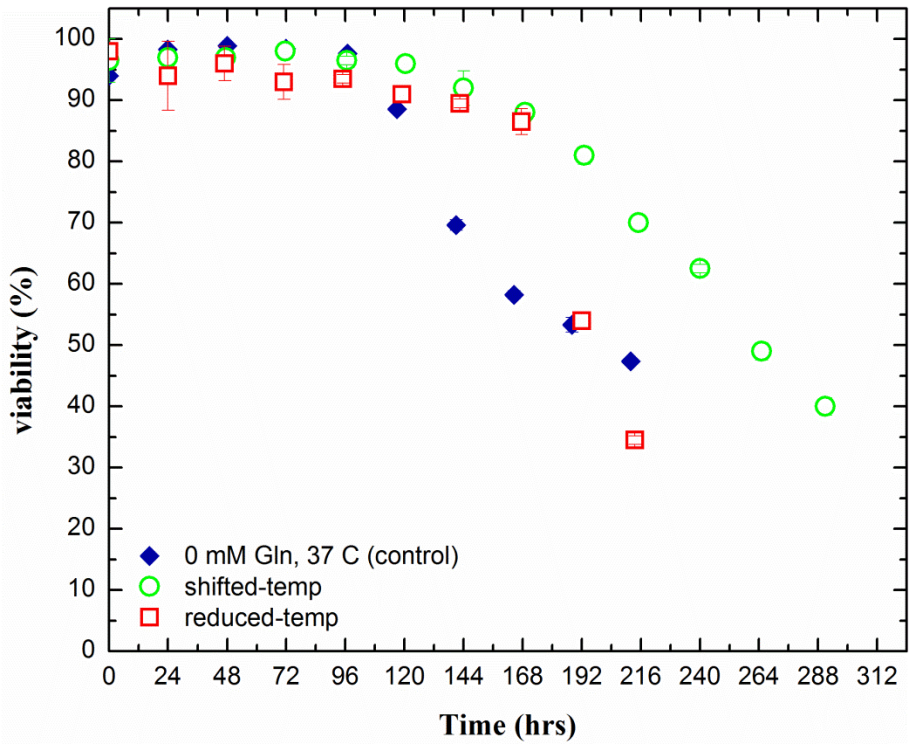

Figure 13, Time profile of viability index of CHO cells cultivated at 0 mM glutamine and different temperature conditions. Data points represent mean ± SD for triplicated experiments. ◆ Control (37ºC), ○ Shifted-Temperature and, □ Reduced-Temperature.

Achieving lower specific cell growths under reduced temperature conditions is in agreement with results reported in previous studies (Trummer et al. 2006; Mason et al. 2014; Vergara et al. 2014). However, it was observed in the current study that for glutamine supplemented cultures under the Reduced-Temperature regime the viable cell density could not reach the same levels as under control condition (4 mM Gln) even at the later days of cultivation, in contrast with previously reported results (Sureshkumar and Mutharasan 1991; Weidemann et al. 1994). On the other hand for the glutamine-free case under the Reduced-Temperature (Figure 12) mode of

operation the cell density reached 2.09±0.11 x10^6 cells/ml, almost the same value of the peak in density obtained for the control but with a delay of one day.

Table 5, Specific growth rate at mild hypothermia condition for cells cultivated at glutamine 4 mM and zero mM glutamine supplementation.

	Exponential phase of growth Specific growth rate (1/h)			**Post-exponential phase of growth Specific Death Rates (1/h)**		
Gln	Control (37˚C)	Shifted-Temp.	Reduced-Temp.	Control (37˚C)	Shifted-Temp.	Reduced-Temp.
4 mM	0.031	0.031	0.021	-0.03	-0.009	-0.006
0 mM	0.026	0.022	0.022	-0.01	-0.004	-0.008

As reported in Chapter 4, the specific growth rate was slower under glutamine-free conditions than in the 4 mM glutamine supplemented culture, regardless of the temperature levels. For both the Reduced-Temperature and Shifted-Temperature modes the specific growth rates were affected but to different extents for the glutamine supplemented and glutamine-free cultures. For example, with initial 4 mM glutamine, the culture under Shifted-Temperature regime had similar specific growth as the control (4 mM Gln and 37˚C), while under the Reduced-Temperature regime the specific growth dropped significantly by 32 % as compared to the control. Under glutamine-free condition, we observed almost the same specific growth rate

for the control, the Shifted-Temperature and the Reduced-Temperature conditions at the exponential phase of growth.

At the post exponential phase of growth (decline phase), for the 4 mM glutamine culture, the specific growth rate dropped by 70 % and 80 % for the Shifted-Temperature and the Reduced-Temperature regime respectively, compared to the control. Thus, for cultures initiated with 4 mM glutamine, the temperature reduction strategies reduced both the cell growth and death rate during both the exponential and post-exponential phases of growth. In contrast, for cultures initiated without glutamine, the lower temperature operation only decreased the death rates but did not affect the growth (Table 5). It was reported by (Wahrheit et al. 2013) that in the absent of glutamine, the latter is synthesize in the early stages of growth and it is consumed at the later stages of the culture. On the other hand, in the shifted temperature operation, the glucose consumption is lower in the post-exponential phase thus postponing the occurrence of cell death with increasing viability as shown in Figure 15 for glucose and Figure 12 for cell viability.

The observed longer cell viability for both glutamine-free and 4 mM glutamine cultures under the lower temperature conditions are in agreement with other studies (Moore et al. 1997; Yoon et al. 2005; Mason et al. 2014). In the current study, the culture operated under the Shifted-Temperature regime and without glutamine, exhibited a longer life span as compared to the Reduced-Temperature cultures with initial 4 mM Gln. In addition, the combination of glutamine-free and Shifting-Temperature conditions was found to be the most effective for extending the cell viability.

5.3.2 Extracellular Metabolite Profiles

➢ *Temperature Effect and 4 mM Glutamine Condition*

The extracellular metabolite concentrations were analyzed for all batches over a period of 10 to 12 days depending on the longevity of the culture. The time profiles of glutamine, glucose, lactate and ammonia at 4 mM Gln are shown in Figure 14.

Residual concentrations of glucose and glutamine were higher in both the Shifted-Temperature and Reduced-Temperature samples than those of the control. The control culture ran out of glucose on day 5, whereas for the Shifted-Temperature and Reduced-Temperature sufficient glucose (3.3±0.4 mM and 6.6±0.8, respectively), was left in the culture for sustaining growth.

Glutamine was consumed even faster than glucose. All the extracellular glutamine was consumed by day 3 for both the control and the Shifted- Temperature batches, while 2.5±0.3 mM glutamine was still left at that day in the Reduced-Temperature samples. In the latter, glutamine was exhausted only after 6 days of cultivation. This fact can be explained by the lower cell growth observed under mild hypothermia conditions, which led to preservation of glucose and glutamine in the culture.

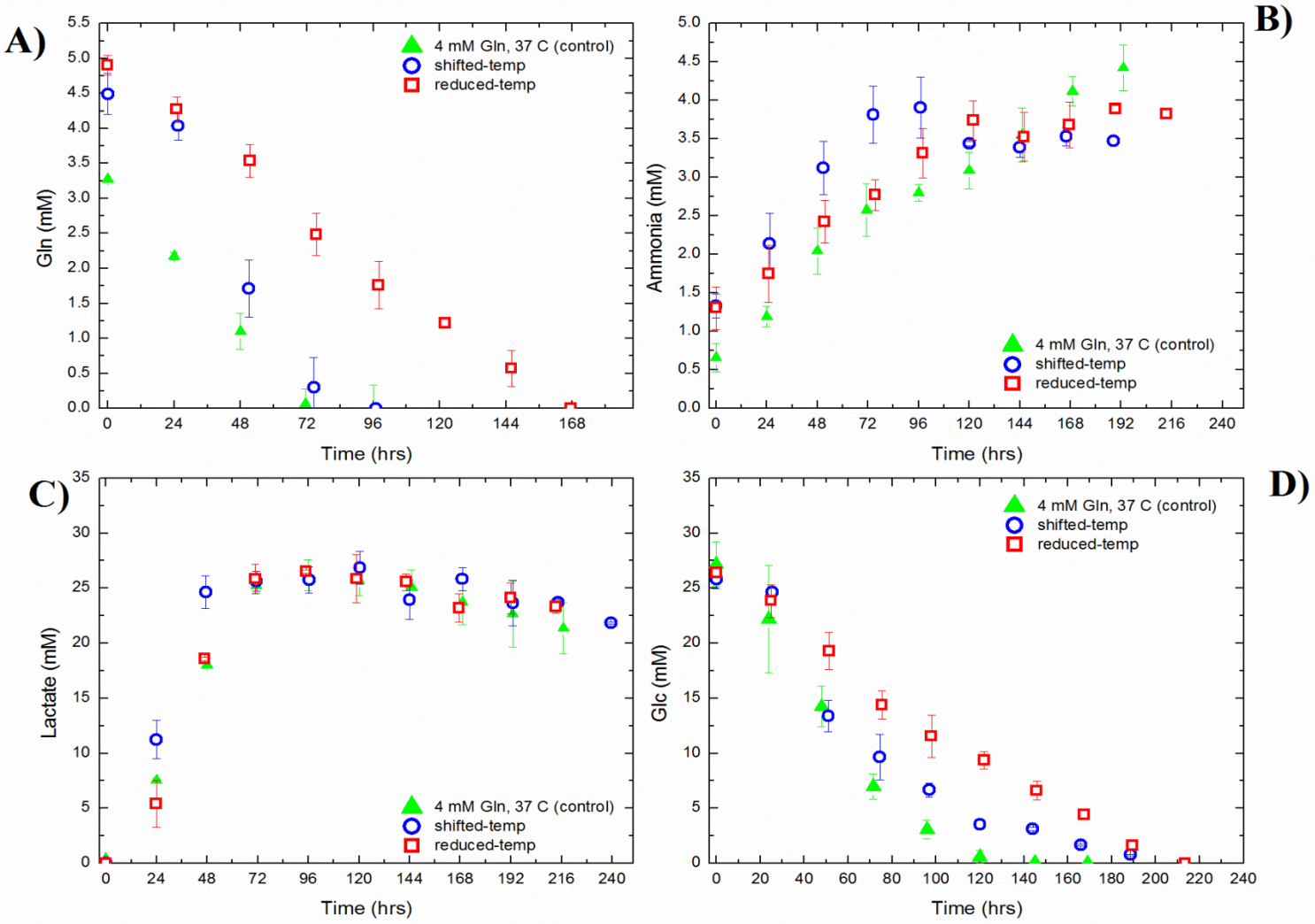

Figure 14, Metabolite profiles of mild hypothermia experiment at 4 mM Gln. Data points represent mean ± SD for triplicate experiments: ▲ Control at 37ºC, ○ Shifted-Temperature, and □ Reduced-Temperature. A) Glutamine (mM), B) ammonia, C) lactate (mM), D) glucose (mM).

Lactate profiles were very similar in all the experiments at the exponential phase. Lactate was produced at a higher rate during the exponential phase of growth and then it was consumed to a slight extent during the post–exponential phase. The maximum lactate production occurred on day 5 up to a value of 31±1.8 mM for all conditions and its levels dropped to 27.5±1.8 on day

9. However, the specific lactate consumption at the decline phase was not similar for Reduced-Temperature conditions. In the latter case, due to high availability of glucose, the used of lactate as an alternative carbon source was limited.

Ammonia accumulation followed a fairly similar pattern in all the experiments. The level of ammonia accumulation drops by almost 90% in the post-exponential phase of growth. The highest level of ammonia at day 9 after inoculation was 4.5±0.3 mM for the Control, 3.91±0.39 mM for Temperature-Shift and 3.89±0.06 for Reduced-Temperature samples.

➢ *Temperature Effect and Glutamine-Free Condition*

The time profiles of extracellular glucose, lactate and ammonia under glutamine-free condition are shown in Figure 15. Residual concentrations of glucose were similar in the exponential phase regardless of the type of experiment. However, the glucose levels continued to drop for both Shifted-Temperature and Reduced-Temperature operating modes because of the prolonged cell growth in the post-exponential phase. It is worth mentioning that due to measurement error, the Control flask was started with a slightly higher level of glucose (27 mM) as compared to 25 mM used in most experiments. However, it is unlikely that this relatively small error in initial glucose can explain that glucose residuals as high as 8±2.2 mM were observed towards the end of culturing.

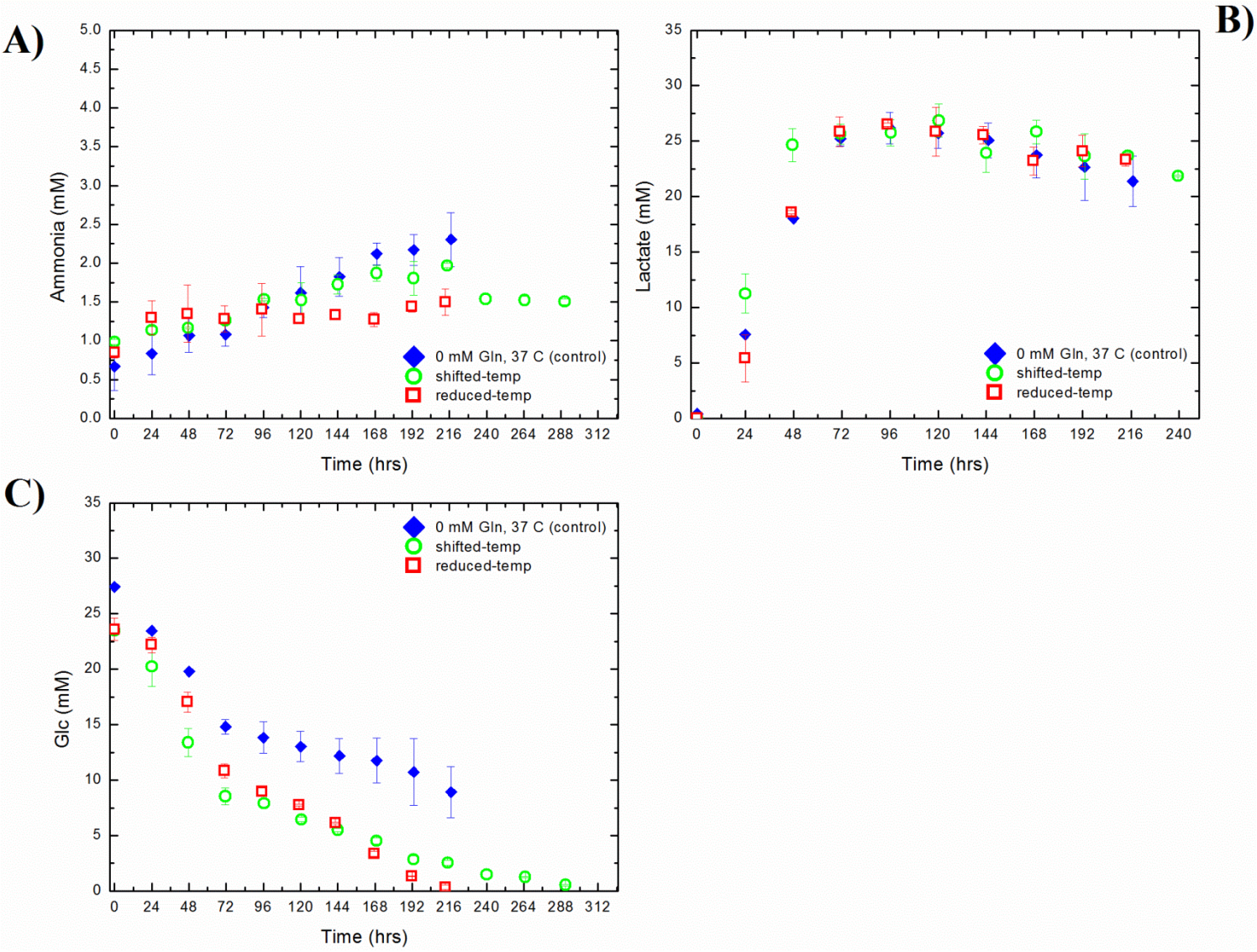

Figure 15, Metabolite profiles of mild hypothermia experiment at 0 mM Gln. Data points represent mean ± SD for triplicate experiments: ◆ Control at 37ºC, ○ Shifted-Temperature, and □ Reduced-Temperature. A) ammonia (mM), B) Lactate (mM), C) glucose (mM)

As for the 4 ml glutamine experiment, lactate was produced at a higher rate during the exponential phase of growth and then was consumed to a slight extent during the post–exponential phase under all conditions. Similar to 4 mM glutamine conditions, lactate

consumption was lower at the lower temperature experiments. The maximum concentrations of lactate were 26.19± 1.41 mM on day 4 for the Control, 26.85±1.48 mM on day 5 for the Shifted-Temperature experiment and 25.85±2.19 mM on day 5 for the Reduced-Temperature experiment. The minimum levels of lactate towards the end of the post-exponential phase were 23.7±0.28 mM.

For the Reduced-Temperature experiment without glutamine supplementation, ammonia initially accumulated and then stayed at the same level of 1.35±0.08 mM, for the entire 9 days of incubation, in contrast to the cultures started with 4 mM glutamine environment where ammonia accumulated for the entire duration of the culture. Also, in the absence of glutamine, ammonia levels increased to 2.3±0.34 mM and 1.97±0.028 mM for the Control and the Shifted-Temperature samples respectively. Thus, for glutamine-free cultures, cells still produced ammonia by metabolizing amino acids other than glutamine (Wahrheit et al. 2013).

The specific production and consumption rates of metabolites under mild hypothermia condition have been calculated based on equations 3-1 and 3-2 and are presented in Table 6. For both 0 mM and 4 mM glutamine condition, reducing the temperature did not affect the specific glucose and glutamine uptake rate significantly. As the specific growth rate was also lower compared to the control condition at mild hypothermia (Table 5), glucose and glutamine were consumed in a larger degree towards protein production relative to cell growth as compared to the operation at normal temperatures. The results of the protein production details are presented later in section 5.3.3. In addition, our observation indicates that in the absence of initial

glutamine similar metabolic pathways are used for synthesis of intracellular glutamine regardless of the temperature conditions.

Table 6, Specific consumption and production rates of metabolites at mild hypothermia and 4 mM glutamine a), mild hypothermia and glutamine-free b).

a) Specific Consumption and Production Rates of Metabolites (pmol/cell.h)

Mild Hypothermia and 4 mM Glutamine

	Exponential phase of growth			Post-exponential phase of growth		
	Control (37˚C)	Shifted-Temp.	Reduced-Temp.	Control (37˚C)	Shifted-Temp.	Reduced-Temp.
Glc	-0.2	-0.2	-0.25	-0.04	-0.04	-0.05
Gln	-0.03	-0.03	-0.04	0	0	-0.013
lac	0.19	0.17	0.2	-0.01	-0.01	-0.003
NH_4	0.02	0.02	0.02	0.003	0	0.001

b) Specific Consumption and Production Rates of Metabolites (pmol/cell.h)

Mild Hypothermia and Glutamine-Free

	Exponential phase of growth			***Post-exponential phase of growth***		
	Control (37˚C)	Shifted-Temp.	Reduced-Temp.	Control (37˚C)	Shifted-Temp.	Reduced-Temp.
Glc	-0.15	-0.18	-0.17	-0.024	-0.023	-0.04
lac	0.51	0.52	0.55	-0.026	-0.015	-0.015
NH_4	0.005	0.003	0.0004	0.005	0.003 -0.001	0.0004

As explained in the Chapter 4, in batches with glutamine supplementation, glucose consumption rate was higher than glutamine-free due to co-metabolism of glucose and glutamine in this cell line. In terms of carbon catabolism under low hypothermia conditions the findings in the literature are somewhat contradictory. For example, Vergara et al (2014) showed that the glucose consumption rate was not affected by lowering the temperature to 33ºC in a process producing a plasminogen activator by CHO cells. On the other hand, Yoon et al (Yoon et al. 2005) showed that glucose and glutamine were consumed at a slower rate at 32.5 ºC as compared to a process of EPO production by CHO cells where lower temperatures did not affect the glucose consumption rate.

Regardless of the initial level of glutamine, lactate production was not affected by the lower temperature strategies. However its consumption reduced in the decline phase due to a higher availability of glucose as the main carbon source at low temperature conditions for cell growth and metabolism. Specific ammonia accumulation was higher in the exponential phase of growth for all conditions and significantly decreased in the decline phase. In the glutamine free condition the rate of ammonia formation was lower as compare to the batches initiated with glutamine concentration. This fact can be explained by the utilization of ammonia for glutamine synthesis (Wahrheit et al. 2013).

5.3.3 mAb' Profiles, Specific and Volumetric Productivity

- ***Temperature Effect and 4 mM Glutamine Condition***

Figure 16, a-b presents the mAb concentration profile and specific productivity, Q_p, for cultures cultivated at 4 mM glutamine under mild hypothermia and control conditions. The concentration of mAbs was found to monotonically increase under Reduced-Temperature conditions throughout the culture while for the Control and Shifted-Temperature samples, the mAb concentration decreased during the post exponential phase of growth. The maximum concentration of mAb at day 9 of cultivation reached 41.5±3.8 mg/l for Reduced-Temperature, 25.8±3.9 mg/l for Shifted-Temperature and 19.3±1 mg/l for the control samples. .

The mAb concentration as a function of the time integral values of viable cell growth (equation 3-2) is presented in Figure 16-b. The specific productivity can be inferred from the slopes of this figure according to (equation 3-2). The slope values are summarized in Table 7 for the exponential and post-exponential phases of growth. For both the Shifted-Temperature and the Control cultures, the slope of mAb productivity dropped in the post exponential phase of growth. However, this drop was not observed under mild hypothermia as compared to the control experiment.

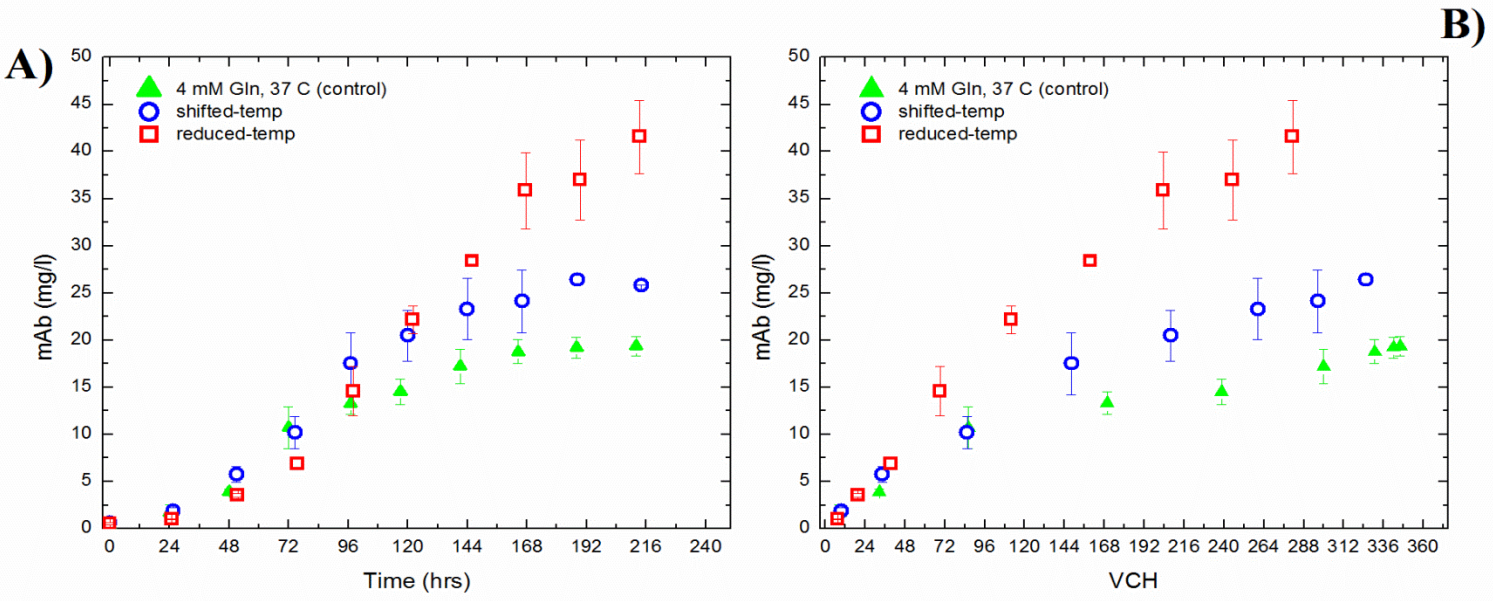

Figure 16, mAbs profiles and mAbs specific productivity of mild hypothermia experiment at 4 mM Gln. Data points represent mean ± SD for triplicate experiments: ▲ Control at 37ºC, ○ Shifted-Temperature and, □ Reduced-Temperature. mAbs' concentration vs time A); mAbs' concentrations vs volumetric cell hours (VCH) B).

Table 7, Specific mAb productivity under mild-hypothermia conditions at exponential and post exponential phase of growth,

Specific mAb Productivity (pg/cell.h)						
	Exponential phase of growth			Post-exponential phase of growth		
Gln	Control (37˚C)	Shifted-Temp.	Reduced-Temp.	Control (37˚C)	Shifted-Temp.	Reduced-Temp.
4 mM	0.12	0.083	0.15	0.036	0.054	0.15
0 mM	0.12	0.12	0.13	0.039	0.078	0.13

The data presented in Table 7 reveals that reducing temperature for the entire duration of the culture (9 days) can improve Q_p up to 25% for the exponential phase; and up to 3 fold increase for the post-exponential phase of growth as compared to the control batches. Reducing the temperature at the middle of the exponential phase of growth was not as effective as reducing the temperature for the entire culture time. However, even for the shifted temperature experiment, Q_p was increased in the post- exponential phase of growth by 50% as compared to the control experiment.

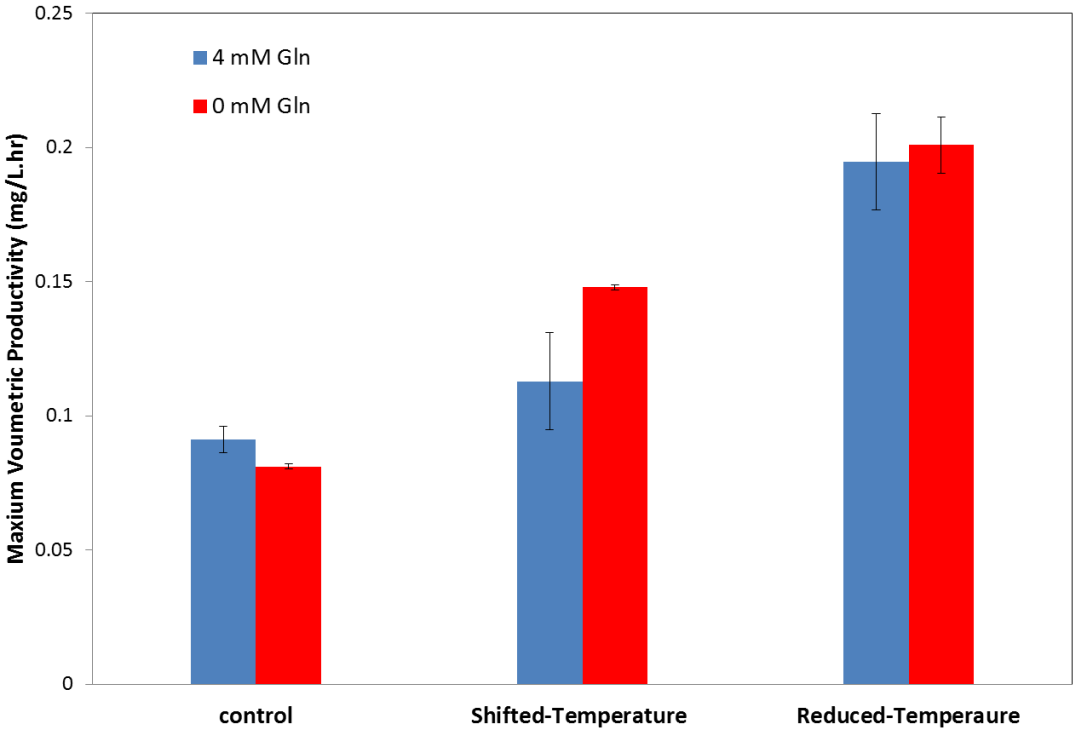

Figure 17, Maximum volumetric productivity, $Q_{v,max}$, under mild-hypothermia conditions compared to the control.

Maximum volumetric productivity rates, $Q_{v,max}$, were calculated from equation 3.3 by dividing the maximum value of mAb concentrations by the culture time. The blue bars in Figure 17, describe the maximum volumetric productivity values at 4 mM glutamine for the 3 experiments, i.e. reduced temperature, shifted temperature and control. The $Q_{v,max}$, under Shifted-Temperature was not significantly increased as compared to the control batches. However, under Reduced-Temperature conditions, the maximum productivity increased by almost 100% as

compared to the Control reaching a level of 0.2±0.01 (mg/l.h). Thus, with an initial 4 mM glutamine concentration, cultivating the cells at a lower temperature (33ºC) was an effective strategy for obtaining both higher volumetric mAb productivity and specific productivity. The improved final mAb concentration in this case, was not due to extended culture longevity, but rather to a marked increase of specific mAb productivity. Possible mechanisms that explain this observation are the increased mRNA stability of recombinant proteins at lower temperature and the improved transcription levels. On the other hand, we did not observe any reduction in metabolism of carbon sources as reported by other researchers (Michael Butler, 2005a; Vergara et al., 2014).

➢ *Temperature Effect and Glutamine-Free Condition*

Figure 18, a-b, describes mAb concentration profiles as a function of time and volumetric cell hours respectively for cultures initiated without glutamine for Reduced-Temperature and Control conditions.

Similar to the experiments initiated with 4 mM glutamine, the concentration of mAbs monotonically increased under Reduced-Temperature conditions throughout the culture. Shifting the temperature at the exponential phase of growth was also effective to increase a high level of protein production. According to Figure 18, the maximum mAbs concentration for Shifted-Temperature was 39.19±0.27 mg/l, on day 11; for Reduced-Temperature was 42.89±2.22 mg/l, on day 9; while for the control it was about two times slower equal to 17.2±4.5 mg/l, on the same

day. The specific mAbs productivity, Q_p , for exponential and post- exponential phases are calculated form the slopes in Figure 18-b, and are summarized in Table 7. Under reduced-Temperature conditions, Q_p, rose until the end of cultivation, and its value reached 0.13 (pg/cell.hr). This is approximately a three times higher productivity as compared to the Control condition during the post exponential phase of growth. Under Shifted-Temperature, Q_p was 0.12 (pg/cell.hr) in the exponential phase of growth; then dropped to 0.08 (pg/cell.hr) at the decline phase. The maximum volumetric productivity, $Q_{v,max}$, is shown in Figure 17 by the red bars. In contrast with the culture initiated with 4 mM glutamine the $Q_{v,max}$ significantly improved for both Shifted and Reduced-Temperature cultures as compared to the control.

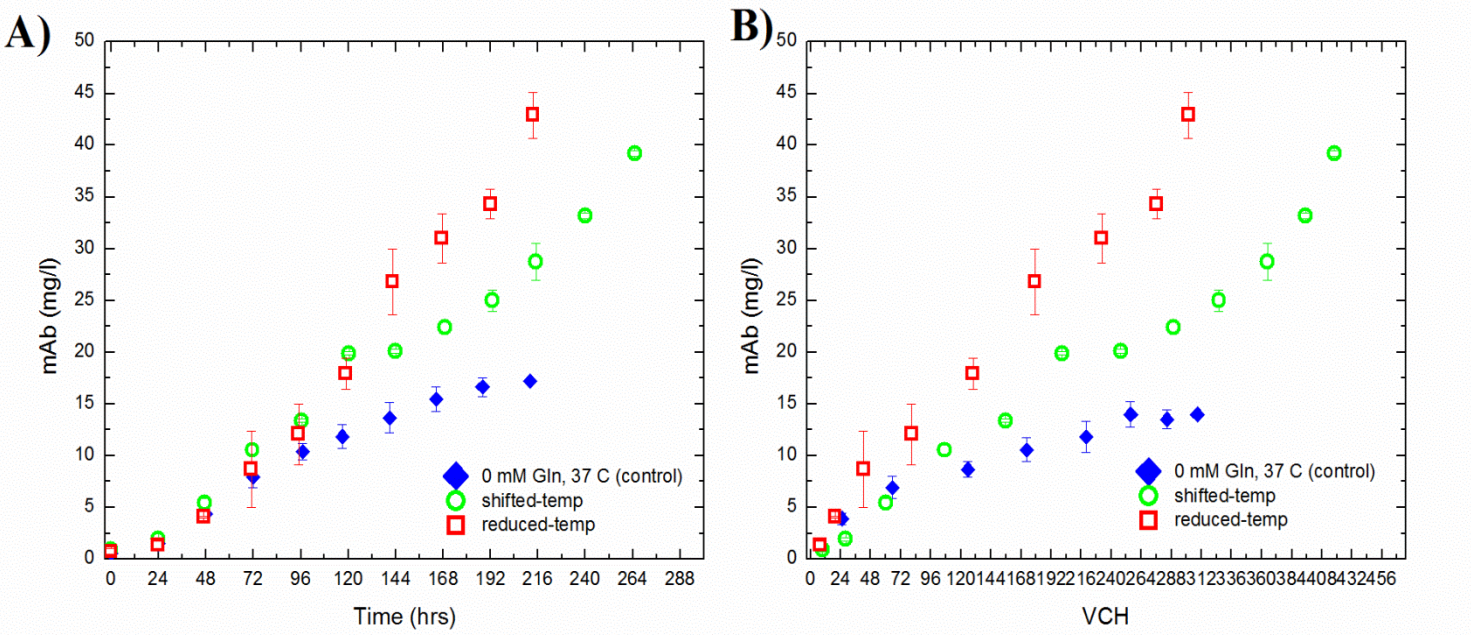

Figure 18, mAbs profiles and mAbs specific productivity of mild hypothermia experiment at 0 mM Gln. Data points represent mean ± SD for triplicate experiments: ◆ Control at 37ºC, ○ Shifted-Temperature, and □ Reduced-Temperature. A mAbs' concentration vs time); B) mAbs' concentrations vs volumetric cell hours (VCH)

This productivity increased by approximately 2 fold and 2.5 fold as compared to the control, for the Shifted and Reduced-Temperature experiments respectively.

Among all the experiments conducted with different levels of initial glutamine and with reduced temperature strategies, the experiment with the Reduced temperature regime and initiated with 4 mM glutamine resulted in the largest improvement in specific productivity in the

exponential phase, whereas the experiment initiated without glutamine and under a Shifted-Temperature operation exhibited the highest volumetric productivity.

In summary, the main effect of mild hypothermia, regardless of the initial concentration of glutamine, was a marked decrease in cell growth. At glutamine-free conditions it resulted in lower ammonia production while the glucose uptake rate was not affected. In addition the lower temperature strategies improved both mAbs' specific productivity and mAbs' volumetric productivity regardless of initial glutamine conditions.

5.3.4 Glycan Profiles and Glycosylation Indices

- ***Temperature Effect and 4 mM Glutamine Condition***

The glycan profiles of mAbs were analyzed using the method presented in Chapter 3, section 3.3.5. Samples were collected during the exponential phase (day 3), early stationary phase (day 4) and death phase of growth (day 5 and 7). The relative abundances (RA) of dominant glycans were normalized on the basis of a total area of 100 % (Table8). The data points on the table show the means of RA % for two replicated batches.

From the abundance of dominant fucosylated glycans, specifically F6A2G0, F6A2G1, F6A2G2, F6A2G2S1 and F6A2G2S1, it can be inferred that the glycan evolutions during the course of the culture were different between the Shifted and Reduced-Temperature experiments.

Table8, Relative abundances of dominant glycans (%) under mild hypothermia and 4 mM glutamine on days 3, 4, 5 and 7 of cultivation. Each data point presents the average of glycan percentage for two replicated flasks a) Shifted-Temperature and 4 mM glutamine, b) Reduced-Temperature and 4 mM glutamine.

a) Shifted- Temperature and 4 mM glutamine				
	Day 3	Day 4	Day 5	Day 7
F(6)A1	0.32± 0.45	0.31±0.11	0.83±0.22	2.06±0.34
A1G1	1.79±1.18	1.048±0.178	0.34±0.23	0.62±0.08
F(6)A2G0	7.06±0.37	12.02±2.1	19.12±1.95	25.13±1.56
A2G1	0.23±0.32	0.47±0.00	1.08±0.23	2.61±0.02
A2G1	0±0	0.24±0.34	0.62±0.88	1.31±1.85
F(6)A1G1	0±0	1.68±2.3	0±0	1.26±1.78
F(6)A2G1 isomer	13.81±0.23	14.93±1.49	14.41±0.3	13.41±0.42
F(6)A2G1isomer	13.81±0.23	14.93±1.49	14.41±0.3	13.41±0.42
A2G2	0.43±0.61	1.35±0.48	1.33±0.27	1.55±0.24
F(6)A2G2	45.87±1.5	38.68±7.13	36.7±1.75	29.23±2.78
F(6)A2G2S1	6.51±0.06	5.64±0.86	4.68±0.28	3.86±0.57
F(6)A2G2S1	6.51±0.06	5.64±0.86	4.68±0.28	3.8±0.57
F(6)A2G2S2	3.64±1.03	3.01±0.24	1.73±0.4	1.68±0.44
b) Reduced- Temperature and 4 mM glutamine				
	Day 3	Day 4	Day 5	Day 7
F(6)A1	0.36±0.05	0.32±0.036	0.23±0.04	0.54±0.02
A1G1	1.24±0.39	0.27±0.08	0.08±0.11	0.11±0.08
F(6)A2G0	14.11±2.42	9.32±0.64	8.3±0.23	15.08±0.36
A2G1	0.38±0.12	0.36±0.06	0.45±0.07	0.52±0.06
A2G1	0.24±0.12	0.21±0.29	0.2±0.28	0.28±0.4
F(6)A1G1	0±0	0.06±0.08	0.27±0.39	0±0
F(6)A2G1 isomer	18.84±0.34	19.65±0.3	19.62±0.13	18.36±0.02
F(6)A2G1isomer	18.84±0.34	19.65±0.3	19.62±0.12	18.36±0.02
A2G2	0.45±0.32	0.43±0.21	1.54±1.34	0.73±0.05
F(6)A2G2	37±1.75	40.09±0.77	39.64±0.73	35.69±0.64
F(6)A2G2S1	3.63±0.19	4.03±0.1	4.26±0.06	4.17±0.07
F(6)A2G2S1	3.63±0.19	4.03±0.1	4.26±0.062	4.17±0.07
F(6)A2G2S2	1.24±0.06	1.63±0.16	1.48±0.04	1.93±0.01

For example, F(6)A2G0, a non galactosylated glycan, reached on day 3 a twofold higher percentage area of 14.11 ±2.24 under the Reduced-Temperature operation as compared to the Shifted-Temperature operation (7.06 ±0.37). Subsequently, the level of this glycan declined to 8.3±0.23 on day 7 under Reduced-Temperature condition and again rose to 15.08±0.36 on day 9. But under Shifted-Temperature, the level of this glycan consistently increased until the end of culturing to the value of 25.13 ±1.56 %. F(6)A2G0 is the main non-galactosylated glycan for this mAb and its higher concentration at day 3 for the Reduced-Temperature samples as compared to the Shifted-Temperature can be explained by the lower residence of mAb of the former in the Golgi complex. The reduction of the residence time is due to a higher rate of production at lower temperature that limits the exposure time of protein to the glycosyltransferase enzymes (Butler 2006b). The lower availability of glucose observed towards the end of the culture is possibly the reason for the consistent increase of this non-galactosylated glycan for the Control and the Shifted-Temperature cultures. Due to depletion of glucose with the associated decrease in galactose, less amount of F(6)A2G0 is further reacted thus explaining its monotonic increase until the end of the batch.

The levels of a monogalactosylated glycan, F(6)A2G1, remained almost constant during culturing for both the Shifted Temperature and Reduced Temperature operations (18.84±0.34 to 18.36±0.02 % on days 3 and 7 respectively, for Reduced-Temperature compared to the 13.81±0.23 to 13.41±0.42 % on the same days, for the Shifted-Temperature samples).

The reduction in temperature affected the fully galactosylated glycans, including F(6)A2G2, F(6)A2G2S1, and F(6)A2G2S2 differently for the Shifted and Reduced-Temperature experiments. For instance, the abundance of these glycans consistently decreased until day 9 under the Shifted-Temperature operation, whereas for the Reduced-Temperature operation their levels were lower on day 3, increased between day 3 and day 7 and dropped again on day 9. The maximum levels of F(6)A2G2 for the Shifted and Reduced-Temperature regimes were 45.87±1.5 % on day 3 and 40.09±0.77% on day 4, respectively. Following the results of F(6)A2G0, the temporal accumulation of this non-galactosylated may explain the subsequent reduction of F(6)A2G2 for the Shifted-Temperature condition since the former glycan is a substrate for the latter glycan. Similarly, the higher level of F(6)A2G0 in the Reduced-Temperature at day 3, my explain the lower level of F(6)A2G2 on the same day.

The highest levels of sialylated glycans mainly, F(6)A2G2S1 and F(6)A2G2S2 were 6.51±0.06% and 3.64±1.03% on day 3 of the Shifted-Temperature culture, and 4.26±0.06% and 1.93±0.01% on day 5 and day 7 of cultivation respectively, for the Reduced-Temperature flasks. We have previously reported that (Chapter 4) ammonia inversely affect on the sialylation evolution (Aghamohseni et al. 2014). However, mild-hypothermia did not alter the ammonia production rate and approximately same concentration of ammonia equal to 4 ±0.3 mM was obtained for all the three conditions. Also, in agreement with previous studies (Ohadi et al. 2013; Liu et al. 2014) there is a clear correlation between galactosylation and sialyation levels as sialic acid can only is attached to a galactose branch of a glycoprotein.

Figure 19, describes the time profiles of the glycosylation indices. These values were calculated according to equations 3.4 and 3.5 based on the RA% values presented in Table8. Under the control and the Shifted-Temperature conditions, the galactosylation index, GI value, (Figure 19-a) reached its maximum level on day 3, and its profile declined approximately by 19 %, for the control and 27% for the Shifted-Temperature between day 3 to day 7. In contrast, significantly different trends of the GI profile were observed for the Reduced-Temperature condition. For example, the GI at day 3 reached a value of 0.66, much lower than the values observed for the Shifted Temperature and Control cultures (0.78 and 0.76 for the Shifted-Temperature and the Control respectively). The highest level of GI occurred on day 5 and it was still lower than the maximum GI values for the Control and Shifted-Temperature conditions. A possible explanation for these differences is that during the exponential phase, higher specific mAb productivity under Reduced-Temperature compared to the Shifted Temperature and Control cultures, resulting in a shorter residence time of mAb within the cell and in less glycosylation thus a lower GI value observed at the lower temperature of 33˚C.

According to above mentioned observations, the galactosylation index (GI) and sialylation index (SI) are strongly correlated. Accordingly, the SI value at day 3 for the Reduced Temperature culture was also lower as compared to the Shifted-Temperature and the control conditions (Figure 19-b) and, similarly to the GI, SI value increased between day 3 and day 7. Thus, mild hypothermia was favorable for mAb production, but not helpful for increasing the

level of glycosylation. This outcome was explicitly considered in the development of the semi-empirical model presented in Chapter 6.

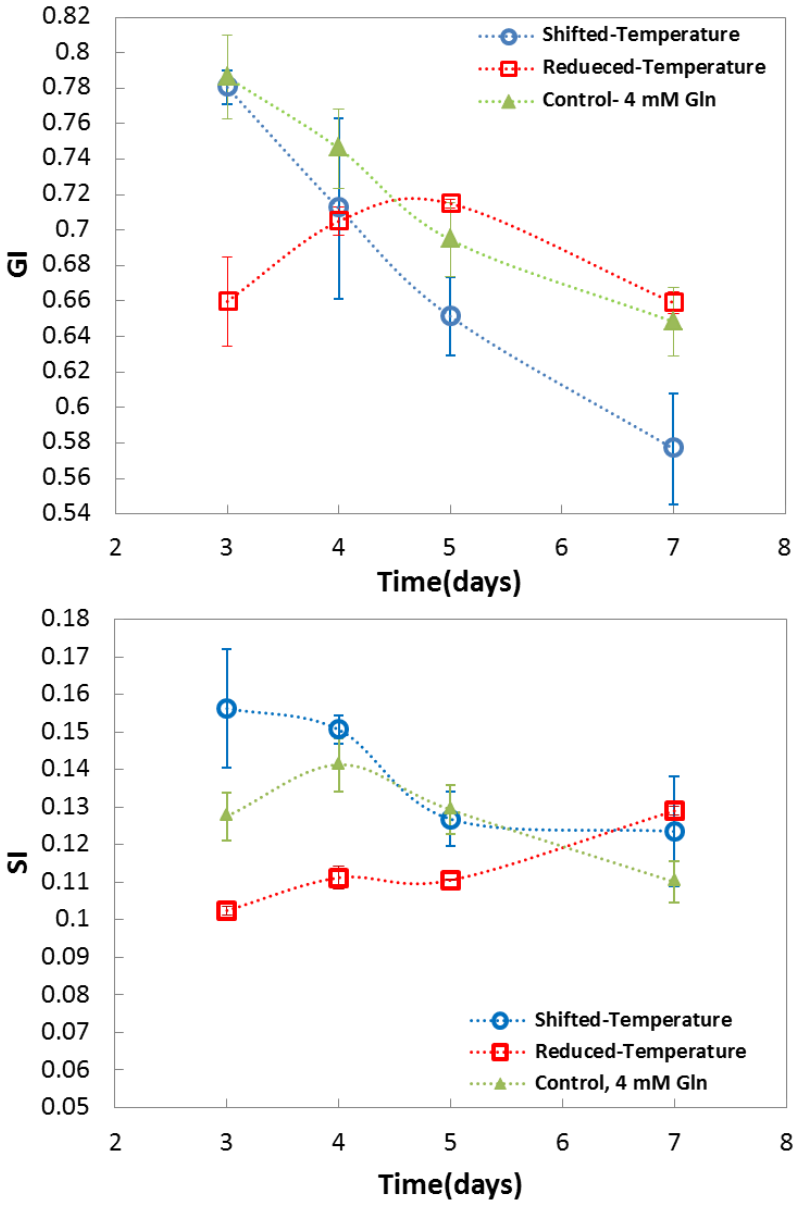

Figure 19, Galactosylation index, GI, profile under mild hypothermia and 4 mM glutamine condition. Data points represent mean for duplicated experiments: ▲ Control at 37ºC, ○ Shifted-Temperature, and □ Reduced-Temperature.

➢ *Temperature Effect and Glutamine-Free Condition*

The data points on the Table 9, show the mean values of RA % , for two replicated batches. Similar to the cultures initiated with 4mM of glutamine, it can be observed from the abundances of F6A2G0, F6A2G1, F6A2G2, F6A2G2S1 and F6A2G2S1 that time evolution of the glycans were different between the Shifted and the Reduced-Temperature batches.

F(6)A2G0, the dominant non-galactosylated glycan, reached on day 3 a higher level of 14.5 ±1.56 % under the Reduced-Temperature regime as compared to the Shifted-Temperature (8.77 ±3.39 %) operation. Subsequently, the levels of this glycan declined to 8.8±1.3 and 6.14±0.17 % on day 4 and 5 respectively, for the Reduced-Temperature condition, and again rose to 12.73±0.83 % on day 7. Similar trends were observed for this glycan for the Shifted-Temperature operation. Its levels declined to 5.53±0.27 and 4.78±0.38 on days 4 and 5 respectively and then increased to 8.15± 0.87 and 13.39±0.65 on days 7 and 9 of cultivation consequently. Similar to the initial 4 mM glutamine case, the high concentration of F(6)A2G0 can be explained by the higher rate of mAb production at this condition that consequently results in a lower residence time of proteins in the Golgi apparatuses. However, the profile of F(6)A2G0 for the cultures initiated without at glutamine was not similar to the ones initiated with 4 mM glutamine supplementation at Shifted-Temperature and its relative abundance did not increase monotonically. It appears that for glutamine limited conditions, the nucleotide sugars were depleted earlier as compared to the cultures initiated with 4 mM glutamine thus resulting in

decreasing galactosylation towards the end of the culture. This observation is more evident in the GI and SI profile as presented later in this section (Figure 20).

The level of a monogalactosylated glycan, F(6)A2G1, under Shifted-Temperature conditions remained almost constant from day 3 (14.58±1.47) until day 7 (16.23±0.98) of the culture. Then it dropped to 13.85±0.25 on day 9 of cultivation. This glycan reached higher values under Reduced-Temperature and glutamine free experiments. In the latter case, the level of F(6)A2G1 decreased from 20.27±1.79 on day 3 to 18.11±0.27 and 18.08±0.48 on days 4 and 5 respectively and then dropped to a lower value of 16.34±0.47 on day 7 of cultivation.

Reduction in temperature affected the fully galactosylated glycans, including F(6)A2G2, F(6)A2G2S1, and F(6)A2G2S2, differently for the Shifted and Reduced-Temperature experiments. The abundance of these three glycans were low on day 3, then improved until day 7 and dropped on day 9 for the Reduced-Temperature batch, while, for the Shifted-Temperature batch, F(6)A2G2 dropped consistently until day 9. On the other hand, the evolution of sialylation with time was similar to the Reduced-Temperature operation. The maximum levels of F(6)A2G2 for Shifted and Reduced-Temperature were 41.7±5.25 on day 3 and 39.75±0.97 on day 5 respectively.

Table 9, Relative abundances of dominant glycans (%) under mild hypothermia and glutamine-free condition, on days 3, 4, 5, and 7 of cultivation. Each data point presents the average glycan percentage for two replicated flasks a) Shifted-Temperature and glutamine-free, b) Reduced-Temperature and glutamine-free.

a) Shifted- Temperature and 4 mM glutamine					
	Day 3	Day 4	Day 5	Day 7	Day 9
F(6)A1	0±0	0.11±0.15	0.1±0.14	0.37±053	0.57±0.81
A1G1	0±0	0±0	0±0	0.17±0.23	0±0
F(6)A2G0	8.77±3.39	5.54±0.27	4.47±0.39	8.16±0.84	13.37±0.65
A2G1	1.21±0.72	0.71±0.09	0.63±0.03	0.92±0.07	1.69±0.15
A2G1	1.21±0.72	0.71±0.09	0.63±0.03	0.92±0.07	1.69±0.15
F(6)A1G1	0±0	0±0	0±0	0±0	0±0
F(6)A2G1 isomer	14.58±1.47	15.51±0.82	14.98±0.33	16.23±0.98	13.85±0.25
F(6)A2G1 isomer	14.58±1.47	15.51±0.82	14.98±0.33	16.23±0.98	13.85±0.25
A2G2	1.61±0.30	1.28±0.01	1.29±0.17	1.27±0.07	1.46±0.38
F(6)A2G2	41.70±5.25	45.57±0.67	41.38±0.05	40.48±0.65	35.93±1.77
F(6)A2G2S1	6.19±0.89	6.04±0.5	7.54±0.28	5.96±1.09	6.78±0.01
F(6)A2G2S1	6.19±0.89	6.04±0.5	7.54±0.28	5.96±1.09	6.78±0.01
F(6)A2G2S2	2.64±0.08	2.97±0.58	6.15±0.63	3.34±0.79	3.3±0.84
b) Reduced- Temperature and 4 mM glutamine					
	Day 3	Day 4	Day 5	Day 7	
F(6)A1	1.4±1.4	0.22±0.31	0.18±0.25	1.17±0.05	
A1G1	0±0	0±0	0.09±0.14	0.08±0.11	
F(6)A2G0	14.51±1.56	8.80±1.30	6.15±0.17	12.73±0.83	
A2G1	0.72±0.00	1.05±0.76	0.53±0.01	1.62±0.26	
A2G1	0.72±0.00	1.05±0.746	0.53±0.01	1.62±0.26	
F(6)A1G1	0±0	0.129±0.09	0.09±0.13	0.09±0.14	
F(6)A2G1 isomer	20.27±1.79	18.11±0.27	18.08±0.48	16.34±0.47	
F(6)A2G1 isomer	20.27±1.79	18.11±0.27	18.08±0.48	16.34±0.47	
A2G2	0.43±0.61	1.31±0.49	0.73±0.28	1.64±0.07	
F(6)A2G2	33.94±2.53	39.52±0.46	39.75±0.97	35.66±0.19	
F(6)A2G2S1	3.08±0.60	4.69±0.96	5.76±0.15	5.15±0.77	
F(6)A2G2S1	3.08±0.60	4.69±0.96	5.76±0.15	5.15±0.77	
F(6)A2G2S2	1.54±0.63	1.55±0.21	4.23±1.00	2.39±0.32	

From the results of F(6)A2G1, it is observed that the temporal accumulation or depletion of this mono-galactosylated glycan is correlated to the corresponding reduction or increase of the fully-galactosylated F(6)A2G2 since the former glycan is a substrate for the latter glycan.

The highest values of F(6)A2G2S1 and F(6)A2G2S2 were 7.54±0.28 and 6.15±0.63 for Shifted-Temperature and, 5.76±0.15 and 4.23±1.00 for Reduced-Temperature, respectively. This trend is because of the observed correlation of galactosylation and sialylation as observed in our previous study (Chapter 4)(Aghamohseni et al. 2014). Figure 20 describes the time profiles of glycosylation indices that were calculated according to equations 3.4 and 3.5 based on the RA% values presented in Table 9.

Similar to 4 mM glutamine condition, for the Reduced-Temperature batch and zero initial glutamine, the GI profile was different from the Control. On day 3, a lower level of GI equal to 0.61 was observed compared to 0.75 and 0.74 GI values for the Shifted-Temperature and the Control batches, respectively. Then the level of GI increased to a value of 0.72 on day 5, almost the same as for the Control batch. The low level of GI on day 3 for the Reduced-Temperature batch can be again explained by the combination of lower growth with associated slower synthesis of nucleotides and high mAb specific productivity with the resulting lower residence time of proteins passing through the Golgi (Butler 2006a).

Reducing the temperature to 33 ˚C, for both the Shifted Temperature and Reduced Temperature operations contributed to increase the sialylation levels specifically on the day 5 of cultivation. In agreement with our previous observation in chapter 4 (Aghamohseni et al. 2014),

the low level of ammonia accumulation in the later days of the culture can be the reason for the high levels of SI observed in these cases (Figure 15).

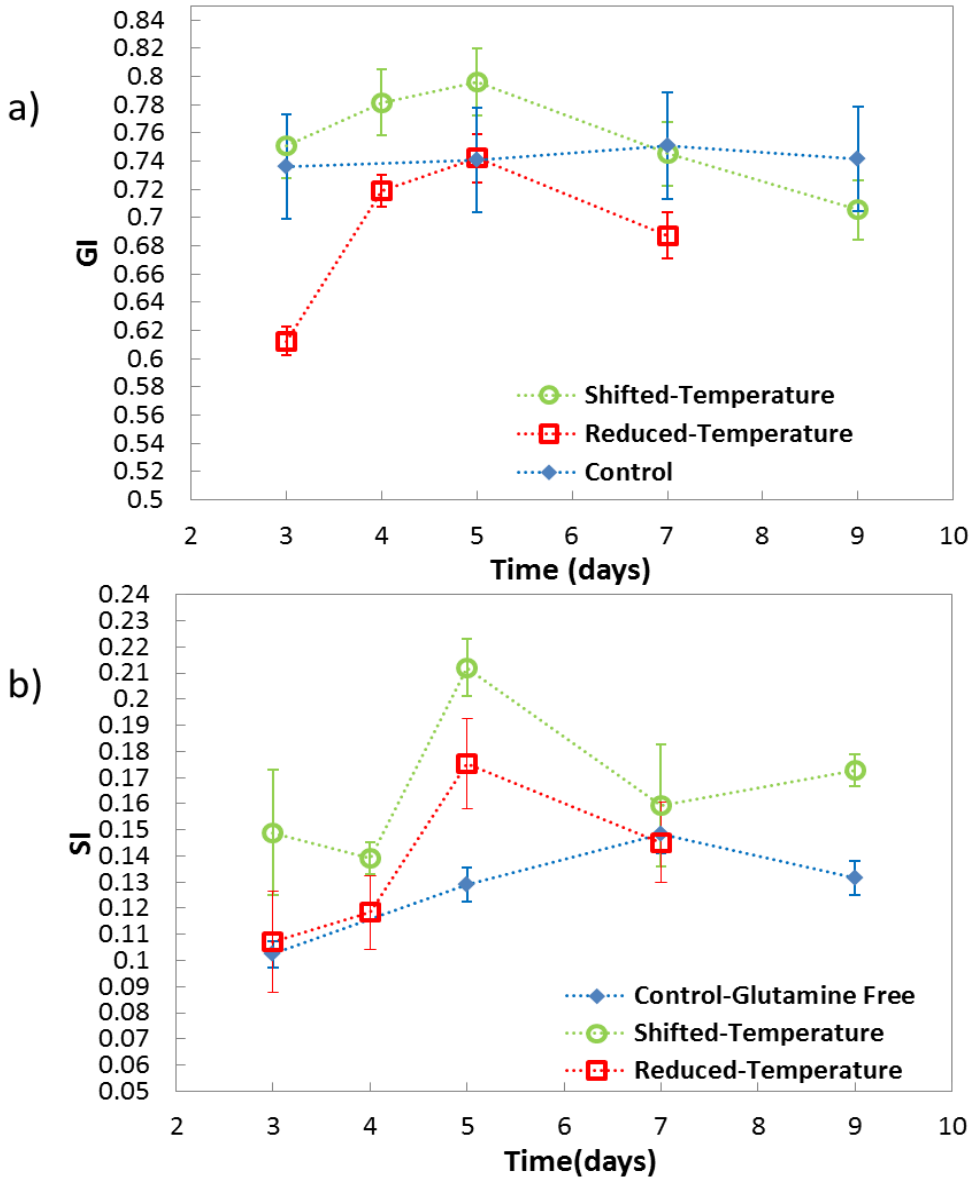

Figure 20, Galactosylation index, GI, profile under mild hypothermia and glutamine-Free condition. Data points represent mean for duplicated experiments: ◆ Control at 37ºC, ○ Shifted-Temperature, and □ Reduced-Temperature.

In summary, the effect of mild-hypothermia conditions on the CHO cells' growth, mAbs productivity and glycosylation have been investigated by two strategies, a shifting of the temperature on day 3 of the culture and operating the entire culture at a lower temperature of 33˚ C. These strategies were investigated for two different initial glutamine concentration, 4 mM and 0 mM. The observed increase in mAb productivity was in agreement with previous studies (Trummer et al. 2006; Vergara et al. 2014) with the exception of the study by Seo at al., (2013) that reported a lack of effect of temperature (33˚C) on productivity for a rF2N78 cell line (Seo et al. 2013).

The volumetric productivityQ_p was found to increase by more than 80% as compared to the control condition, during the exponential phase of growth for both the initial glutamine-Free and 4 mM glutamine conditions and by up to threefold increase during the post-exponential phase of growth when the cells were cultivated at Reduced-Temperature conditions. Q_{vmax} also increased by almost 100% for the Reduced-Temperature conditions for cultures initiated with zero or 4 mM glutamine concentrations. Applying mild hypothermia techniques in this research study was also helpful for increasing cells' viability but reduced the cells growth rate which is in agreement with previous studies (Chen and Harcum 2006; Rodriguez et al. 2010; Vergara et al. 2014).

In terms of the effect of temperature on glycosylation we observed a different progression of the galactosylation index (GI) during 9 days of cultivation for the Reduced-Temperature and Shifted-Temperature compared to the Control batches for both 4 mM and 0 mM initial glutamine

levels. The GI Index reached a low value during the exponential phase of growth and its level improved by day 5 of the culture. Our results revealed that reducing the optimum temperature for cell growth reduces glycosylation. This reduction may be related to: i- a reduction in cell growth that is associated to a decrease in nucleotides and nucleotide sugars synthesis and ii- an increase in mAb specific productivity which results in a shorter residence time in the Golgi. This correlation between temperature reduction and glycosylation is further discussed and modeled in the mathematical modeling chapter (Chapter 6). It should also be noticed that several previous studies did not reported any changes on the glycosylation profiles while cells were cultivated at lower temperatures (Rodriguez et al. 2010; Taschwer et al. 2012; Seo et al. 2013).

Chapter 6

Mathematical Modeling

The dynamic model presented in the first section of this chapter is based on the modeling section of an earlier work (Aghamohseni et al. 2014) and cited accordingly by permission of the J*ournal of Biotechnology.* The thesis author's specific contributions to the modeling section of this publication were to perform the experimental design, running experiments and analysis, and to provide all the data used for the dynamic models. In addition, she carried out the metabolic flux analysis, macro reaction implementation and formulation of the model structure according to the experimental results. Then, she collaborated with Kaveh Ohadi, one of the co-authors of the publication above on the coding of the mathematical equations and optimization of the dynamic model in the MATLAB environment.

6.1 Introduction

A dynamic model for describing the evolution of extracellular metabolites' concentrations with time during a batch culture was formulated based on a metabolic flux analysis (MFA) approach developed by our research group (Naderi et al. 2011). The objectives for developing a model to describe the extracellular metabolites were: i) to systematically understand and quantify the metabolic behavior of nutrients and by products for different experimental conditions, ii) to correlate cell growth and death with the metabolites' dynamics and iii) to ultimately correlate the evolution of extracellular metabolites to the dynamic evolution of glycans. Figure 21 describes the network of reactions considered for the MFA. This network serves as the basis for the formulation of the dynamic balances for extracellular metabolites. Fluxes were calculated from the changes with respect to time of the extracellular metabolites' concentrations, as per the method given by Naderi et al., 2011. In this calculation, it was assumed that the intermediates of glycolysis and the TCA cycle do not accumulate over time (Aghamohseni et al. 2014).

From the calculated flux distribution, a set of macro-reactions was obtained that relates the concentrations of nutrients to those of by-products. Based on these reactions, a set of dynamic mass balances relating the most significant nutrients to by-products were formulated using the Michaelis-Menten kinetics for each reaction. A biomass balance was formulated based on growth and death rates and accounts separately for the populations of growing and non-growing cells (Aghamohseni et al. 2014). Further details about the model are given in the "Modeling of

the Extracellular Environment", section 6.2.1 of this chapter. The impacts of Reduced-pH and Reduced-Temperature were also modeled through the resulting changes in growth rate. The dynamic equations updated for describing the effect of pH and temperature are presented in section 6.2.2 of this chapter.

To describe the interrelation between the extracellular environment and the glycosylation reactions we initially examined a rigorous mechanistic model in a work co-authored with (Ohadi et al. 2013). However, it was found that this model is very difficult to calibrate due to the large number of model parameters and the relative scarcity of data. Instead, we proposed in the second part of this chapter a novel semi-empirical model to connect extracellular properties of cell metabolism to the intracellular process of mAbs' glycosylation. This semi-empirical model is composed of two different equations: i) an ordinary differential equation describing a lump sum of the nucleotides' sugars as a function of extracellular glucose and glutamine concentration and, specific growth rates and ii) a steady state equation describing the correlation between the galactosylation index (GI) equation with the nucleotides' sugars levels calculated in the part I of the model, the specific mAb production rates and, the extracellular glucose concentrations. The dependency of the nucleotide sugar model and GI model equations was based on our understanding of the process and the experimental data collected during the current research study and previously published studies.

The semi-empirical model proposed above was found to be easy to calibrate as compared to the rigorous mechanistic model mentioned above. As such it can serve to efficiently elucidate

correlations between extracellular properties and glycosylation while avoiding the very challenging parameter estimation task required for a more rigorous model (Ohadi et al. 2013). The results obtained with the semi-empirical model are presented in Section 6.3 of this chapter and compared to experimental data.

6.2 Modeling of the Extracellular Environment

6.2.1 Metabolic Flux Analysis

Metabolic flux analysis (MFA) is a method used for determining intracellular metabolic fluxes in live cells (Sanfeliu and Stephanopoulos 1999; Ahn and Antoniewicz 2012). MFA provides fundamental understanding about the metabolic pathways involved in the overall cellular metabolism by quantifying fluxes from measured metabolites' production or consumption rates. The flux analysis is based on the steady-state mass balance of intracellular species (Gao, 2007).

A metabolic flux analysis has been implemented for the current study, based on the flux values for the CHO DUXB and the network presented in Figure 21. This metabolic network includes the four metabolic pathways of interest here, glycolysis, pentose phosphate, TCA cycle and amino acid metabolism, which are the main carbon consuming pathways and are responsible for energy and biomass production. With the exception of tryptophan, which has insignificant

involvement in protein and energy production (Gambhir et al. 2003), all amino acids are involved in the analysis. Reversible reactions were accounted for by assuming in the flux calculations that these reactions proceed in both directions for the conversions of pyruvate to oxalacetate, α-ketoglutarate to glutamate, and glutamate to glutamine, i.e., reactions 7, 25, and 26. The network comprises 30 metabolites and 37 intercellular fluxes. The corresponding set of stoichiometric equations is summarized in Appendix B.

The calculation of the fluxes was performed based on experimentally measured consumption rates of nutrients and production rates of by-products. Fluxes were calculated separately for the exponential and post-exponential phases where the time corresponding to the peak in cell density was used as the boundary between the two phases. To calculate the fluxes, average consumption and production rates were calculated from experimental data collected during the exponential or post-exponential phases.

The entire set of mass balance equations, which were obtained based on the stoichiometric reactions (F), can be formulated in the following matrix equality:

$$\mathbf{R} = A\,J \tag{6-1}$$

where J= [ji] is a vector of unknown fluxes, and A= [αim] is the stoichiometric matrix of reactions in which each entry αim is the stoichiometric coefficient for metabolite m={1,…,nm} in reaction i={1,…,ni}. The fluxes are expressed in units of mol of the corresponding metabolite per hour and per mol of biomass.

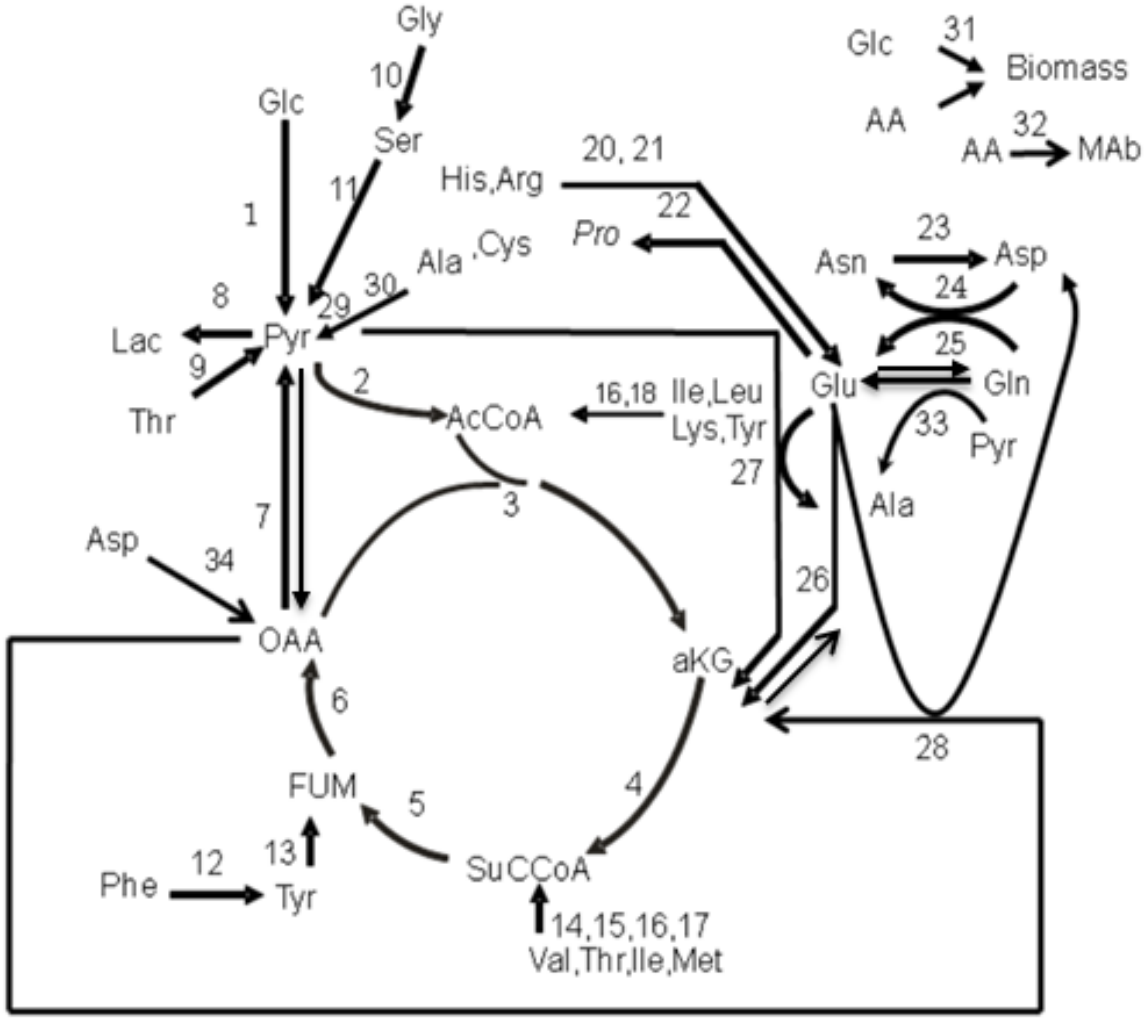

Figure 21, The complete reaction network utilized for metabolic flux analysis (Gao et al. 2007)**.**

R is a vector of consumption and production rates of all the metabolites that can be calculated from experimental data. The vector R satisfies mass balance equations represented by the matrix equation (6-2).

$$\frac{d\boldsymbol{\psi}(t)}{dt} = \mathbf{R}X_V(t) \qquad (6\text{-}2)$$

where $\boldsymbol{\psi}$ is the vector of metabolite concentrations of all intercellular metabolites (in this study $R_{i,}$ i=1,.., 6) and extracellular metabolites ($R_{i,}$ i=7,…, 30), t is the culture time (exponential and post-exponential phase of growth) and $X_v(t)$ is the viable cell concentration.

For the intracellular reactions, such as the ones related to metabolites involved in the TCA cycle and glycolysis, $R_{i,}$ i=1,.., 6 were set to zero based on the assumption that under balanced growth condition, intracellular metabolites are at a quasi-steady state and do not accumulate with time within the cell (Gao et al. 2007).

Assuming that **R** is constant, during a specific time interval t, equation (6-2) can be integrated as follows:

$$\int_0^t d\boldsymbol{\psi}(t) = \mathbf{R}\int_0^t X_V(t)\,dt \qquad (6\text{-}3)$$

The integral in the right hand side of equation (6.3) is referred to the volumetric cell hours (VCH) (Dutton et al., 1999), and can be approximated piecewise by using the logarithmic mean cell density between time intervals t and t + Δt as follows:

$$VCH = \sum_{0}^{t} \frac{\left(X_{v_{t+\Delta t}} - X_{v_t} \right)}{\ln\left(\frac{X_{v_{t+\Delta t}}}{X_{v_t}} \right)} \times \left(t_{t+\Delta t} - t_t \right) \qquad (6\text{-}4)$$

The system of equations defined by the matrix equality (6-1) for the network considered in this study was found to be underdetermined, i.e. the number of unknowns is larger than the number of equations. To solve the fluxes a constrained optimization approach was applied (Naderi et al. 2011). Only positive values for each flux, corresponding to the directions assumed for the reactions in the network, were considered as a set of constraints. A quadratic programming (using the MATLAB function qp) approach was used to minimize the differences between the measured and modeled rates as follows:

$$Min(\mathbf{R} - \mathrm{AJ})^{\mathrm{T}} (\mathbf{R} - \mathrm{AJ}) \qquad (6\text{-}5)$$

Subjected to …

$\mathbf{j} > 0$

where, the vector $\mathbf{R}$ corresponds to the measured consumption or production rates, whereas the vector obtained from the product AJ corresponds to the corresponding predicted rates.

Figure 22 presents the flux distribution of a control batch (4 mM Gln, 25 mM Glc) during the exponential and post-exponential phases of growth. It should be noticed that the MFA was conducted in this work with the purpose of identifying the significant metabolic reaction and based on those, to formulate a simplified dynamic mass balances' model. Then, to achieve this objective, the insignificant fluxes contributing less than 0.1% of total flux were omitted from the network. This simplification does not imply that the eliminated fluxes and corresponding amino acids are not necessary for growth but rather that they are not major contributors to the requirements of the cells in terms of energy and biomass formation. As a result

fluxes $j_{i,}$, i={*1,2,3,4,5,6,7,8,23,24,25,26,27,28,30,31,32,33,34*}

were found to be significant, and the rest of the fluxes were eliminated from the metabolic network. The simplified network for CHO DUXB is shown in Figure 23.

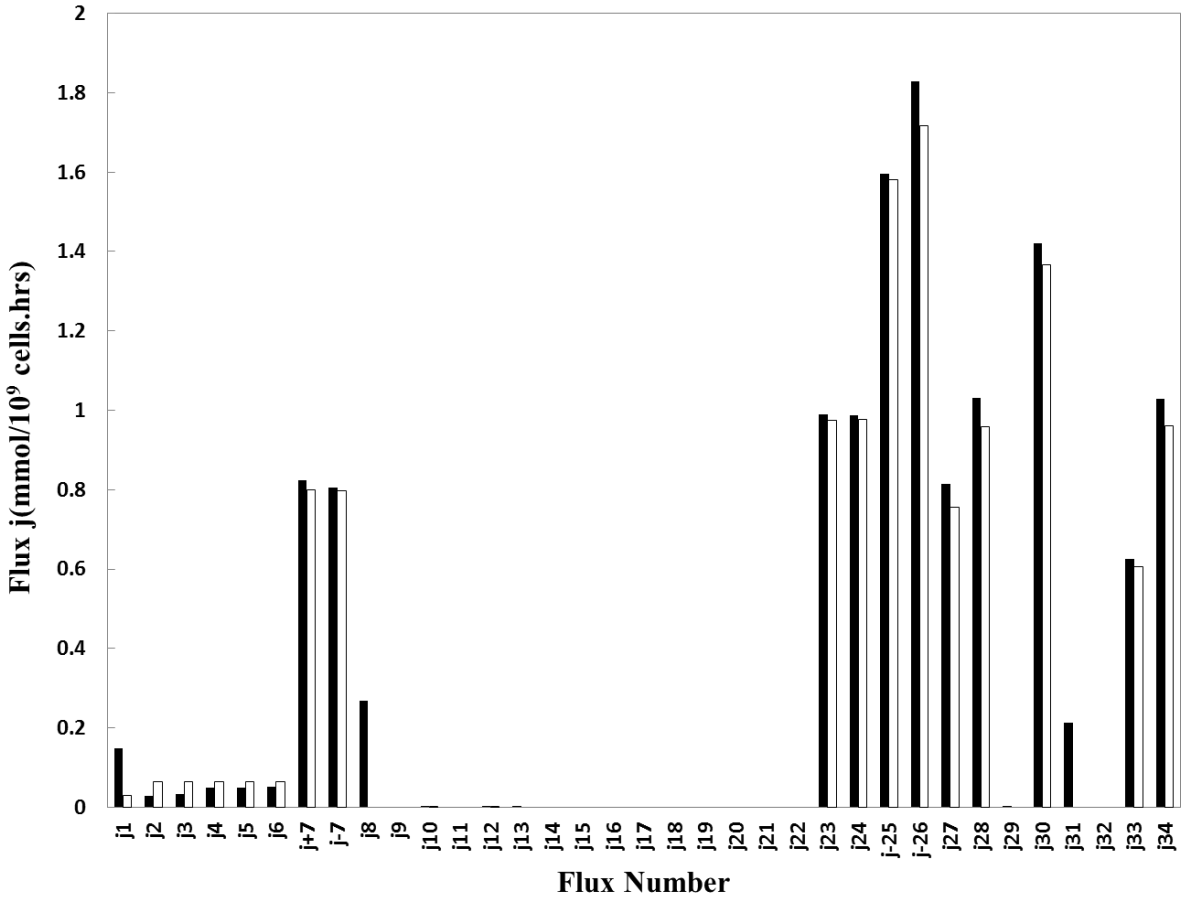

Figure 22, Distribution of fluxes for a batch culture with initial 4 mM glutamine and 25 mM glucose for exponential (black bars) and post-exponential (white bars) phases of growth (Aghamohseni et al. 2014)

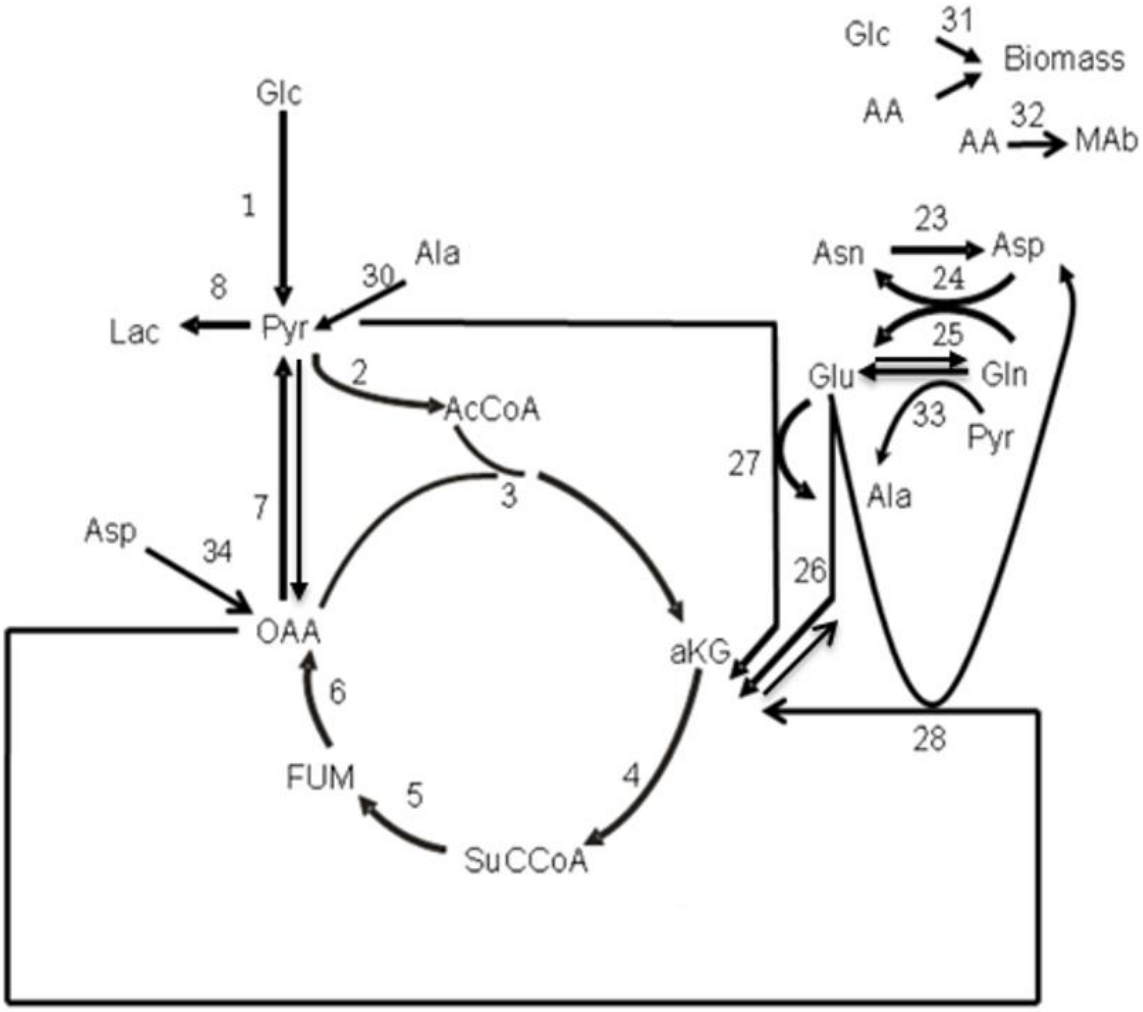

Figure 23, The simplified metabolic network for CHO DUXB (Aghamohseni et al. 2014)**.**

6.2.2 Dynamic Modeling

➢ *Glucose and Glutamine Depletion effects*

The dynamic model was formulated based on MFA analysis combined with data collected from batches cultivated at different initial levels of glutamine and glucose. Based on the reduced network shown in (Figure 23) and using the quasi-steady assumption for the intracellular species we obtain a set of macro-reactions that directly relate substrates to the products. The resulting 8 macro-reactions are listed in Table 10.

Table 10, Essential macro-reactions of extracellular metabolites

E1	Glc → 2Lac
E2	Glc → 6CO2
E3	Asn → Asp + NH3
E4	Ala → NH3 + 3 CO2
E5	Gln + 0.5 Glc→ Asp+Ala+ Co2
E6	Asp→ NH3 + 4 CO2
E7	Glc+2 NH3→2CO2 + Gln
E8	Gln+Asp → Asn+Ala+2Co2

A dynamic model was developed for cell density that discriminates between viable and dead cell populations. In this model the viable biomass population was assumed to consist of both growing (*fgr*) and non-growing (1 – *fgr*) fractions as described in (Aghamohseni et al. 2014). Based on the observation that growth stopped when glucose was depleted, the *fgr* was assumed to be correlated to the glucose concentration and described accordingly by equation 6-6.

.

$$\frac{dfgr}{dt} = -K_{11}\frac{fgr}{1+[Glc]/K_{12}} \tag{6-6}$$

According to the experimental results, the viable cell population was dependent on glucose and glutamine concentrations. The ammonia [Amm] and lactate [Lac] concentrations in the denominator of the cell growth term (the third and fourth terms in the right hand side of equation 6-7), reflect the fact that ammonia and lactate accumulation in the culture were found to be inhibitors of cell growth (Naderi et al., 2011; Quek et al., 2010). Since the level of ammonia could not explain by itself the rate of death, an additional term was used to represent the death rate which is inversely proportional to glucose level. Increasing ammonia concentration and glucose starvation induced the rate of dead cells in agreement with previously reported studies (Ahn & Antoniewicz, 2012; Zustiak, et al., 2008). This dependency of death on glucose concentration was hypothesized to be caused by autophagic death where the cell consumes itself in the absence of nutrients (Kim et al., 2013; Zustiak et al., 2008). Equations 6-7 and 6-8

describe the dynamic evolution of viable cells and dead cells respectively. The fifth parameter (K_{28}) of equation 6-8 was added to account for cell lysis during the cell cultivation.

$$\frac{dX_v}{dt} = \mu_{\max}.fgr.X_v\left(\frac{[Glc]}{K_{21}+[Glc]}\times\frac{[Gln]}{K_{26}+[Gln]}\times\frac{1}{1+[Amm]/K_{23}}\times\frac{1}{1+[Lac]/K_{27}}\right)$$
$$-k_d.(1-fgr)X_v\left(\frac{1}{1+\left(K_{24}/[Amm]\right)^n}+\frac{K_{25}}{[Glc+\varepsilon]}\right) \quad (6\text{-}7)$$

$$\frac{dX_d}{dt} = k_d.(1-fgr).X_v\left(\frac{1}{1+(K_{24}/[Amm])^n}+\frac{K_{25}}{[Glc+\varepsilon]}\right)-k_{28}X_d \quad (6\text{-}8)$$

Dynamic models for nutrients and byproducts were developed according to the macro-reactions listed in Table 10 as follows:

$$\frac{d[Glc]}{dt} = -X_v\left(\frac{K_{31}[Glc][Gln]}{(K_{32}+[Glc])(K_{36}+[Gln])}+\frac{K_{33}[Glc]}{(K_{34}+[Glc])}\right)-K_{35}X_v \quad (6\text{-}9)$$

$$\frac{d[Gln]}{dt} = -K_{41}X_v\left(\frac{[Glc][Gln]}{(K_{42}+[Glc])(K_{43}+[Gln])}\right) \quad (6\text{-}10)$$

$$\frac{d[Lac]}{dt} = -\frac{K_{51}[Glc]}{[Glc]+K_{52}}X_v\frac{d[Glc]}{dt} \quad (6\text{-}11)$$

$$\frac{d[Asn]}{dt} = -K_{61}X_v\frac{[Asn]}{K_{62}+[Asn]} \quad (6\text{-}12)$$

$$\frac{d[Asp]}{dt} = X_v\left(\frac{K_{61}[Asn]}{K_{62}+[Asn]} - \frac{K_{71}[Asp]}{K_{72}+[Asp]} + \frac{K_{63}[Glc][Gln]}{(K_{64}+[Glc])(K_{65}+[Gln])}\right) \quad (6\text{-}13)$$

$$\frac{d[Ala]}{dt} = X_v\left(\frac{K_{65}[Glc][Gln]}{(K_{64}+[Glc])(K_{65}+[Gln])} - \frac{K_{81}[Ala]}{K_{82}+[Ala]}\right) \quad (6\text{-}14)$$

$$\frac{d[Amm]}{dt} = -K_{91}\frac{d[Gln]}{dt} + K_{92}X_v\left(\frac{K_{61}[Asn]}{K_{62}+[Asn]} + \frac{K_{71}[Asp]}{K_{72}+[Asp]} + \frac{K_{81}[Ala]}{K_{82}+[Ala]}\right) \quad (6\text{-}15)$$

$$\frac{dmAb}{dt} = X_v\left(K_{101} + K_{102}[Glc]\right) \quad (6\text{-}16)$$

Lactate production (equation 6-9) was assumed to be proportional to glucose consumption pre-multiplied by a yield where the latter was used to account for deviations from the assumption of zero accumulation of intermediates in glycolysis. Following the reactions listed in Table 10, ammonia accumulation was correlated to the metabolism of glutamine, asparagine, aspartate and alanine (equation 6-15).

Based on the experimental data, glucose was found to be positively correlated with the Mab production, as described in equation 6-16.

The parameters of the eleven ordinary differential equations (ODEs) (equations 6-6 to 6-16) were optimized by minimizing the sum of squared error (SSE) between experimental and model predicted results. The data of a batch culture initiated with 4 mM of glutamine (presented in Chapter 4) was used for calibration of parameters. The parameter values resulting from calibration of the model are provided in Appendix C.

The prediction ability of the model was tested with data obtained for the cultures with 0 and 8 mM initial glutamine levels. These data were not used to calibrate the model. The comparison between experiments and model predictions are shown in Figure 24. Acceptable agreement was obtained between the predictions, thus corroborating different important experimental observations: i) glutamine and glucose are co-metabolized during the culture, ii) Cell death depends on both ammonia and glucose, iii) Mab productivity is correlated with glucose and iv) Mab is produced by both growing and non-growing cells (Aghamohseni et al. 2014).

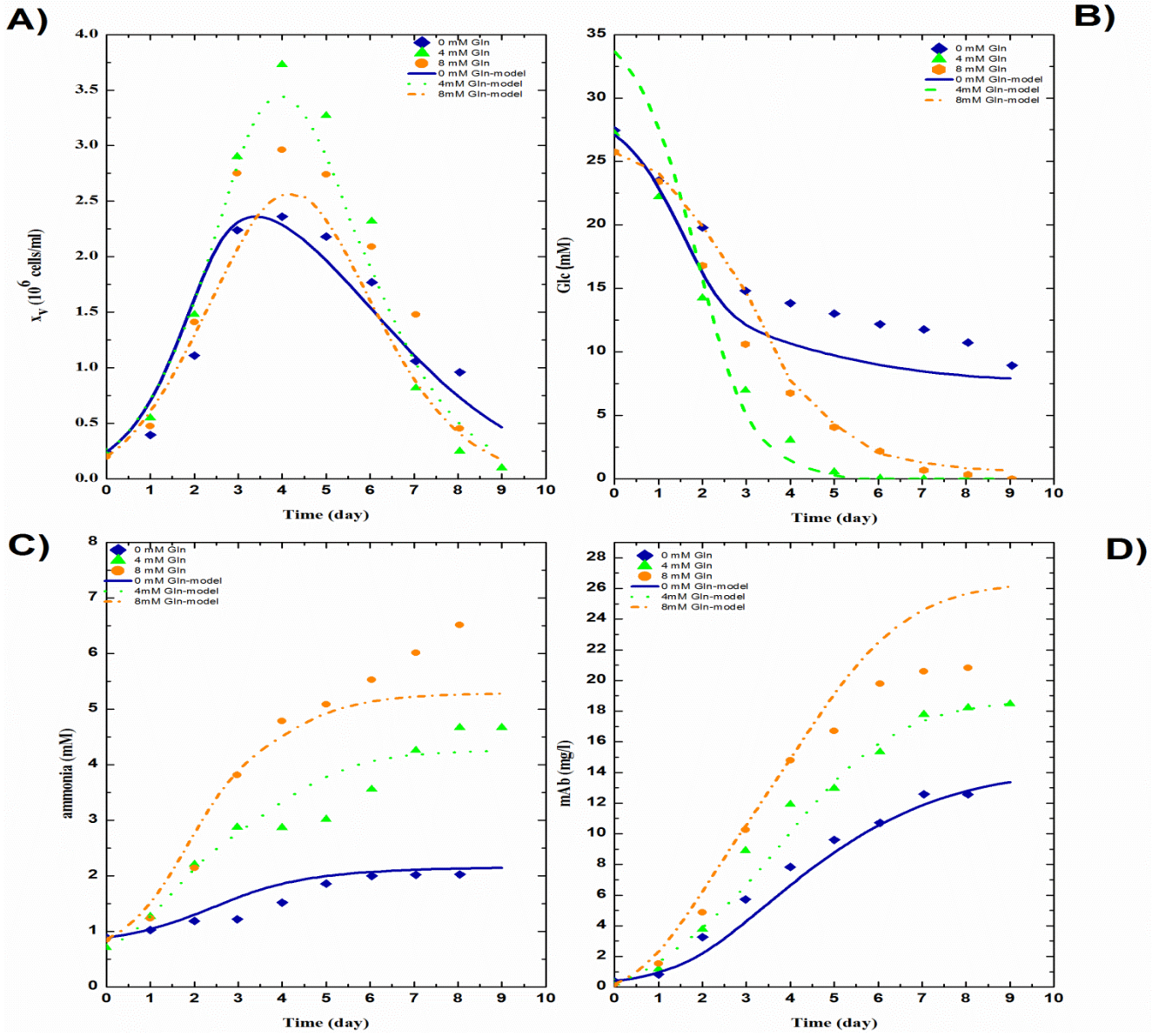

Figure 24, Results of model validation with ◆ 0 mM Gln, ▲ 4 mM Gln, and ● 8 mM Gln conditions. The data points present real data, and dashed lines present the model prediction. A) Total viable cell concentration (10^6 cells/ml); B) Glc concentration (mM); C) ammonia concentration (mM); D) mAb concentration (mg/l).

➢ *pH and Temperature Effect*

The experimental studies describing the impact of lowering pH and temperature on cell growth and protein production have been presented in Chapter 4 and Chapter 5. In this chapter the mathematical model presented in section 6.2.2 is modified to account for these effects. Although experimental studies regarding the effect of pH and temperature on cell growth and protein productivity have been previously reported (Ahn et al., 2008; Kaufmann et al., 2001; Rodriguez et al., 2010; Yoon et al., 2006), mathematical models describing these effects have not been presented as yet.

To develop a mathematical model that accounts for the effect of pH, batches initiated with different concentrations of glutamine for different pH conditions were monitored daily and regression equations representing the evolution of pH with time were obtained. In the control batch pH was not externally manipulated and pH levels never drop below a level of 6.9±0.05. For the rest of the batches, pH was manipulated by the addition of an acid to a level of 6.8±0.05. This reduction was done, as described in Chapter 3, according to either one of two strategies: i) the pH was reduced from the beginning and from the entire duration of the culture (Reduced-pH strategy) or ii) the pH lowered after the completion of the exponential growth phase (Shifted pH strategy). Our experiments and previous experimental studies (Seo et al. 2013) indicated that lowering of pH mostly impacts the cell growth. Accordingly the dependency of growing cells with respect to pH was formulated by the combination of equations 6-17 and 6-18. These equations contain two new parameters (k29 and k30), and after calibration with data they

successfully accommodated the impact of pH on the fraction of growing cells. The parameters of this equation were calibrated together with the equations presented above.

$$p_1 = 2 - \frac{1}{1 + k_{29} \exp \frac{-(pH(t) - 6.9)}{k_{30}}} \tag{6-17}$$

$$\frac{dfgr}{dt} = -p_1 K_{11} \frac{fgr}{1 + [Glc]/K_{12}} \tag{6-18}$$

In addition to its effect on cell growth, pH was also found to affect the rate of glucose depletion (Aghamohseni et al. 2014) in agreement with previous studies (Trummer et al. 2006; Seo et al. 2013). Initially it was hypothesized that this slower depletion of glucose is caused by a lower growth resulting from the reduction in pH. However, it was found that the reduction in growth alone could not explain the observed glucose depletion rate. Then, it was further argued that the lactic acid used for pH adjustment will indirectly affect the rate of glucose depletion since it may serve as an additional source of carbon. Accordingly the glucose and lactate balances were adjusted as follows:

$$\frac{d[Glc]}{dt} = -X_v \left(\frac{K_{31}[Glc][Gln]}{(K_{32} + [Glc])(K_{36} + [Gln])} + \frac{K_{33}[Glc]}{(K_{34} + [Glc])} \right) - K_{35} X_v + K_{37} F X_v \tag{6-19}$$

$$\frac{d[Lac]}{dt} = -\frac{K_{51}[Glc]}{[Glc] + K_{52}} X_v \frac{d[Glc]}{dt} + K_{38} F \tag{6-20}$$

in which F represents moles of lactic acid added per volume of culture at 24-hour intervals for pH adjustment, and K37 and K38 were new parameters added for calibration of the glucose and

lactate profiles . $K_{37}FX$, in the right hand side of the glucose balance represents a possible consumption of lactic acid by CHO as a carbon source. The remaining seven dynamic ODE equations were left unchanged.

The experiments on the effects of mild-hypothermia described in Chapter 5, indicated that cell cultivation at a lower temperature of 33ºC resulted in reduced cell growth, improved cell viability and increased mAb productivity (Rodriguez et al. 2010; Vergara et al. 2014). Thus, an Arrhenius-type dependence, equation 6-21, was introduced into the viable cells balance to describe the effect of temperature on growth (Mensonides, et al., 2014). The viable cell dynamic balance equations consist of both growing and non-growing cells and temperature was assumed to affect both groups by decreasing the specific growth rate of viable cells while extending their life span. Thus, in equation 6-22, the coefficients Q_1 and Q_2 were calibrated to capture the effects of temperature on decreasing cell growth rates and cell death rates respectively.

mAb production was also found to be affected by temperature and therefore the corresponding balance was adjusted by a pre-multiplying parameter to capture this effect. The modified equations of Xv and mAb are as follows:

$$Q = A.\exp\frac{-E}{RT} \qquad (6\text{-}21)$$

$$\frac{dX_v}{dt} = Q_1\mu_{\max}.fgr.X_v\left(\frac{[Glc]}{K_{21}+[Glc]}\times\frac{[Gln]}{K_{26}+[Gln]}\times\frac{1}{1+[Amm]/K_{23}}\times\frac{1}{1+[Lac]/K_{27}}\right)$$
$$-Q_2k_d.(1-fgr)X_v\left(\frac{1}{1+\left(K_{24}/[Amm]\right)^n}+\frac{K_{25}}{[Glc]}\right)$$

(6-22)

.

$$\frac{dMab}{dt} = Q_3X_v\left(K_{101}+K_{102}[Glc]\right) \quad (6\text{-}23)$$

Equation 6-23 presents the effect of temperature on the mAb productivity at mild-hypothermia conditions as it was observed that mild hypothermia improved the specific mAb productivity consistently for over 9 days of cultivation. The remaining eight ODE equations were left unchanged and the parameters of the model were re-optimized. The optimized parameters are shown in Appendix C.

The prediction ability of the modified dynamic model was tested with data obtained from the cultures with 4 Mm glutamine with the Reduced-pH strategy, 4 and 0 mM glutamine with the Reduced-Temperature strategy and, 4 and 0 mM glutamine with the Shifted-Temperature strategy. These set of experiments were not used to calibrate the model. The compared experiments and model predictions are presented in Figure 25, Figure 26, and Figure 27 indicating good agreement with the experimental data. The differences between mAb

measurements and their corresponding predictions can be partially explained by the occurrence of an approximate 20% error in the ELISA analysis.

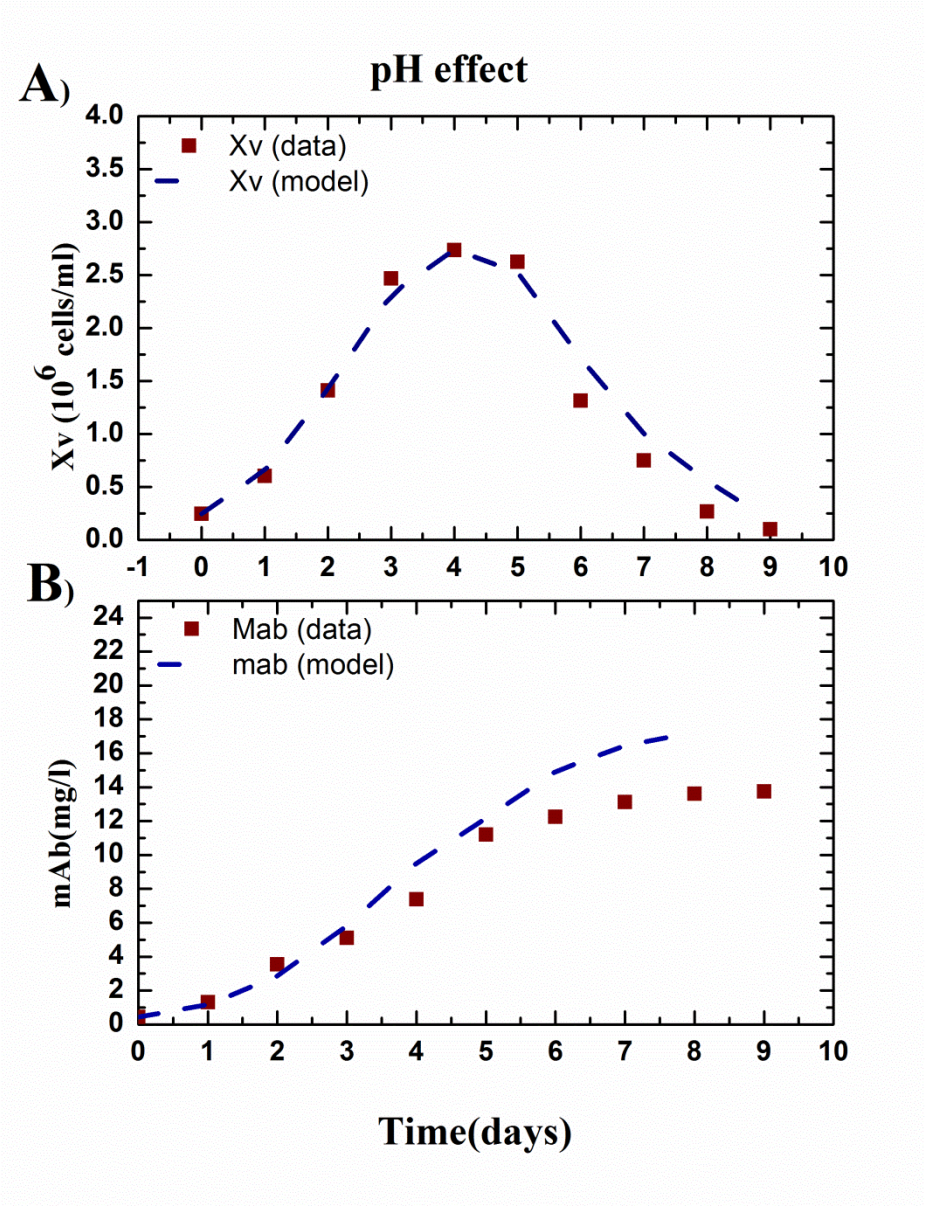

Figure 25, Results of dynamic model validation with initial 4 mM and Reduced-pH experiment. The data points present real data, and dashed lines present the model prediction. A) Total viable cell concentration (10^6 cells/ml), B) Mab concentration (mg/l).

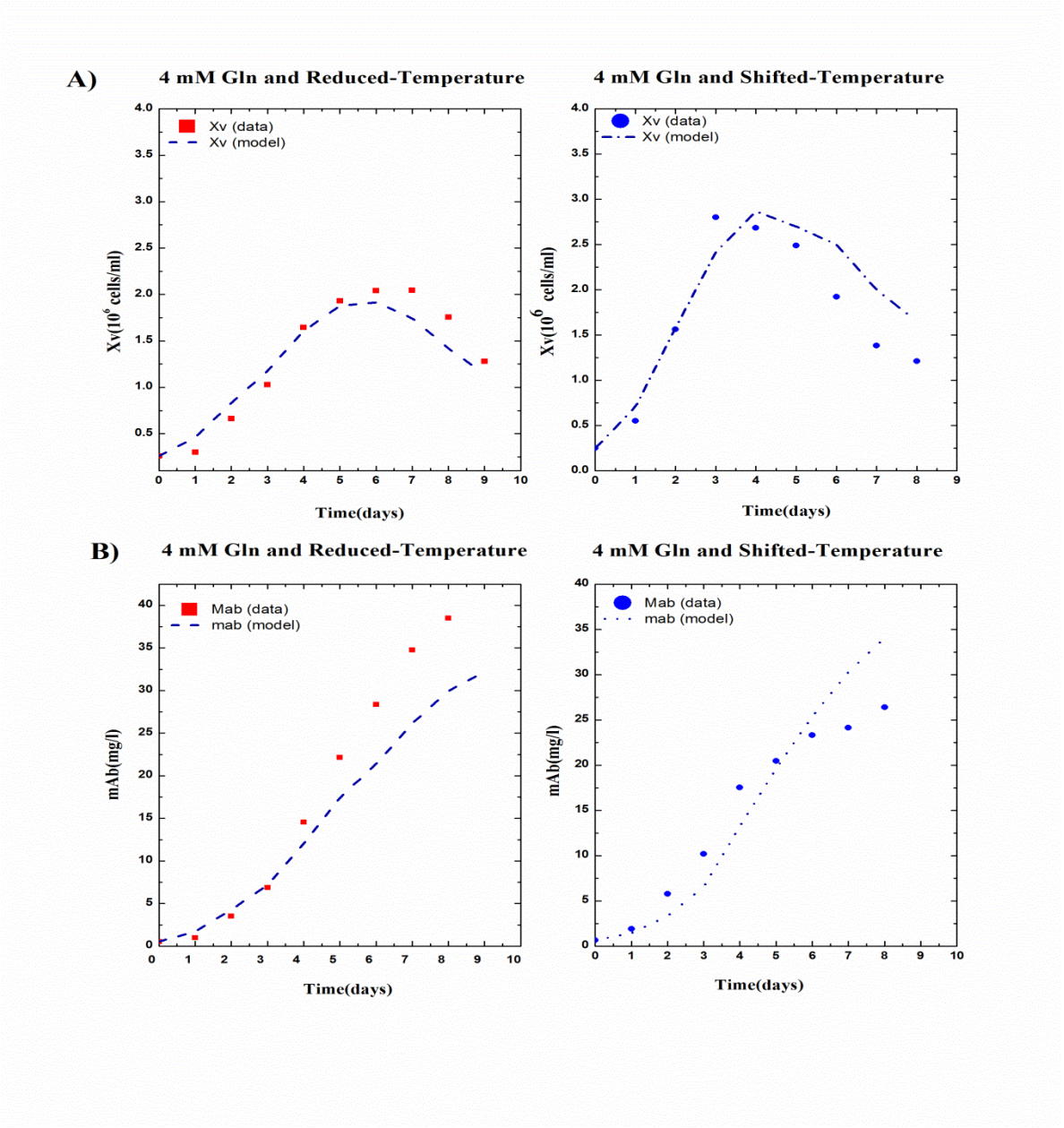

Figure 26, Results of dynamic model calibration with initial 4 mM glutamine and model prediction for 4mM glutamine and Reduced-Temperature and Shifted-Temperature experiments. The data points present real data, and dashed lines present the model prediction. A) Total viable cell concentration (10^6 cells/ml), B) mAb concentration (mg/l).

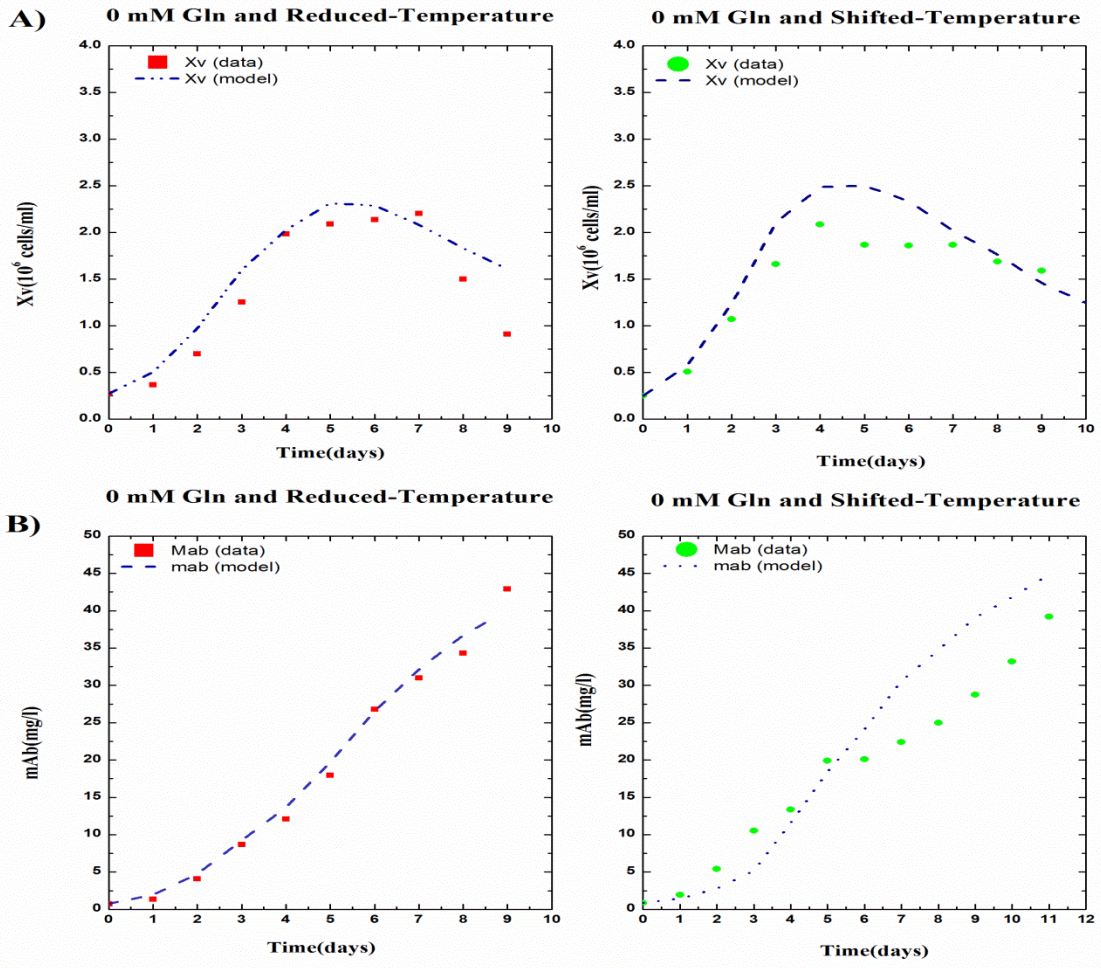

Figure 27, Results of dynamic model calibration with initial 4 mM glutamine and model prediction for 0 mM glutamine and Reduced-Temperature and Shifted-Temperature experiments. The data points present real data, and dashed lines present the model prediction. A) Total viable cell concentration (10^6 cells/ml), B) mAb concentration (mg/l).

6.3 Modeling of the Glycosylation Process

The glycan profile of mAb expressed by a particular cell line in a culture may be affected by different factors such as the cells' environmental conditions, the method of culture, and the host cell line (Restelli and Butler 2002; Hossler 2012). Thus, it is necessary to identify the culture conditions that control the bioprocess for synthesizing mAbs with the desired spectrum of glycans. An appropriate model with the capability of correlating the mAb glycan profile to the cell culture conditions can be useful for bioprocess design and control, culture media formulation, and possible genetic engineering strategies (Del Val, et al., 2011).

In view of the above, the purpose of the present section is to develop a systematic approach for manipulating cell culture conditions so as to produce a desired glycan profile. To achieve this goal, a mathematical modeling approach was proposed that allowed correlating the extracellular culture conditions to the resulting galactosylation of the antibody. This model can thus serve to control the glycosylation process.

Although several studies have been conducted to evaluate the effects of culture conditions on glycan profiles, including the impacts of particular nutrient concentrations such as glucose, glutamine, and galactose (Burleigh et al. 2011; Taschwer et al. 2012; Grainger and James 2013; Liu et al. 2014), culture supplementation and inhibitors such as ammonia (Yang and Butler 2002; Chen and Harcum 2006; Crowell et al. 2007), nucleotide sugar feeding (Gu and Wang 1998; Wong et al. 2010) and, environmental pH and temperature alternation (Yoon et al. 2005; Ahn et

al. 2008; Rodriguez et al. 2010; Seo et al. 2013), studies exploring how the combination of these factors affects the glycosylation are not numerous. Models reported in the literature mostly focused on the glycosylation process occurring in the Golgi (Hossler et al., 2006; Del Val et al., 2011) but did not discuss the interconnection between the culture conditions and the glycosylation of the proteins. For example, Del Val et al., (2011) presented a model describing the N-glycosylation process occurring within the Golgi apparatus while considering the transport of nucleotide sugar donors from the cytosol to the Golgi lumen. However, this model was not coupled to the culture conditions (Del Val et al., 2011) while such coupling is essential for model based control because the process can be manipulated solely through these conditions.

Association of extracellular conditions to the intracellular glycosylation process has been implemented in our group based on a developed comprehensive matrix of reactions for the glycosylation process in mammalian cells (Hossler et al. 2006). This novel dynamic consists (Figure 28) of three main sub-models: i) a metabolic flux analysis (MFA) based dynamic model, ii) a nucleotide sugars model and iii) a glycosylation model in the Golgi apparatus (Ohadi et al. 2013). The predicted results of temporal glycosylation indices were in good agreement with the experimental glycosylation indices of mAbs produced by CHO cells under batch condition with two initial glutamine concentrations. However, this model is of very high dimensions involving over 100 differential equations and a large number of calibration parameters thus making it difficult to fit for a wide range of operating conditions. Therefore, this research study is being further investigated in our group.

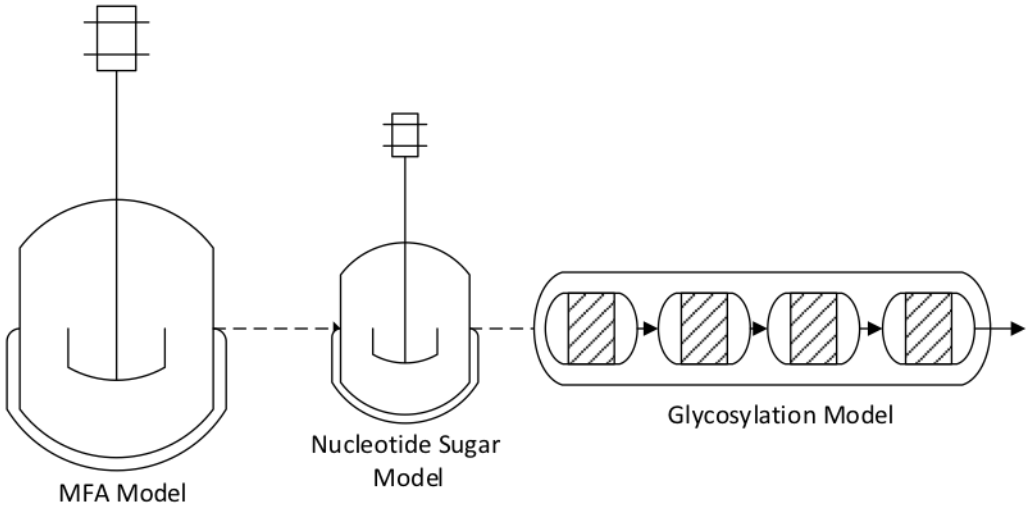

Figure 28, Schematic representation of the comprehensive model: Metabolic Flux Analysis (left), Nucleotide Sugar (center), Glycosylation based on Golgi Maturation (right) (Ohadi et al. 2013)**.**

More recently, Jedrzejewki et al., (2014), presented a model frame work connecting the extracellular conditions to the intracellular nucleotide sugar donors and glycosylation process for a mAb produced by a hybridoma cell line (Jedrzejewski et al. 2014). However, the model of Jedrzejewki et al was only calibrated to experiments of one single batch and its prediction ability has not been investigated.

Although, the mechanistic models of (Ohadi et al. 2013) and (Jedrzejewski et al. 2014) are rigorous but require a very large number of parameters thus requiring large data sets for calibration and making it difficult to accurately estimate the parameters. The other challenging aspect of this type of modeling is that, it requires measurements of intracellular nucleotides and nucleotide sugars and those measurements require collecting large volumes of cell culture

supernatants that impact the evolution of the culture. Also, the nucleotide sugars data available in this work have been found to be very noisy. To circumvent the problems associated to the mechanistic models, we propose in the next section a semi-empirical model that can still serve to correlate the extracellular culture conditions and glycosylation while avoiding the very challenging parameter estimation task required for a more rigorous model.

6.3.1 Glycosylation Model

➢ *Mathematical Model Development*

A semi-empirical glycosylation model was developed to explain the experimental observations presented in Chapters 4 and 5 in terms of correlations between extracellular culture conditions and the level of mAb galactosylation. Although the current model cannot predict the level of sialylation, it can be expanded in future to accomplish this goal. The proposed semi-empirical model consists of two parts: i) a dynamic balance of a lumped quantity representing the total nucleotide sugar intracellular concentration ii) a static correlation to predict the galactosylation index as a function of parameters that are expected to affect this index such as the nucleotides sugars levels, the specific antibody productivity and the glucose level. These two components of the model are given by equations 6-24 and 6-25 respectively:

$$\frac{dSug}{dt} = a_1 \mu(t)^m \frac{[Glc]^p}{a_2 + [Glc]} (1 + [G\ln])^q - a_3([Sug]) \quad (6\text{-}24)$$

$$GI^{inst} = \frac{1}{(S_p(t) + a_4)^r} \left(\frac{[Glc]\ [Sug]}{(a_5 + [Glc])(a_6 + [Sug])}\right) \quad (6\text{-}25)$$

where $[Sug]$ is the lumped concentration of all types of nucleotide as nucleotide sugars present within viable cells at one-day intervals. GI^{inst} represents a galactosylation index resulting from the galactosylation process occurring within the Golgi at a particular time interval. These equations only predict the GI for a specific time instance but do not consider the accumulation of glycan concentration along the culture cultivation. Then, the average galactosylation index of the mAb present in the batch culture at any given time requires the calculation of a cumulative average based on the productivity and the instantaneous GI values given by 6-25 as described later in this section.

The Nucleotide sugar model, equation 6-24, was assumed to be a function of extracellular glucose and glutamine concentrations, and the specific growth of CHO-DUXB cells cultivated at different culture condition. The effects of glucose availability on the nucleotide sugar pools have been reported previously (Grammatikos,et al., 1998; Jedrzejewski et al., 2014; Liu et al., 2014; Valley et al., 1999). In addition, it has been found that glucose and glutamine are co-metabolites for the current cell line (Ohadi et al. 2013; Aghamohseni et al. 2014). The assumed dependency of the nucleotides sugars synthesis term on growth rate is based on the fact that these sugars are

synthesized from nucleotides which serve as substrates for nucleic acids' that are needed for biomass formation (Jedrzejewski et al. 2014).

equation 6-25 is dependent on the lumped nucleotides' sugar level solved by equation 6-24, specific mAb production rates and extracellular glucose concentrations. The dependency of galactosylation on nucleotides sugars is evident since the latter are substrates for all the glycosylation reactions (Gu and Wang 1998; Valley et al. 1999; Wong et al. 2010; Ohadi et al. 2013). The assumed effect of specific productivity on galactosylation is based on the fact that the productivity will determine the residence time of proteins within the Golgi thus determining the extent of glycosylation. A large residence time is expected to result in a high glycosylation. For example, we observed that at lower temperature conditions the specific mAb productivity was consistently higher for the entire duration of the batch as compared to the control culture (Chapter 5) while the galactosylation was lower. This observation is in agreement with the assumption that a higher productivity implies a smaller residence time of protein through the Golgi complex and reduced exposure time to the galactosyltransferases present in the Golgi complex (Wang et al. 1991; Butler 2006a). The third parameter on the GI^{inst} model is [Glc]. In our earlier study we have demonstrated that higher availability of glucose in the batches initiated with lower pH and glutamine concentrations resulted in the availability of glucose for longer time periods and further glycosylation (Ohadi et al. 2013; Aghamohseni et al. 2014). The glucose availability also has been reported to affect the site occupancy or macro-heterogeneity of the glycan profile through alteration of lipid-linked oligosaccharides (Rearick et al. 1981; Liu et al.

2014). As glucose itself is involved as a substrate in the synthesis of nucleotide and nucleotide sugars, a Michaelis-Menten expression involving glucose was assumed for this reaction.

As mentioned, equation 6-25, depict the instantaneous GI level in one individual cell while the GI measurement of a supernatant sample will reflect a cumulative value of the glycosylated mAbs cultivated consistently until the time of sample analysis. In order to convert the predicted value of GI^{inst} into a cumulative GI^{Acc}, the following equation is used:

$$[GI]^{Acc} = \frac{\int_0^t \overset{*}{mAb}\,[GI]^{inst}\,dt}{\int_0^t \overset{*}{mAb}\;dt} \tag{6-26}$$

in which mAb is the concentration of mAb produced in one day interval. The parameters of the above two equations were optimized by minimizing the sum of squared error (SSE) between experimental and model predicted results. The data of batch cultures initiated with 4 mM and 0 mM glutamine for control conditions (normal pH conditions and 37˚C), for reduced pH and for reduced temperature were used for calibration of parameters. In addition, the initial value for GI and $[Sug]$ at time=0 was also estimated by the two model-equations. For brevity, the parameter values are provided in the Appendix D.

Figure 29, presents the value of GI predicted by the index model in comparison with the experimental data. The developed index model was able to successfully capture the galactosylation index profile during the course of the culture. The maximal errors were of the

order of 10%. In addition, this model covered a variety of culture conditions, glutamine effect, pH effect and temperature effect. Some of the discrepancies between data and model predictions under mild-hypothermia conditions can be explained by the fact that for simplicity the effect of lower temperature on expression level of glycosyltransferase enzymes was not considered in this approach (Sou et al. 2014).

In summary, our approach for developing a semi-imperial model was successful enough to correlate the effects of different culture condition and galactosylation indices. This mathematical frame work can be extended for other conditions as well for control the glycosylation process.

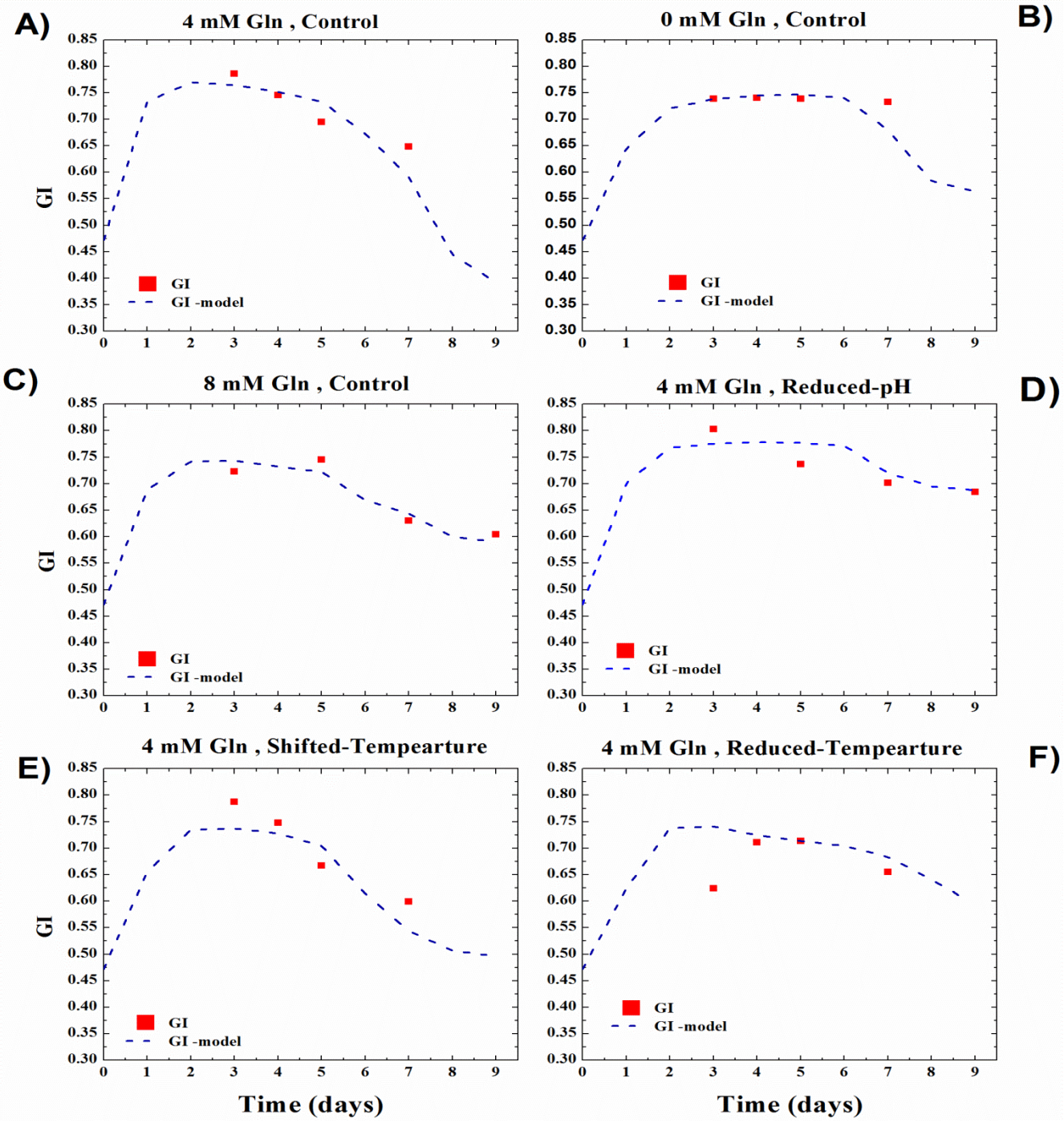

Figure 29, Profile of experimental and predicted GI at different culture conditions. Data points presents experimental data and dash lines display model observations , A) 4 mM glutamine without pH and temperature; B) 0 mM Gln without pH and temperature; C) 8 mM glutamine without pH and temperature D) 4 mM glutamine and Reduced-pH to 6.8 ; E) 4 mM glutamine and Shifted-Temperature to 33˚C ; F) 4 mM glutamine and Reduced-Temperature to 33˚C.

Chapter 7

Conclusion and Future Work Suggestions

7.1 Conclusion

Monoclonal antibodies (mAbs) are one of the key therapeutic glycoprotein products in the pharmaceutical industry. However, production of these glycoproteins is associated with many challenges in terms of productivity and quality. The glycan conformations are important quality-measurements because they can influence the biological characteristics of mAb including secretion, solubility, receptor recognition, antigenicity, bioactivity and pharmacokinetics. The post translational process of glycosylation can be affected by many environmental conditions and it can be quantified in terms of site–occupancy (macro-heterogeneity) or in the structure of added glycans (micro-heterogeneity).

The goal of this research was to investigate the impacts of different cell culture parameters on the glycosylation pattern of a novel mAb, Eg2-hFc, produced by a newly developed cell line, CHO DUXB. Then, based on the experimental observations, the goal was extended to develop a mathematical model that could serve in the future to control and optimize the glycosylation process. It was argued that a model relating culture conditions including essential nutrient levels,

byproduct concentration as well as pH and temperature conditions to the resulting glycoprofiles, may serve in the future to calculate a set of operating conditions to obtain a desired glycan distribution. The following discussion summarizes the challenges and approaches that have been pursued to establish connections between the cell metabolism and the glycosylation processes to provide a systematic approach for controlling glycan profiles.

The thesis is organized into 7 Chapters. Chapters 1, 2 and 3 present and introduction to the problem, a literature review and the materials and methods used in the experimental and modeling studies.

In **Chapter 4** the effects of glucose, glutamine, ammonia and pH levels on growth, mAb productivity and the glycans' evolutions were studied. Cells were cultivated at 0, 2, 4 and, 8 mM of initial of glutamine and 25 mM of glucose. We found that increasing the initial level of glutamine from 0 to 8 mM glutamine for a constant level of glucose, resulted in higher consumption rate of glucose and consequently lower galactosylation levels. The faster depletion of glucose was associated to a co-metabolic consumption of glutamine and glucose mostly related to the requirement of both metabolites for biomass formation. It has been previously reported that a reduced level of intracellular uridine triphosphate N-Acetyl glucosamine (UDP-GlcNAc) is the main reason for the lower level of glycosylation in both glucose and glutamine depleted media (Nyberg et al. 1999). Although, increasing the level of glutamine from 0 mM to 4 mM resulted in a lower level of GI, it improved the cell growth and a higher peak of cell density was observed when cells were cultured with 4 mM initial glutamine. Increasing the

initial glutamine concentration to 8 mM was found to slightly inhibit cell growth possibly due to the high concentration of ammonia resulting from glutamine conversion. In addition, since the mAb specific productivity was found to be correlated with growth, an increase of initial glutamine from 0 mM to 4 mM resulted in more mAb but lower GI. Hence, there was a clear tradeoff between increasing mAb productivity versus reaching a higher level of galactosylation which is often preferred in mAbs' therapeutic applications.

The sialic acid content of N-glycans is also important in the regulation of anti-inflammatory immune response of IgG (Anthony et al. 2008) and improvement of the serum half-life of therapeutic proteins (Butler 2006b). Thus, we investigated ways to affect the sialylation especially through the concentration of ammonia. The experiments showed that higher ammonia levels resulting from cultures initiated with higher glutamine concentrations led to less galactosylation and less sialylation. In addition, since some of the experiments with different levels of ammonia resulted in similar levels of pH, it was possible to discern between the effects of pH and ammonia on sialylation. Previous reported studies in the literature have hypothesized that the mechanisms by which pH and ammonia affect sialylation are indeed different. For example, it was reported that ammonia is correlated with the synthesis of UDP–GlcNAc which may in turn inhibit sialic acid transport (Valley et al. 1999). To further investigate the individual effects of ammonia and pH and their possible correlation to the glycosylation process, we designed and conducted a series of experiments and analyzed the experimental results by a computer code (GLYCOVIZ) that calculates the level of reactions for all possible glycosylation

reactions occurring within the Golgi. The experiments consisted in adding a lactic acid solution for lowering pH to a level of 6.8±0.05 for batches started with 4 mM glutamine and 25 mM glucose (Chapter 3). Then, the GLYCOVIS (Hossler et al. 2006) software was used to elucidate the individual mechanisms by which ammonia and pH affect the galactosylation and sialylation levels. Cultivation of cells at lower pH showed that the effect of pH was independent of changes in ammonia. pH reduction increased the GI and SI levels but at the cost of a reduction in Mab productivity. Then, once again there is a tradeoff between productivity and the desired glycosylation levels. Based on the GLYCOVIS analysis, pH is likely to impact sialylation through the activity of the sialyltransferases. Thus, besides availability of glucose and glutamine, ammonia and pH play crucial roles on GI and SI evolution for this specific cell line.

In **Chapter 5**, we examined the impacts of mild-hypothermia on cell growth, metabolic profile, mAb production and, mAb glycosylation process. It was initially hypothesized that reducing the temperature will slow down the passage of mAbs through the Golgi thus increasing glycosylation levels but without affecting the overall batch productivity of mAb. In that way one could improve both mAb productivity and glycosylation levels in contrast with manipulation of nutrients or pH that resulted, as shown in Chapter 4, in a trade-off between productivity and glycosylation. Two strategies were applied to investigate the effect of the lower temperature of 33˚C, i) cultivation cells at 33˚C consistently for 10 days ii) shifting temperature from the optimum of 37˚C to 33˚C on day 3 of culture when cells were still in their exponential phase of their growth according to the explained method in Chapter 3**.** Batches with 4 mM and 0 mM

initial glutamine concentrations were selected for investigating temperature impacts as we observed in the studies summarized in Chapter 4 that high level of GI and SI occurred for 0 mM initial glutamine whereas high levels of mAb and cell population occurred at 4 mM glutamine. It was found from these experiments that reducing the temperature of the culture to 33˚C, either from the beginning (Reduced Temperature strategy) or after the exponential phase of growth (Shifted Temperature strategy) and regardless of the initial level of glutamine, had a significant effect on cell growth, mAb productivity and glycosylation profile. Cell growth was, as expected, lower at 33˚C while cell viability remained high for a longer time of cell cultivation. In contrast to other reports regarding the increase (Yoon et al. 2003) or the decrease (Sou et al. 2014) of glucose metabolism at lower temperature, the specific glucose consumption rate did not change in our experiments. In the other word, the yield of cell formation per glucose consumption during the exponential phase of growth was equal to 0.12 (10^6 cells/mM Glc) for all batches. However, the yield of cell formation per glutamine consumption in the exponential phase of growth decreased under hypothermia conditions. This value was 1.02 (10^6 cells/mM Gln) for control condition, 0.68 (10^6 cells/mM Glc) for Shifted-Temperature, and 0.48 (10^6 cells/mM Glc) for Reduced-Temperature respectively. Thus, glutamine appears to be utilized for protein production rather than for cell growth at lower temperatures as we found significant improvements in mAb production. So, the requirements of glutamine and glucose for biomass formation seem to be different when operating at 33˚C versus normal temperature levels. The maximum volumetric productivity was equal to 0.2 (mg/L.h) for both batches cultivated at 0 and 4 mM glutamine and

the Reduced-Temperature condition, i.e. the temperature was reduced from the beginning of the batch. The improved mAb concentration was not because of extended culture longevity, but to a marked increase of specific mAb productivity. Although mild hypothermia was favorable for mAb production, it was not helpful for increasing the level of glycosylation. It is argued that a reduction of the residence time of mAbs through the Golgi apparatus due to a higher rate of production at lower temperature resulted in a lower value of GI compared to control conditions. This fact was confirmed by the experiments and explicitly considered in the development of the semi-empirical model presented in Chapter 6. The GI and SI trends with culture time were different for 4 and 0 mM glutamine under Reduced-Temperature and they reached a low value on day 3 and gradually rose until day 5, in contrast with the monotonically decreasing trend that was observed for the control condition.

In **Chapter 6**, a modeling framework was proposed to correlate extracellular culture conditions to the intracellular mAb glycosylation. Based on the observations presented in chapters 4 and 5 regarding the effects of nutrient availability, ammonia, specific productivity, temperature and pH conditions on the glycosylation of Eg2-hFc mAb, we formulated a model with the capability of correlating the mAb glycan profile to the aforementioned factors. We argue that this model would be useful for glycosylation control and optimization. The model consists of two sub-models where the first sub-model describes the extracellular metabolites evolutions with time and the second sub-model correlates the outputs from the first part of the model to the glycosylation levels. For the first sub-model the most dominant metabolic pathways

of CHO cells was in terms of energy and biomass formation were considered and a metabolic flux analysis was performed. The fluxes were calculated based on a quadratic programming formulation where a norm of the differences between measured and predicted consumption and production rates of metabolites was minimized. Based on the dominant fluxes, nine different micro-reactions were formulated. According to these macro- reaction and based on the experimental results eleven dynamic balances for cell growth, cell death, amino acids, ammonia, lactate and mAb profiles were formulated. The calibrated dynamic models were found in good agreement with experimental data. They correctly described the co-metabolism of glucose and glutamine, the dependency of death rate with respect to ammonia and glucose depletion and the correlation of mAb to cell growth and availability of glucose. Subsequently, the model was successfully modified to describe the effects of reduced pH and temperature conditions on cell growth and metabolites dynamic profiles.

To correlate the outputs from the first sub-model with the glycosylation conditions we initially formulated in collaboration with another member of our research group, a mechanistic model that takes into account detailed balances of nucleotides and nucleotides sugars and all possible glycosylation reactions occurring in the Golgi. Although this model was very rigorous, but it was of very high dimensions and has been found to be very difficult to calibrate for the different operating conditions used in the experiments. I co-authored a paper on the subject but I have not used it in this thesis due to the aforementioned calibration challenges (Ohadi et al. 2013). Instead, a second sub-model consisting of a semi-empirical formulation was constructed

to correlate the culture conditions to glycosylation. This semi empirical model uses a dynamic balance of a lumped sum of nucleotides sugars thus assuming that the nucleotides sugars are correlated with each other. Then, the concentration of nucleotides sugars calculated from this balance is used as an input for an equation that represents the instantaneous galactosylation process occurring in the Golgi. In terms of time scale the galactosylation process is assumed to be instantaneous because it represents the passage of the antibody through the Golgi apparatus where the glycosylation reactions occur while, the dynamic balances for nucleotides are representing reactions occurring during the life of one cell. The nucleotide sugar concentration $[Sug]$ is solved at one day interval as a function of glucose and glutamine concentrations and the specific growth rate of that day. The dependency of the nucleotides synthesis on growth rate is based on the recognition that nucleotides sugars derive from nucleotides where the latter are mostly used for cell growth. The GI^{inst} model correlates to $[Sug]$ profile, glucose concentration and mAb specific productivity. The combination of this model was accomplished to predict the galactosylation indices for a wild range of culture condition over 7 days of cell cultivation. Considering the simplicity of this semi-empirical model, the agreement between experiments and model predictions was acceptable. For example the model correctly predicted the trends of the cumulative GI for cultures operated at both normal and reduced temperature conditions.

From the research presented in this thesis it can be concluded that cell culture environment has notable impacts on the glycan distribution of the new developed camelid humanized mAb. However, there are clear trade-offs between glycosylation levels and productivity thus implying

that productivity has to be sacrificed for higher therapeutic efficacy that is obtained with higher glycosylation. For example, higher initial glutamine levels resulted in better growth and productivity but less galactosylation and sialylation due to glucose deprivation and ammonia accumulation respectively. Similarly low temperature operation increased the specific productivity but negatively impacted the glycosylation.

7.2 Future Work Suggestions

7.2.1 Use of a Controlled pH and Temperature Bioreactor

The results presented in this research (Chapter 4 and 5) rely on shaker flask batch cultivation. The control of pH in shaker flask was approximately achieved by manual periodic additions of acid thus resulting in oscillations in pH between instances of acid addition. On the other hand, pH can be closely monitored and controlled in a bioreactor. In addition oxygen concentration can be adjusted at optimum level for controlling the glycosylation process. This may allow for more accurate assessment of the effect of different levels of pH for extended periods of time and for collecting data that is more repeatable for the purpose of model calibration. However, volume effects and shear stress are additional factors that may negatively impact glycosylation (Senger and Karim 2003; Ivarsson et al. 2014).

7.2.2 Use of Fed-Batch and Perfusion Operations

In Chapter 6, it was demonstrated that both the extracellular metabolites and the glycosylation levels are strongly dependent on the level of glucose. In fed-batch cultures, glucose is typically maintained at low levels but away from zero concentration by carefully controlled feeding strategies according to the cell's requirements for appropriate cell growth and maximal productivity to obtain a unique glycan profiles. Maintaining the major carbon sources at low concentrations leads to keep the concentrations of toxic metabolic by-products such as ammonia

at low levels (Butler 2006a). In perfusion cultures, the constant supply of nutrients and continuous or intermittent removal of media result in higher cell densities. An optimum dilution rate may exist that provides acceptable mAb productivity due to prolonged cell viability and, at the same time, a high residence time of proteins within the cells (Golgi) to produce more completely glycosylated products.

7.2.3 Cell Adaptation to a lower Temperature conditions

In Chapter 5, it was indicated that temperature has a significant effect on increasing the specific mAb productivity of the current cell line. However, the increase in the product titre was accompanied by a significant decrease of cell growth. Isolation of a cell population which is adapted to grow at lower temperature may allow for extending glycosylation evolution through reducing the specific productivity, i.e. lower residence time, while maintaining a high level of mAb concentration because of higher cell growth of the adapted culture. Fast growing cells can be selected during continuous passaging while cell cultivation performs at a lower temperature such as 33˚C.

7.2.4 Improvement of the Glycosylation Model

It has been reported by other researchers that Mild hypothermia condition influences the expression level of galactosylation enzymes involved in the process of glycosylation (Sou et al. 2014). Additionally, the evolution of glycosylation processes occurring in the Golgi apparatus

could be affected by changes in the enzymatic activity under lower pH conditions. These factors could be integrated into the models presented in Chapter 6 to better describe the experimental results. This will require the experimental analysis of enzyme levels which is currently pursued at the University of Manitoba.

7.2.5 Real Time Glycosylation Monitoring

As it was presented in Chapters 4 and 5, glycosylation is a crucial property of mAb that usually drops towards the end of the batch culture due to lack of nutrient availability and ammonia accumulation. The other culture environment including, oxygen concentration, pH and temperature levels also can influence the final product quality. In addition GI value is not constant during cell cultivation (except for glutamine free condition) and usually drops till the end of batch operation. Accumulation of mAb at the end of batch or fed-batch operation would induce protein aggregation or glycan removal due to activity of sialidase enzyme released by lysed cells. These expected changes in glycosylation along the culture require proper monitoring if control of the process is desired. Recent industrial research has focused into real time online monitoring techniques with the ability to reflect the culture variation into product quality in real time. For example, researchers of the Amgen pharmaceutical company combined the micro sequential injection (μSI) system with an ultra-performance liquid chromatography (UPLC) system in an attempt to perform real-time monitoring of the antibody glycan profile (Tharmalingam, et al., 2014).

Appendix A

Metabolites and glycosylation Indices profiles with HCl pH adjustment

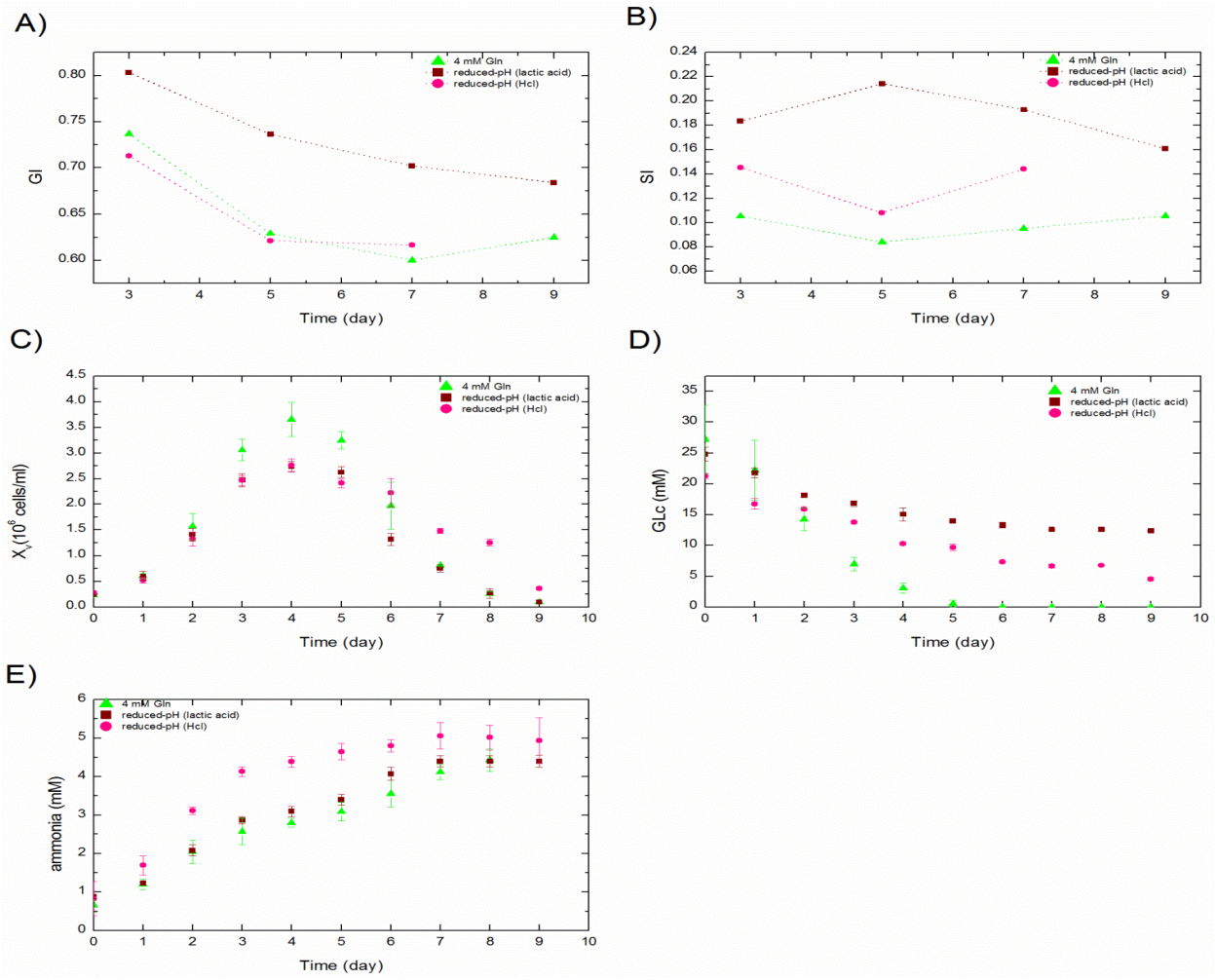

Metabolite profiles of reduced- pH by HCl addition. Closed symbols: ▲ 4 mM glutamine, ■ reduced-pH (lactic acid), ● reduced-pH (HCl). A) GI level, B) SI level, C) cell growth profile, D) glucose profile, E) ammonia profile.

Appendix B

HILIC Profiles of Glycans

Appendix A, HILIC profile of glycan analysis for cultures supplemented with different level of glutamine and cultivated at different pH adjustment by lactic acid. A) day 3, B) day 5, C) day 7 , D) day 9

A) ***Glutamine Effect (day 3)***

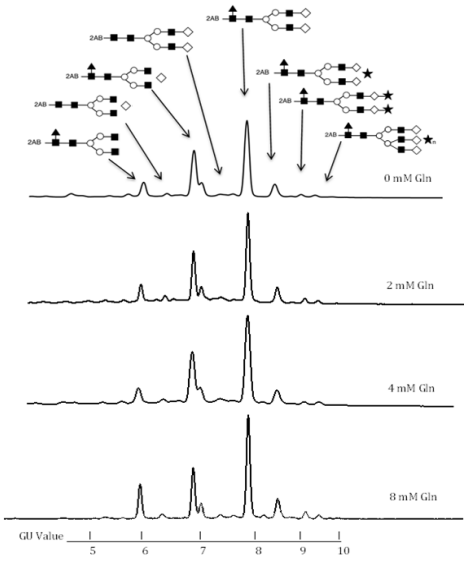

B) ***Glutamine Effect (day 5)***

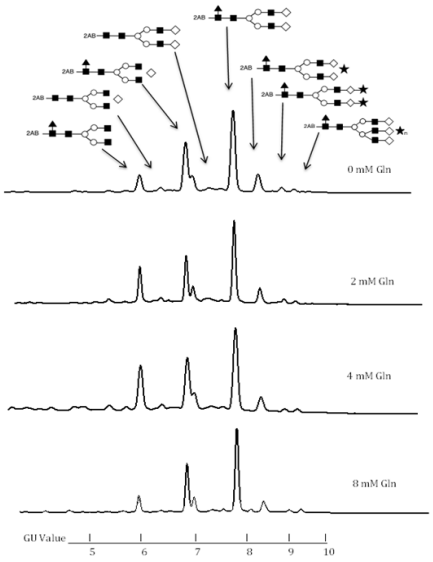

C) *Glutamine Effect (day 7)*

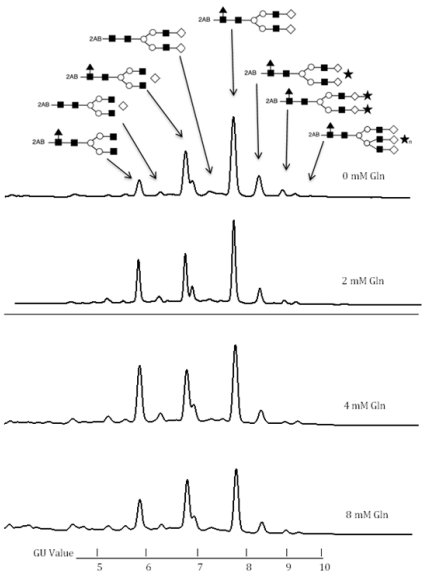

D) *Glutamine Effect (day 9)*

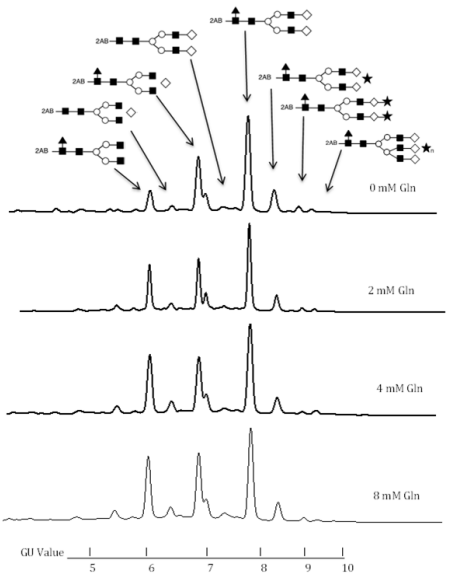

A) *pH Effect (day 3)*

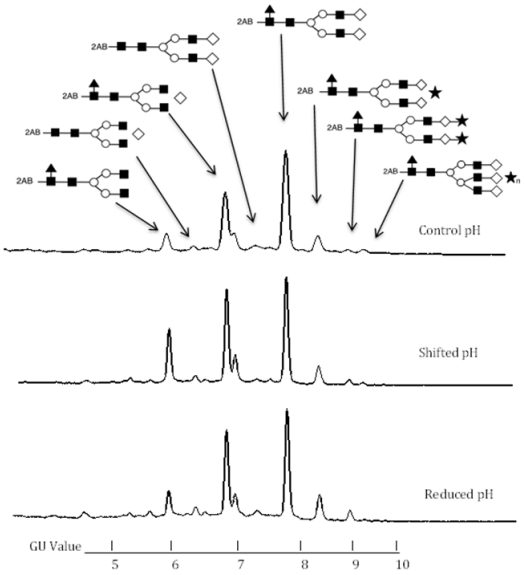

B) *pH Effect (day 5)*

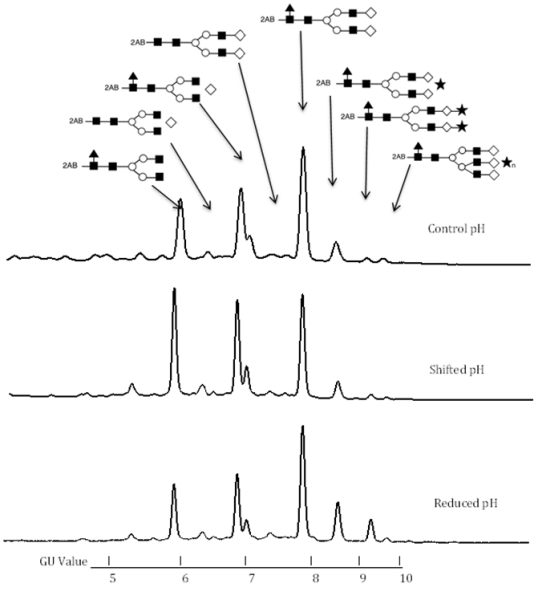

C) *pH Effect (day 7)*

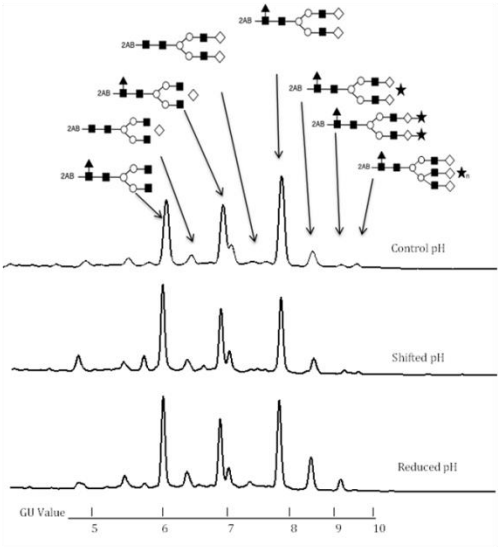

D) *pH Effect (day 9)*

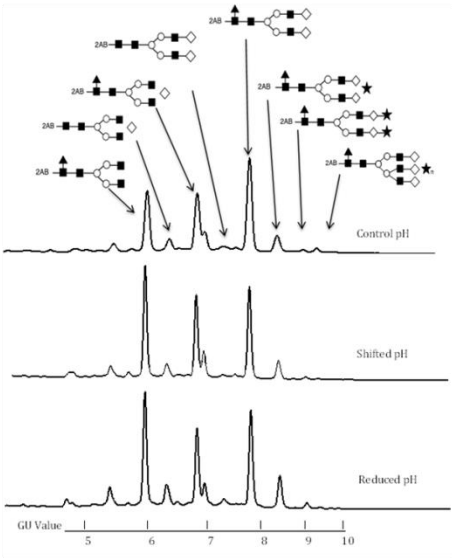

Appendix C
Metabolic Pathways

Appendix B, the general metabolic pathways of CHO DUXB cell line

Flux Numbers	*Metabolic Pathways Reactions*
j1	*GLC→ 2PYR + 2NADH + 2ATP*
j2	*PYR→ AcCoA + CO2+NADH*
j3	*AcCoA + OAA→ aKG + NADH + CO2*
j4	*aKG→ SuCCoA+ NADH + CO2*
j5	*SuCCoA→ FUM + NADH*
j6	*FUM→ OAA + NADH*
j7	*OAA⇔ PYR + NADPH + CO2*
j8	*PYR + NADH→ LAC*
j9	*THR→ PYR + CO2 + NH3 + 2NADH*
j10	*2GLY→ SER+CO2+NH3 + NADH*
j11	*SER→ PYR+NH3*
j12	*PHE→ TYR + NADH*
j13	*TYR→ FUM + 2AcCoA + NH3 + CO2 + NADPH*
j14	*VAL→ SuCCoA + CO2 + NH3 + NADPH*
j15	*THR→ SuCCoA + NH3*
j16	*ILE→ SuCCoA + AcCoA + NADPH + NH3*
j17	*MET + O2→ SuCCoA + SO2 + NADPH + NH3*
j18	*LEU→ NH3 + 3AcCoA + NADPH*
j19	*LYS→ 2 AcCoA + 2CO2 + 2NADPH + 2NH3*
j20	*HIS→ GLU+2NH3+CO2*
j21	*ARG→ aKG + 2NH3 + UREA + 3 NADH*
j22	*GLU + ATP + 2 NADPH→ PRO*
j23	*ASN→ ASP + ATP + NH3*
j24	*GLN + ASP + 2 ATP→ ASN + GLU*
j25	*GLN⇔ GLU + ATP + NH3*
j26	*GLU⇔AKG + NADPH + NH3*
j27	*PYR + GLU→ ALA + AKG*
j28	*GLU + OAA→ ASP + AKG*
j29	*CYS + O2→ PYR + SO2 + NADH + NH3*
j30	*ALA→ PYR + NADH + NH3*
j33	*Gln + Pyr→Glu+Ala*
j34	*Asp →OAA+NH3*

Appendix D

Dynamic Model's Parameters

Appendix C, The parameters values refer to the coefficients in the differential equations.

Parameter	value	Parameter	value
K_{11}	0.254	K_{43}	4.96
K_{12}	9.99	K_{51}	0.5338
μ	1.38	K_{52}	1×10^{-7}
K_{21}	1	K_{61}	1.9053
K_{23}	6.243	K_{62}	27.032
K_{24}	2	K_{63}	0.3899
K_{25}	0.00621	K_{64}	0.00001
n	2.854	K_{65}	0.0306
K_{31}	12	K_{71}	3.026
K_{32}	46	K_{72}	7.897
K_{33}	0.922	K_{81}	5.522
K_{34}	47.506	K_{82}	34.7
K_{35}	0.1636	K_{91}	0.44
K_{36}	0.0437	K_{92}	0.249
K_{41}	9.12	K_{101}	0.87
K_{42}	10.18	K_{102}	0.032
K_d	1.2		
K29	0.07	K30	0.05
K37	-4.3	K38	0.19
Q1	0.7	Q2	0.45
Q3	2.3	ε	0.001

Appendix E

Glycosylation Index Model's Parameters

Appendix D, Glycosylation index model's parameters

Parameter	Value
a1	4.579
a2	0.5871
a3	1
a4	2.378
a5	1.408
a6	0.0526
m	2.5
p	2.5
q	0.5
s	0.0861
r	0.0861
Nuc(t=0)	0.4299
GI(t=0)	0.472

Bibliography

Aghamohseni H, Ohadi K, Spearman M, Krahn N, Moo-Young M, Scharer JM, et al. Effects of nutrient levels and average culture pH on the glycosylation pattern of camelid-humanized monoclonal antibody. J Biotechnol. Elsevier B.V.; 2014 Sep 30;186:98–109.

Ahn WS, Antoniewicz MR. Towards dynamic metabolic flux analysis in CHO cell cultures. Biotechnol J. 2012 Jan;7(1):61–74.

Ahn WS, Jeon J-J, Jeong Y-R, Lee SJ, Yoon SK. Effect of culture temperature on erythropoietin production and glycosylation in a perfusion culture of recombinant CHO cells. Biotechnol Bioeng. 2008 Dec 15;101(6):1234–44.

Altamirano C, Illanes A, Becerra S, Cairó JJ, Gòdia F. Considerations on the lactate consumption by CHO cells in the presence of galactose. J Biotechnol. 2006 Oct;125(4):547–56.

Andersen DC, Goochee CF. The effect of cell-culture conditions on the oligosaccharide structures of secreted glycoproteins. Curr Opin Biotechnol. 1994 Oct;5(5):546–9.

Anthony RM, Nimmerjahn F, Ashline DJ, Reinhold VN, Paulson JC, Ravetch J V. Recapitulation of IVIG anti-inflammatory activity with a recombinant IgG Fc. Science. 2008 Apr 18;320(5874):373–6.

Bell A, Wang ZJ, Arbabi-Ghahroudi M, Chang T a, Durocher Y, Trojahn U, et al. Differential tumor-targeting abilities of three single-domain antibody formats. Cancer Lett. Elsevier Ireland Ltd; 2010 Mar 1;289(1):81–90.

Bigge JC, Patel TP, Bruce JA, Goulding P., Charles S., Parekh R. nonselective and efficeient fluorescent labeling of glycans using 2-amino benzamide and anthranilic acid. Anal Biochem. 1995;30(2):229–38.

Borys MC, Linzer DL., Papoutsakis ET. Culture pH Affcets Expression rates and Glycosylation of Recombinant Mouse Placental Lactogen Proteins by Chinese Hamster Ovary (CHO) Cells. Nat Biotechnol. 1993;11:720–4.

Brodsky AN, Caldwell M, Bae S, Harcum SW. Glycosylation-related genes in NS0 cells are insensitive to moderately elevated ammonium concentrations. J Biotechnol. Elsevier B.V.; 2014 Oct 10;187:78–86.

Burleigh SC, van de Laar T, Stroop CJM, van Grunsven WMJ, O'Donoghue N, Rudd PM, et al. Synergizing metabolic flux analysis and nucleotide sugar metabolism to understand the control of glycosylation of recombinant protein in CHO cells. BMC Biotechnol. BioMed Central Ltd; 2011 Jan;11(1):95.

Butler M. Animal cell cultures: recent achievements and perspectives in the production of biopharmaceuticals. Appl Microbiol Biotechnol. 2005 Aug;68(3):283–91.

Butler M. Optimisation of the cellular metabolism of glycosylation for recombinant proteins produced by Mammalian cell systems. Cytotechnology. 2006a Mar;50(1-3):57–76.

Butler M. Optimisation of the cellular metabolism of glycosylation for recombinant proteins produced by Mammalian cell systems. Cytotechnology. 2006b Mar;50(1-3):57–76.

Campbell MP, Royle L, Radcliffe CM, Dwek RA, Rudd PM. GlycoBase and autoGU: Tools for HPLC-based glycan analysis. Bioinformatics. 2008;24:1214–6.

Chee Furng Wong D, Tin Kam Wong K, Tang Goh L, Kiat Heng C, Gek Sim Yap M. Impact of dynamic online fed-batch strategies on metabolism, productivity and N-glycosylation quality in CHO cell cultures. Biotechnol Bioeng. 2005 Jan 20;89(2):164–77.

Chen F, Kou T, Fan L, Zhou Y, Ye Z, Zhao L, et al. The combined effect of sodium butyrate and low culture temperature on the production, sialylation, and biological activity of an antibody produced in CHO cells. Biotechnol Bioprocess Eng. 2011 Dec 3;16(6):1157–65.

Chen P, Harcum SW. Effects of elevated ammonium on glycosylation gene expression in CHO cells. Metab Eng. 2006 Mar;8(2):123–32.

Chotigeat W, Watanapokasin Y, Mahler S, Gray PP. Role of environmental conditions on the expression levels, glycoform pattern and levels of sialyltransferase for hFSH produced by recombinant CHO cells. Cytotechnology. 1994;15(1-3):217–21.

Chu L, Robinson DK. Industrial choices for protein production by large-scale cell culture. Curr Opin Biotechnol. 2001;12:180–7.

Cohen SA, De Antonis K., Michaud D. Compositional Protein Analysis Using 6-Aminoquinolyl-N-Hydroxysuccinimidyl Carbamate, a novel derivatization reagent. Tech Protein Chem IV. San Diego: Academic Press; 1993. p. 289–98.

Crowell CK, Grampp GE, Rogers GN, Miller J, Scheinman RI. Amino Acid and Manganese Supplementation Modulates the Glycosylation State of Erythropoietin in a CHO Culture System. 2007;96(3):538–49.

Cruz HJ, Moreira L, Carrondo MJT. Metabolically optimised BHK cell fed-batch cultures. 2000;80:109–18.

Domann PJ, Pardos-Pardos AC, Fernandes DL, Spencer DIR, Radcliffe CM, Royle L, et al. Separation-based glycoprofiling approaches using fluorescent labels. Proteomics. 2007 Sep;7 Suppl 1:70–6.

Doyle C, Butler M. The effect of pH on the toxicity of ammonia to a murine hybridoma. J Biotechnol. 1990 Jul;15(1-2):91–100.

Dutton RL, Scharer JM, Moo-Young M. Hybridoma growth and productivity: effects of conditioned medium and of inoculum size. Cytotechnology. 1999 Jan;29(1):1–10.

Elvin JG, Couston RG, van der Walle CF. Therapeutic antibodies: market considerations, disease targets and bioprocessing. Int J Pharm. Elsevier B.V.; 2013 Jan 2;440(1):83–98.

Fekete S, Gassner A-L, Rudaz S, Schappler J, Guillarme D. Analytical strategies for the characterization of therapeutic monoclonal antibodies. TrAC Trends Anal Chem. Elsevier Ltd; 2013 Jan;42:74–83.

Gambhir A, Korke R, Lee J, Fu P, Europa A, Hu W. Analysis of Cellular Metabolism of Hybridoma Cells at Distinct Physiological States. 2003;95(4).

Gao J, Gorenflo VM, Scharer JM, Budman HM. Dynamic Metabolic Modeling for a MAB Bioprocess. 2007;168–81.

Gawlitzek M, Papac DI, Sliwkowski MB, Ryll T. Incorporation of 15N from ammonium into the N-linked oligosaccharides of an immunoadhesin glycoprotein expressed in Chinese hamster ovary cells. Glycobiology. 1999 Mar;9(2):125–31.

Gawlitzek M, Valley U, Nimtz M, Wagner R, Conradt HS. Characterization of changes in the glycosylation pattern of recombinant proteins from BHK-21 cells due to different culture conditions. J Biotechnol. 1995;42:117–31.

Grainger RK, James DC. CHO cell line specific prediction and control of recombinant monoclonal antibody N-glycosylation. Biotechnol Bioeng. 2013 Nov;110(11):2970–83.

Grammatikos SI, Valley U, Nimtz M, Conradt HS, Wagner R. Intracellular UDP - N - Acetylhexosamine Pool Affects N -Glycan Complexity : A Mechanism of Ammonium Action on Protein. 1998;410–9.

Gu X, Wang DI. Improvement of interferon-gamma sialylation in Chinese hamster ovary cell culture by feeding of N-acetylmannosamine. Biotechnol Bioeng. 1998 Jul 20;58(6):642–8.

Hammond S, Kaplarevic M, Borth N, Betenbaugh MJ, Lee KH. Chinese hamster genome database: an online resource for the CHO community at www.CHOgenome.org. Biotechnol Bioeng. 2012 Jun;109(6):1353–6.

Hauser H, Wagner R. Mammalian cell biotechnology in protein production /editors, Hansjörg Hauser, Roland Wagner. Berlin ; New York: Walter de Gruyter; 1997.

Hossler P. Protein Glycosylation Control in Mamalian Cell Culture:Past Precedents and Contemporary prospects. In: Wei-Shou Hu, A -P Zeng, editors. Genomics Syst Biol Mamm Cell Cult. Advances i. Heidelberg ; New York: Springe; 2012. p. 187–219.

Hossler P, Goh L, Lee MM, Hu W. GlycoVis : Visualizing Glycan Distribution in the Protein N -Glycosylation Pathway in Mammalian Cells. Biotechnol Bioeng. 2006;95:946–60.

Hossler P, Khattak SF, Li ZJ. Optimal and consistent protein glycosylation in mammalian cell culture. Glycobiology. 2009 Sep;19(9):936–49.

Human R, Hayter PM, Curling EMA, Baines AJ, Jenkins N, Salmon I, et al. Glucose-Limited Chemostat Culture of Chinese Hamster Ovary Cells Producing. Biotechnol Bioeng. 1992;39:327–35.

Ivarsson M, Villiger TK, Morbidelli M, Soos M. Evaluating the impact of cell culture process parameters on monoclonal antibody N-glycosylation. J Biotechnol. Elsevier B.V.; 2014 Aug 28;188C:88–96.

Jedrzejewski PM, del Val IJ, Constantinou A, Dell A, Haslam SM, Polizzi KM, et al. Towards controlling the glycoform: a model framework linking extracellular metabolites to antibody glycosylation. Int J Mol Sci. 2014 Jan;15(3):4492–522.

Jimenez del Val I, Nagy JM, Kontoravdi C. A dynamic mathematical model for monoclonal antibody N-linked glycosylation and nucleotide sugar donor transport within a maturing Golgi apparatus. Biotechnol Prog. 2011;27(6):1730–43.

Karsten CM, Pandey MK, Figge J, Kilchenstein R, Taylor PR, Rosas M, et al. Anti-inflammatory activity of IgG1 mediated by Fc galactosylation and association of FcγRIIB and dectin-1. Nat Med. 2012 Sep;18(9):1401–6.

Kaufmann H, Mazur X, Marone R, Bailey JE, Fussenegger M. Comparative analysis of two controlled proliferation strategies regarding product quality, influence on tetracycline-regulated gene expression, and productivity. Biotechnol Bioeng. 2001 Mar 20;72(6):592–602.

Kim DY, Chaudhry MA, Kennard ML, Jardon MA, Braasch K, Dionne B, et al. Fed-Batch CHO Cell t-PA Production and Feed Glutamine Replacement to. Biotechnol Prog. 2013;29:165–75.

Konno Y, Kobayashi Y, Takahashi K, Takahashi E, Sakae S, Wakitani M, et al. Fucose content of monoclonal antibodies can be controlled by culture medium osmolality for high antibody-dependent cellular cytotoxicity. Cytotechnology. 2012 May;64(3):249–65.

Kunkel JP, Jan DCH, Jamieson JC, Butler M. Dissolved oxygen concentration in serum-free continuous culture affects N-linked glycosylation of a monoclonal antibody. J Biotechnol. 1998;62:55–71.

Kuystermans D, Al-rubeai M. Animal Cell Culture. In: Al-Rubeai M, editor. Cham: Springer International Publishing; 2015. p. 717–57.

Li F, Vijayasankaran N, Shen A (Yijuan), Kiss R, Amanullah A. Cell culture processes for monoclonal antibody production. MAbs. 2010 Sep 1;2(5):466–79.

Li J, Wong CL, Vijayasankaran N, Hudson T, Amanullah A. Feeding lactate for CHO cell culture processes: impact on culture metabolism and performance. Biotechnol Bioeng. 2012 May;109(5):1173–86.

Liu B, Spearman M, Doering J, Lattová E, Perreault H, Butler M. The availability of glucose to CHO cells affects the intracellular lipid-linked oligosaccharide distribution, site occupancy and the N-glycosylation profile of a monoclonal antibody. J Biotechnol. Elsevier B.V.; 2014 Jan 20;170:17–27.

Mason M, Sweeney B, Cain K, Stephens P, Sharfstein S. Reduced Culture Temperature Differentially Affects Expression and Biophysical Properties of Monoclonal Antibody Variants. Antibodies. 2014 Aug;3(3):253–71.

McCracken N a, Kowle R, Ouyang A. Control of galactosylated glycoforms distribution in cell culture system. Biotechnol Prog. 2014;30(3):547–53.

Mensonides FIC, Brul S, Hellingwerf KJ, Bakker BM, Teixeira de Mattos MJ. A kinetic model of catabolic adaptation and protein reprofiling in Saccharomyces cerevisiae during temperature shifts. FEBS J. 2014 Feb 13;281(3):825–41.

Meuwly F, Weber U, Ziegler T, Gervais a, Mastrangeli R, Crisci C, et al. Conversion of a CHO cell culture process from perfusion to fed-batch technology without altering product quality. J Biotechnol. 2006 May;123(1):106–16.

Moore A, Mercer J, Dutina G, Donahue CJ, Bauer KD, Mather JP, et al. Effects of temperature shift on cell cycle , apoptosis and nucleotide pools in CHO cell batch cultues. 1997;47–54.

Munro TP, Mahler SM, Huang EP, Chin DY, Gray PP. Bridging the gap: facilities and technologies for development of early stage therapeutic mAb candidates. MAbs. 2011;3(5):440–52.

Müthing J, Kemminer SE, Conradt HS, Sagi D, Nimtz M, Kärst U, et al. Effects of buffering conditions and culture pH on production rates and glycosylation of clinical phase I anti-melanoma mouse IgG3 monoclonal antibody R24. Biotechnol Bioeng. 2003 Aug 5;83(3):321–34.

Nabi IR, Dennis JW. The extent of polylactosamine glycosylation of MDCK LAMP-2 is determined by its Golgi residence time. Glycobiology. 1998 Sep;8(9):947–53.

Naderi S, Meshram M, Wei C, McConkey B, Ingalls B, Budman H, et al. Development of a mathematical model for evaluating the dynamics of normal and apoptotic Chinese hamster ovary cells. Biotechnol Prog. 2011;27(5):1197–205.

Nyberg GB, Balcarcel RR, Follstad BD, Stephanopoulos G, Wang DI. Metabolic effects on recombinant interferon-gamma glycosylation in continuous culture of Chinese hamster ovary cells. Biotechnol Bioeng. 1999 Mar 5;62(3):336–47.

Ohadi K, Aghamohseni H, Gädke J, Moo-Young M, Legge RL, Scharer J, et al. Novel Dynamic Model to Predict the Glycosylation Pattern of Monoclonal Antibodies from Extracellular Cell Culture Conditions. 12th IFAC Symp Comput Appl Biotechnol. 2013.

Ohadi K, Aghamohseni H, Legge RL, Budman HM. Fluorescence-based soft sensor for at situ monitoring of chinese hamster ovary cell cultures. Biotechnol Bioeng. 2014 Aug 16;111(8):1577–86.

Ozturk SS, Hu W. cell culture technology for pharmaceutical and cell-based technology. New york; 2006.

Quek L-E, Dietmair S, Krömer JO, Nielsen LK. Metabolic flux analysis in mammalian cell culture. Metab. Eng. 2010. p. 161–71.

Raju TS, Briggs JB, Borge SM, Jones AJ. Species-specific variation in glycosylation of IgG: evidence for the species-specific sialylation and branch-specific galactosylation and importance for engineering recombinant glycoprotein therapeutics. Glycobiology. 2000;10:477–86.

Rearick J, Chapman A, Kornfeld S. Glucose Starvation Alters Lipid-linked Oligosaccharide Biosynthesis in Chinese Hamster Ovary Cells*. J Biol Chem. 1981;256(12):6255–61.

Restelli V, Butler M. 2. the effect of cell culture parameters on protein glycosylation. In: Al-Rubeai M, editor. cell enginering. Springer Netherlands; 2002. p. 61–92.

Rodriguez J, Spearman M, Tharmalingam T, Sunley K, Lodewyks C, Huzel N, et al. High productivity of human recombinant beta-interferon from a low-temperature perfusion culture. J Biotechnol. Elsevier B.V.; 2010 Dec;150(4):509–18.

Royle L, Radcliffe CM, Dwek RA, Rudd PM. Detailed structural analysisof N-glycans released from glycoproteins in SDS-PAGE gel bands using HPLCcombined with exoglycosidase array digestions. Methods Mol Biol. 2006;347:125–43.

Sanfeliu A, Stephanopoulos G. Effect of glutamine limitation on the death of attached Chinese hamster ovary cells. Biotechnol Bioeng. 1999;64:46–53.

Schneider M, Marison IW, Stockar U von. the importancce of ammonia in mamamlian cell culture.pdf. J Biotechnol. 1996;46:161–85.

Senger RS, Karim MN. Effect of shear stress on intrinsic CHO culture state and glycosylation of recombinant tissue-type plasminogen activator protein. Biotechnol Prog. 2003;19(4):1199–209.

Seo JS, Kim YJ, Cho JM, Baek E, Lee GM. Effect of culture pH on recombinant antibody production by a new human cell line, F2N78, grown in suspension at 33.0 °C and 37.0 °C. Appl Microbiol Biotechnol. 2013 Jun;97(12):5283–91.

Sethuraman N, Stadheim T a. Challenges in therapeutic glycoprotein production. Curr Opin Biotechnol. 2006 Aug;17(4):341–6.

Shields RL, Lai J, Keck R, O'Connell LY, Hong K, Meng YG, et al. Lack of fucose on human IgG1 N-linked oligosaccharide improves binding to human Fcgamma RIII and antibody-dependent cellular toxicity. J Biol Chem. 2002 Jul 26;277(30):26733–40.

Sou SN, Sellick C, Lee K, Mason A, Kyriakopoulos S, Polizzi KM, et al. How does mild hypothermia affect monoclonal antibody glycosylation? Biotechnol Bioeng. 2014 Dec 29;1–29.

Spearman M, Butler M. Animal Cell Culture. In: Al-Rubeai M, editor. Cham: Springer International Publishing; 2015. p. 237–58.

Stanley P. Golgi Glycosylation. Cold Spring Harb Perspect Biol. 2011;3:a005199:1–13.

Sureshkumar GK, Mutharasan R. The Influence of Temperature on a Monoclonal Antibody Production. 1991;37:292–5.

Taschwer M, Hackl M, Hernández Bort J a, Leitner C, Kumar N, Puc U, et al. Growth, productivity and protein glycosylation in a CHO EpoFc producer cell line adapted to glutamine-free growth. J Biotechnol. Elsevier B.V.; 2012 Jan 20;157(2):295–303.

Tharmalingam T, Wu C-H, Callahan S, Goudar CT. A Framework for Real-time Glycosylation Monitoring (RT-GM) in Mammalian Cell Culture. Biotechnol Bioeng. 2014 Dec;n/a – n/a.

Trummer E, Fauland K, Seidinger S, Schriebl K, Lattenmayer C, Kunert R, et al. Process Parameter Shifting : Part I . Effect of DOT , pH , and Temperature on the Performance of Epo-Fc Expressing CHO Cells Cultivated in Controlled Batch Bioreactors. 2006;

Umaña P, Jean-mairet J, Moudry R, Amstutz H, Bailey JE. Engineered glycoforms of an antineuro- blastoma IgG1 with optimized antibody- dependent cellular cytotoxic activity. 1999;17(February).

Del Val IJ, Kontoravdi C, Nagy JM. Towards the implementation of quality by design to the production of therapeutic monoclonal antibodies with desired glycosylation patterns. Biotechnol Prog. 2010;26(6):1505–27.

Valley U, Nimtz M, Conradt HS, Wagner R. Incorporation of Ammonium into N-Acetylhexosamines and into Carbohydrate Structures in Glycoproteins. Biotechnol Bioeng. 1999;64:401–17.

Vergara M, Becerra S, Berrios J, Osses N, Reyes J, Rodríguez-Moyá M, et al. Differential effect of culture temperature and specific growth rate on CHO cell behavior in chemostat culture. PLoS One. 2014 Jan;9(4):e93865.

Wahrheit J, Nicolae A, Heinzle E. Dynamics of growth and metabolism controlled by glutamine availability in Chinese hamster ovary cells. Appl Microbiol Biotechnol. 2013 Dec 22;

Wang W-C, Lee N, Aoki D, Fukuda MN, Fukuda M. The Poly-N-acetyllactosamines Attached to Lysosomal Membrane Glycoproteins Are Increased by the Prolonged Association with the Golgi Complex *. J Biol Chem. 1991;266.

Weidemann R, Ludwing A, Kretzmer G. Low temperature cultivation - A step towards process optimisation. 1994;111–6.

Wong NSC, Wati L, Nissom PM, Feng HT, Lee MM, Yap MGS. An investigation of intracellular glycosylation activities in CHO cells: effects of nucleotide sugar precursor feeding. Biotechnol Bioeng. 2010 Oct 1;107(2):321–36.

Xie L, Nyberg G, Gu X, Li H, Mo F, Wang DIC. Gamma-Interferon Production and Quality in Stoichiometric Fed-Batch Cultures of Chinese Hamster Ovary (CHO) Cells under Serum-Free Conditions. Biotechnol Bioeng. 1997;56(5):577–82.

Yang M, Butler M. Effects of ammonia on CHO cell growth, erythropoietin production, and glycosylation. Biotechnol Bioeng. 2000 May 20;68(4):370–80.

Yang M, Butler M. Effects of ammonia and glucosamine on the heterogeneity of erythropoietin glycoforms. Biotechnol Prog. 2002;18(1):129–38.

Yang WC, Lu J, Kwiatkowski C, Yuan H, Kshirsagar R, Ryll T, et al. Perfusion seed cultures improve biopharmaceutical fed-batch production capacity and product quality. Biotechnol Prog. 2014;30(3):616–25.

Yoon SK, Choi SL, Song JY, Lee GM. Effect of culture pH on erythropoietin production by Chinese hamster ovary cells grown in suspension at 32.5 and 37.0 degrees C. Biotechnol Bioeng. 2005 Feb 5;89(3):345–56.

Yoon SK, Kim SH, Song JY, Lee GM. Biphasic culture strategy for enhancing volumetric erythropoietin productivity of Chinese hamster ovary cells. Enzyme Microb Technol. 2006 Jul;39(3):362–5.

Yoon SK, Song JY, Lee GM. Effect of low culture temperature on specific productivity, transcription level, and heterogeneity of erythropoietin in Chinese hamster ovary cells. Biotechnol Bioeng. 2003 May 5;82(3):289–98.

Zhang J, Mackenzie R, Durocher Y. Therapeutic Antibodies. In: Dimitrov AS, editor. Totowa, NJ: Humana Press; 2009. p. 323–36.

Zustiak M., Pollack J., MR M, Betenbaugh MJ. Feast or famine: autophagy control and engineering in eukaryotic cell culture. Curr Opin Biotechnol. 2008;19:518–26.